



XXII. Symposium on Atomic, Cluster and Surface Physics (SASP'20)

**St. Moritz, Switzerland
02 – 07 February 2020**



CONTRIBUTIONS

EDITORS

Karl-Heinz Ernst, Christine Tran

XXII. Symposium on Atomic, Cluster and Surface Physics (SASP'20)

St. Moritz, Switzerland

02 – 07 February 2020

CONTRIBUTIONS

EDITORS

Karl-Heinz Ernst, Christine Tran

XXII. Symposium on Atomic, Cluster and Surface Physics (SASP'20)

St. Moritz, Switzerland

02 – 07 February 2020

Local Organizing Committee

Karl-Heinz Ernst, Christine Tran

Contact address:

Empa, Swiss Federal Laboratories for Materials Science and Technology
Überlandstrasse 129
CH-8600 Dübendorf
Switzerland
Tel. +41 (0) 58 765 60 85
sasp2020@empa.ch

International Scientific Committee

Daniela Ascenzi (Università degli Studi di Trento)	Stephen Price (University College London)
Martin Beyer (Universität Innsbruck)	Tom Rizzo (EPFL Lausanne)
Tilmann D. Märk (Universität Innsbruck)	Jürgen Stohner (ZHAW Zürich)
Roberto Marquardt (Université de Strasbourg)	Paul Scheier (Universität Innsbruck)
Nigel Mason (Open University, UK)	Roland Wester (Universität Innsbruck)
Martin Quack (ETH Zürich)	

Venue

Hotel Laudinella
Via Tegiatscha 17
CH – 7500 St. Moritz
Switzerland
T +41 (0) 81 836 00 00
info@laudinella.ch

Sponsors

The Organizing Committee gratefully acknowledges financial support by

- | | |
|---------------------|------------------------------|
| ▪ CreaTec Fischer | ▪ Royal Society of Chemistry |
| ▪ Empa | ▪ Scienta Omicron |
| ▪ Hiden | ▪ SPECS |
| ▪ Prevac | ▪ Swiss Chemical Society |
| ▪ Radian Dyes Laser | ▪ Zurich Instruments |

Preface

We welcome all participants and accompanying persons to the XXII. Symposium on Atomic, Cluster and Surface Physics in St. Moritz.

The Symposium on Atomic, Cluster and Surface Physics (SASP) is a series of biennial international conferences, which seeks to promote the growth of scientific knowledge and effective exchange of information among scientists in the field of atomic, cluster and surface physics. The symposium deals in particular with collisional interactions involving different types of collision partners, i.e. electrons, photons, molecules, nano particles, and surfaces.

There will be invited expert lectures covering recent advances in the topics of the symposium. Contributed papers will be presented in two poster sessions. These poster sessions provide the main forum for presentation of new work and for discussion of recent progress. A few contributed papers will be selected for oral presentation in Hot Topic sessions.

Since 1986, SASP takes place every second time in Austria, from 2006 onwards in Obergurgl. The respective following year it was switching between Italy, France and Switzerland. Throughout the years SASP became a truly global conference, with participants from the US and Canada, China, Japan and all over Europe.

We hope that all participants will experience a lively and successful meeting while enjoying the surrounding in the beautiful Engadin region.

Karl-Heinz Ernst

Christine Tran

Your innovative UHV growth

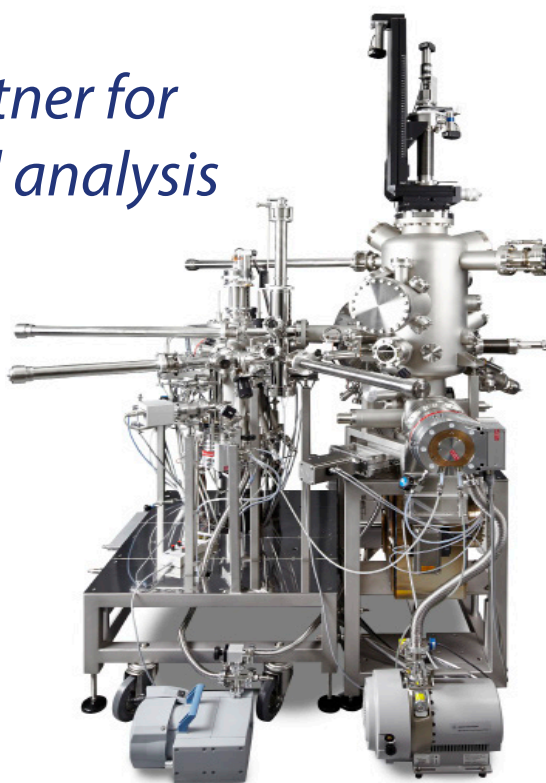
Since 2000, the combined low-temperature scanning tunneling and atomic force microscope (LT-STM/AFM) is an essential part of the CreaTec product range. With more than 25 years of experience in construction, design, and manufacturing of UHV equipment, we can easily implement complex customer requirements. Continuous performance improvement, innovation, and development in close collaboration with leading research institutions allow us to guarantee high quality and reliable systems. Our experienced scientists will promptly support our customers and provide long term maintenance as well as technical upgrades of existing systems.



CreaTec Fischer & Co. GmbH
Industriestr. 9
74391 Erligheim
+49 (7143) 9670-0
sales@createc.de



partner for and analysis



LT-STM/AFM

For a precise manipulation of atoms and molecules at temperatures in the range of 1 to 300 K.



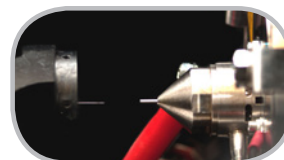
MINI MBE SYSTEM

All features of a MBE production in extremely compact design, scaled for perfect homogeneity on small samples.



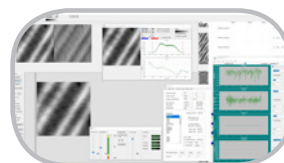
ESI SYSTEM

With the CreaTec ESI System, we offer an ultra-clean source for molecules that cannot be thermally evaporated / sublimated.



SOFTWARE + ELECTRONICS

CreaTec SPM electronics are based on all digital design, with all scanning / feedback parameters fully controlled by our SPM software.



www.createc.de

Upgrade options



AWG



Impedance
Analyzer



Boxcar
PWA



PID, PLL
Controller

All Instruments include



Spectrum
Analyzer



Oscilloscope
with FFT



Image
Recorder



Matlab®, LabVIEW®, .NET,
C and Python interface

Lock-in Amplifiers

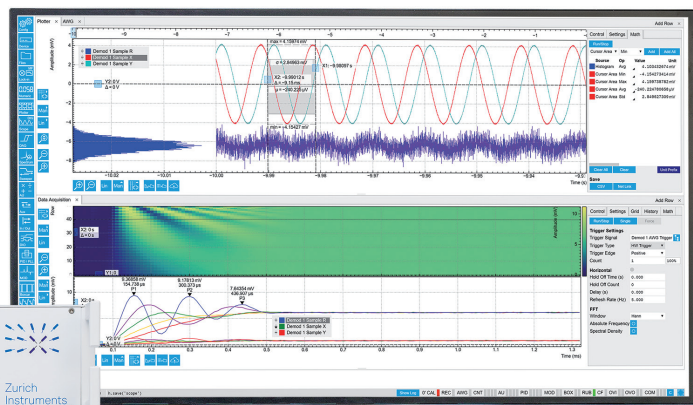
... and more,
from DC to 600 MHz

Typical applications

- **Spectroscopy**
Pulsed lasers, THz, choppers,
optical phase locking (oPLL)
- **Imaging**
AFM, Kelvin-Probe, CARS, SRS, SNOM
- **Quantum research**
Ion traps, cQED, Quantum Dots,
NV centers
- **Sensors**
MEMS, NEMS, gyros,
photoacoustic sensors

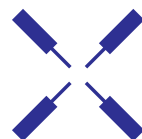
starting at

CHF 6050.–



Intl. +41 44 515 0410
info@zhinst.com
www.zhinst.com

Let's discuss your application
Start the conversation today



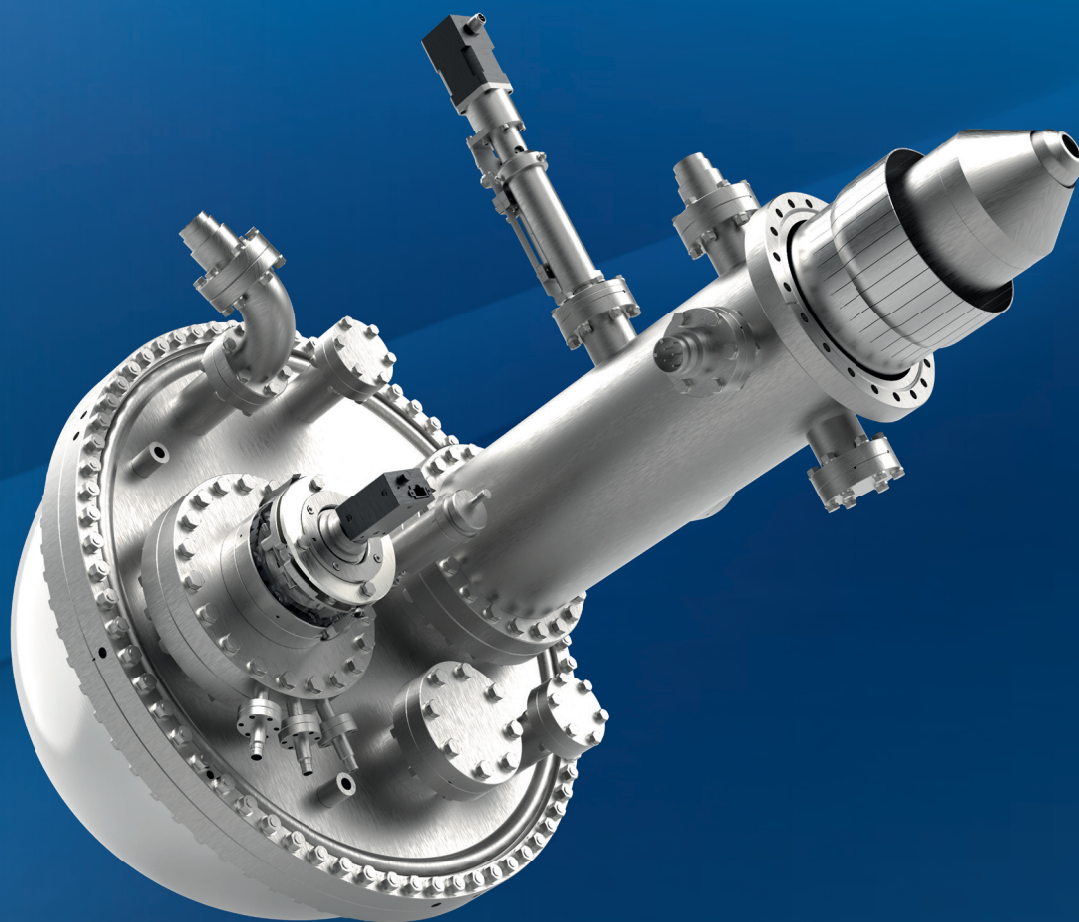
Zurich
Instruments

ASTRAIOS 190

2D MOMENTUM MAPPING ELECTRON ANALYZER
FOR UNRIVALED ARPES PERFORMANCE

KEY FEATURES

- Single spot parallel shifting lens (patent applied)
- $\pm 30^\circ$ acceptance angle
($\pm 1 \text{ \AA}^{-1}$ k-range for He I,
 $\pm 2.5 \text{ \AA}^{-1}$ k-range for (S)XPS)
- k-resolution $< 0.003 \text{ \AA}^{-1}$
- Energy resolution $< 1.5 \text{ meV}$
- Motorized virtual analyzer entrance slit



SPECS Surface Nano Analysis GmbH

T +49 30 46 78 24 0

E info@specs.com

H www.specs-group.com

SPECS™

A member of SPECSGROUP

SASP'20 - PROGRAM

Sunday 02 Feb	Monday 03 Feb <i>Chair: Stöhr</i>	Tuesday 04 Feb <i>Chair: Götzhäuser</i>	Wednesday 05 Feb <i>Chair: Merkt</i>	Thursday 06 Feb <i>Chair: Osterwalder</i>	Friday 07 Feb <i>Chair: Barth</i>
08:00	Arnolds	08:00 Giessibl	08:00 Saalfrank	08:00 Stähler	08:00 Kunze-Liebhäuser
08:35	Maier	08:35 Stöhr	08:35 Rossi	08:35 Domke	08:35 Aumayr
09:10	Niedner-Schatteburg	09:10 Baljovic	09:10 Zimmermann	09:10 Bourguignon	09:10 Stohner
09:30	Coffee	09:30 Coffee	09:30 Coffee	09:30 Coffee	09:30 Coffee
10:00	Beck	10:00 Osterwalder	10:00 Quack	10:00 Bürgi	10:00 Merkt
10:35	Break/ Discussions	10:35 Break/ Discussions	10:35 Break/ Discussions	10:35 Break/ Discussions	10:35 SASP Award
					10:50 SASP 2022
					11:00 Departure
15:45	15:45 Coffee/ Snack	15:45 Coffee/ Snack	15:45 Coffee/ Snack	15:45 Coffee/ Snack	
	<i>Chair: Giessibl</i>	<i>Chair: Beck</i>	<i>Chair: Quack</i>	<i>Chair: Wackerlin</i>	
	16:30 Widdra	16:30 Wodtke	16:30 Fedor	16:30 Franke	
	17:05 Steinrück	17:05 Grill	17:05 Brünken	17:05 Götzhäuser	
	17:40 Kitsopolous	17:40 Sinhal	17:40 Rizzo	17:40 Faure	
	18:00 Melani	18:00 Bastian	18:00 Ellis-Gibbings	18:00 Barth	
	18:20 Tiefentaler	18:20 Kilaj	18:20 Schmid	18:20 Break/ Discussions	
18:30	18:40 Break/ Discussions	18:40 Break/ Discussions	18:40 Break/ Discussions		
	19:00 Dinner	19:00 Dinner	19:00 Dinner	19:30 Conference Dinner	
19:50	<i>Chair: Xantheas</i>		<i>Chair: Xantheas</i>		
20:00	20:30 Poster Session		20:30 Poster Session		
20:40					
21:20					

XXII. Symposium on Atomic, Cluster and Surface Physics (SASP'20)

St. Moritz, Switzerland

02 – 07 February 2020

Time Schedule

Sunday, 02 February 2020

15:45 – 18:30 **Registration**

18:30 – 19:50 **Dinner**

19:50 – 20:00 **Welcome**

Session Chair: Karl-Heinz Ernst

20:00 – 20:40 **B. Feringa**
Molecular Switches and Motors at Interfaces

20:40 – 21:20 **J. Küpper**
Strong-field physics in the molecular frame and the recording of the molecular movie

Monday, 03 February 2020

Session Chair: Meike Stöhr

08:00 – 08:35

H. Arnolds

Insulin and other proteins at interfaces – from amyloidosis to fabric stains

08:35 – 09:10

S. Maier

On-surface synthesis of low-dimensional carbon-based nanostructures

09:10 – 09:30

G. Niedner-Schatteburg

Nitrophobia of size selected iron clusters under cryo isolation

10:00 – 10:35

R. D. Beck

Methane chemisorption on stepped Ni and Pt surfaces studied by vibrational spectroscopy

Session Chair: Franz Giessibl

16:30 – 17:05

W. Widdra

Vibrations and dielectric properties at perovskite surfaces

17:05 – 17:40

H.-P. Steinrück

Ionic liquid adsorption and ion exchange processes at single crystal surfaces

17:40 – 18:00

T. N. Kitsopoulos

Kinetics and dynamics of CO oxidation on atomically stepped Pd surfaces

18:00 – 18:20

G. Melani

Vibrational spectroscopy and non-equilibrium dynamics at aqueous metal oxide interfaces

18:20 – 18:40

L. Tiefenthaler

Highly charged Helium Nanodroplets: a cool tool for well-defined cluster formation

Session Chair: Sotiris Xantheas

20:30 - 22:00

Poster session

S. Armenta Butt

The dynamics of the reactions of Ar^{2+} with small molecules: complexation and bond formation

M. Baljovic

Lack of chirality induced spin selectivity (CISS) in molecular layers of helicenes

M. Baljovic

Diastereoselective on-surface synthesis of bisheptahelicene, their (cyclo)dehydrogenation and consequent HBr desorption

J. Berger

Chiral recognition in the self-assembly of trioxa[11]helicene molecules on metal surfaces

F. Dünsing

Fusion relevant reactive ion surface collision investigation using the SurfTOF tandem mass spectrometer

K.-H. Ernst

On the density of racemic and homochiral crystals: Wallach, Liebisch and Sommerfeld in Göttingen

S. Espinoza

A versatile experimental platform for ultrafast time-resolved ellipsometry from VUV to NIR

D. Field

Spontaneously electrical solids: how ammonia misbehaves

G. Gonella

Interaction of biomolecules with soft surfaces: from blood proteins and polymeric surfaces to partially disordered peptides and biomembranes

T. R. Govers

Predissociation of N_2^+ isotopologues studied by TPEPICO imaging spectrometry

N. Hertl

Theoretical simulations of non-adiabatic H atom scattering from tungsten

N. Hölsch

Precision measurements in H_2 and H_2^+ using nonpenetrating Rydberg states

J. Küpper

Creating and controlling cryogenically-cooled beams of shock-frozen, isolated, biological and artificial nanoparticles

J. Küpper

Creating, imaging, and controlling chiral molecules with electric fields

V. Mazankova

Study of oxygen reactions on polymer surfaces previously treated by ozone

T. Niepel

Tip-enhanced raman spectroscopy on two-dimensional polymers

Y. Pandey

Plasmonically enhanced raman spectroscopy of surface bound molecular electrocatalyst

T. F. Pascher

Electronic structure of copper formate clusters probed by UV/Vis spectroscopy

M. Probst

Sputtering from a beryllium surface: neural-network based molecular dynamics simulations without empirical parameters

M. Rebarz

Ultrafast spectroscopy at the ELI Beamlines facility: available capabilities for applications in molecular, biomedical and materials science

P. Stranak

New high-density radical source for investigating conformational and state-specific effects in chemical reactions

D. Trunec

Plasma polymerized oxazoline based thin films for biomedical applications

J. Voigt

Chirality transfer in a non-covalent molecular network

C. Wäckerlin

Electronic transport through 1D coordination polymers

Tuesday, 04 February 2020

Session Chair: Armin Gölzhäuser

08:00 – 08:35

F. J. Giessibl

A study of small iron clusters on Cu(111) by atomic force microscopy

08:35 – 09:10

M. Stöhr

Molecular nanostructures on metals vs. graphene

09:10 – 09:30

M. Baljozovic

Structural changes of buckybowls via selective on-surface hydrogenation

10:00 – 10:35

A. Osterwalder

Low-energy stereodynamics in merged beams

Session Chair: Rainer Beck

16:30 – 17:05

A. Wodtke

Vibrational energy pooling studied by mid-infrared laser induced fluorescence with a superconducting nanowire single photon detector

17:05 – 17:40

L. Grill

Single-molecule motion at surfaces

17:40 – 18:00

M. Sinhal

Quantum non-demolition state detection and spectroscopy of single trapped molecules

18:00 – 18:20

B. Bastian

Nucleophilic substitution and ligand exchange dynamics in bimolecular collisions with microhydrated anions

18:20 – 18:40

A. Kilaj

Reaction kinetics of trapped molecular ions with conformer- and isomer-selected neutral molecules

Wednesday, 05 February 2020

Session Chair: Frédéric Merkt

08:00 – 08:35

P. Saalfrank

*Photochemistry and spectroscopy of molecules at surfaces:
Insights from ab initio molecular dynamics*

08:35 – 09:10

M. Rossi

*Quantum mechanics for intramolecular reactions and
conformational space exploration of organic molecules on
metallic surfaces*

09:10 – 09:30

R. Zimmermann

*Simultaneous detection of polycyclic aromatic hydrocarbons and
inorganic ions in on-line single aerosol particle laser mass
spectrometry using molecular as well as atomic resonances*

10:00 – 10:35

M. Quack

*Precision tests of nuclear spin symmetry and parity conservation
in polyatomic molecules*

Session Chair: Martin Quack

16:30 – 17:05

J. Fedor

Electron-induced processes in novel dielectric gases

17:05 – 17:40

S. Brünken

Unravelling isomers of reactive ionic intermediates

17:40 – 18:00

T. R. Rizzo

*Combining ultrahigh-resolution ion mobility with cryogenic ion
vibrational spectroscopy for the analysis of glycans*

18:00 – 18:20

L. Ellis-Gibbings

*Gas-phase dications: Creation, coincidences, charges and
chemistry*

18:20 – 18:40

M. Schmid

Recent advancements in surface science instruments

Session Chair: Sotiris Xantheas

20:30 - 22:00

Poster session

Thursday, 06 February 2020

Session Chair: Andreas Osterwalder

08:00 – 08:35

J. Stähler

ZnO: Ultrafast generation and decay of a surface metal

08:35 – 09:10

K. F. Domke

Nanoscale insights into surface electrochemistry - Au oxidation revisited

09:10 – 09:30

B. Bourguignon

Molecules in interaction with nanoparticles grown on alumina film: the benefits of combined SFG spectroscopy and STM microscopy

10:00 – 10:35

T. Bürgi

Thiolate-protected metal clusters: Chirality and dynamic nature

Session Chair: Christian Wäckerlin

16:30 – 17:05

K. Franke

Spin excitations and interactions on superconductors – probed and manipulated by scanning tunneling microscopy

17:05 – 17:40

A. Götzhäuser

Carbon nanoconduits: 2D Materials for water purification and osmosis

17:40 – 18:00

A. Faure

Interstellar organic molecules and (anti-)masers

Friday, 07 February 2020

Session Chair: Johannes Barth

08:00 – 08:35

J. Kunze-Liebhäuser

Electroreduction of water and CO₂: competition or synergism on Mo₂C film electrodes?

08:35 – 09:10

F. Aumayr

Neutralization dynamics of highly charged ions in 2D materials

09:10 – 09:30

J. Stohner

Small chiral molecules: Progress in synthesis and beyond

10:00 – 10:35

F. Merkt

Ion-molecule reactions below 1 K

10:35 – 10:50

SASP Award

10:50 – 11:00

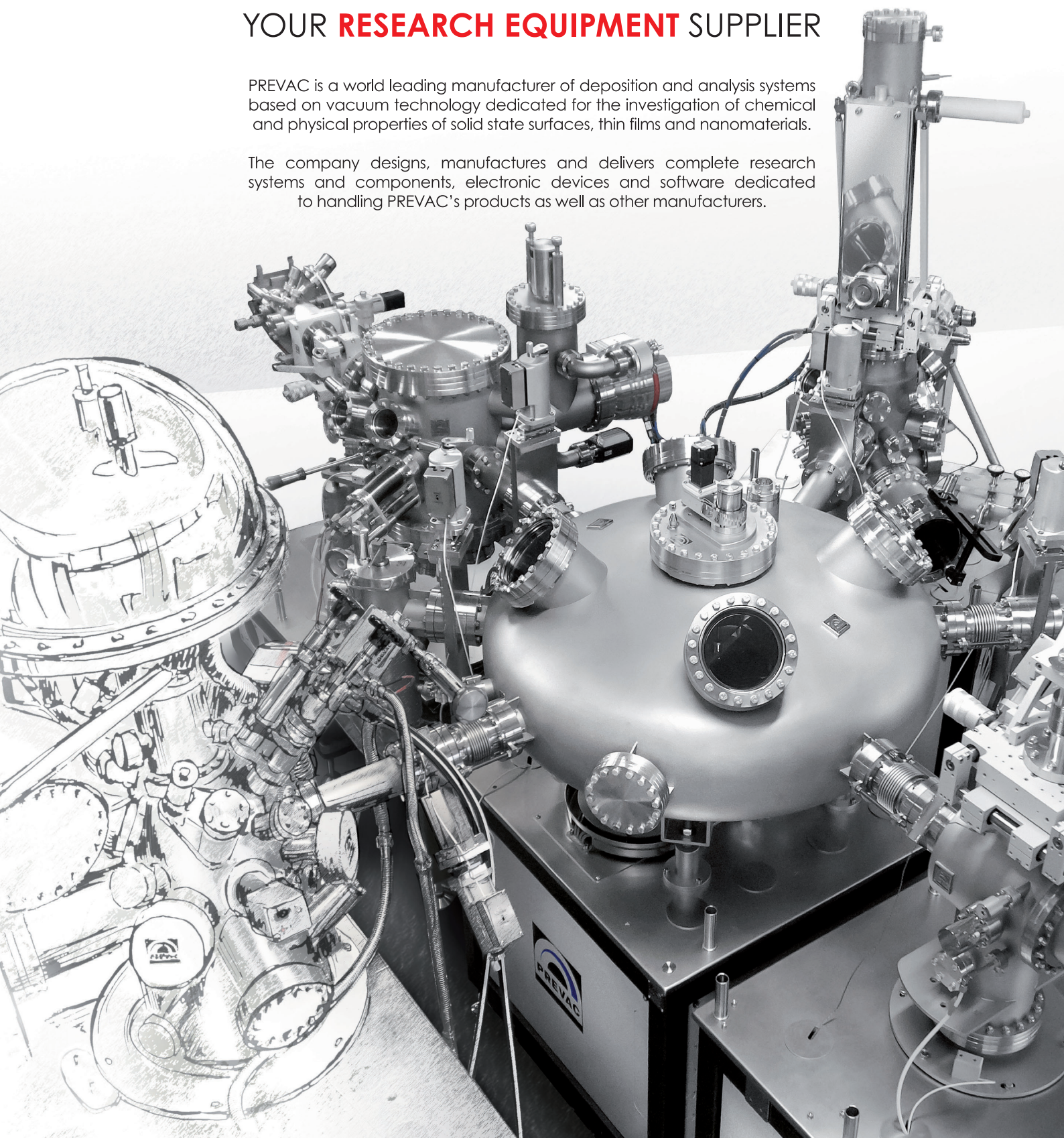
SASP 2022



YOUR **RESEARCH EQUIPMENT** SUPPLIER

PREVAC is a world leading manufacturer of deposition and analysis systems based on vacuum technology dedicated for the investigation of chemical and physical properties of solid state surfaces, thin films and nanomaterials.

The company designs, manufactures and delivers complete research systems and components, electronic devices and software dedicated to handling PREVAC's products as well as other manufacturers.



Radiant Dyes Laser Acc. GmbH

NarrowScan Dye Laser



Laser Accessories



Optomechanics



Radiant Dyes Laser & Acc. GmbH, Germany,
www.radiant-dyes.com, info@radiant-dyes.com

Table of Contents

Molecular switches and motors at interfaces <u>Ben L. Feringa</u>	26
Strong-field physics in the molecular frame and the recording of the molecular movie <u>Jochen Küpper</u>	27
Insulin and other proteins at interfaces – from amyloidosis to fabric stains Jamaica-Marie Bucag, Xinyang Li, Alice Mason, Jack Quayle, <u>Heike Arnolds</u>	28
On-surface synthesis of low-dimensional carbon-based nanostructures <u>Sabine Maier</u>	29
Nitrophobia of size selected iron clusters under cryo isolation A. Steiner, S. Dillinger, Jennifer Mohrbach, Christopher Wiehn, M. P. Klein, D. V. Fries, P. B. Armentrout, <u>G. Niedner-Schatteburg</u>	30
Methane chemisorption on stepped Ni and Pt surfaces studied by vibrational spectroscopy <u>Rainer D. Beck</u>	31
Vibrations and dielectric properties at perovskite surfaces Florian O. Schumann, Krassimir L. Kostov, Veronica Goian, Jonas Pantzer, <u>Wolf Widdra</u>	32
Ionic liquid adsorption and ion exchange processes at single crystal surfaces <u>Hans-Peter Steinrück</u>	33
Kinetics and dynamics of CO oxidation on atomically stepped Pd surfaces Dmitry Borodin, Michael Schwarzer, Jannis Neugebahren, Barratt G. Park, Alec M. Wodtke and <u>Theofanis. N. Kitsopoulos</u>	34
Vibrational spectroscopy and non-equilibrium dynamics at aqueous metal oxide interfaces <u>Giacomo Melani</u> , Yuki Nagata, R. Kramer Campen, Peter Saalfrank	36
Highly charged Helium Nanodroplets: a cool tool for well-defined cluster formation Felix Laimer, Lorenz Kranabetter, <u>Lukas Tiefenthaler</u> , Simon Albertini, Fabio Zappa, Andrew M. Ellis, Michael Gatchell, Paul Scheier	38
The dynamics of the reactions of Ar²⁺ with small molecules: complexation and bond formation <u>Sam Armenta Butt</u> , Stephen D. Price	41
Lack of chirality induced spin selectivity (CISS) in molecular layers of helicenes <u>Milos Baljozovic</u> , Anaïs Mairena, Benito Arnoldi, André Luis Fernandes Cauduro, Eduardo Bonini Guedes, Christian Wäckerlin, Jan Voigt, Bahaaeddin Irziqat, Jan Hugo Dill, Benjamin Stadtmüller, Andreas Schmid, Karl-Heinz Ernst	43
Diastereoselective on-surface synthesis of bisheptahelicene, their (cyclo)dehydrogenation and consequent HBr desorption <u>Milos Baljozovic</u> , Anaïs Mairena, Maciej Kawecki, Konstantin Grenader, Martin Wienke, Kévin Martin, Laetitia Bernard, Narcis Avarvari, Andreas Terfort, Karl-Heinz Ernst, Christian Wäckerlin	44

Chiral recognition in the self-assembly of trioxa[11]helicene molecules on metal surfaces	45
Bahaaeddin Irziqat, <u>Jan Berger</u> , Jesus Mendieta, Shyam Sundar, Ashutosh Bedekar, Pavel Jelinek, Karl-Heinz Ernst	
Fusion relevant reactive ion surface collision investigation using the SurfTOF tandem mass spectrometer	46
<u>Felix Duensing</u> , Lorenz Ballauf, Faro Hechenberger, Paul Scheier	
On the density of racemic and homochiral crystals: Wallach, Liebisch and Sommerfeld in Göttingen	47
<u>Karl-Heinz Ernst</u>	
A Versatile experimental platform for ultrafast time-resolved ellipsometry from VUV to NIR	48
<u>Shirley Espinoza</u>	
Spontaneously electrical solids: how ammonia misbehaves	50
<u>David Field</u> , Andrew Cassidy, Rachel James	
Interaction of biomolecules with soft surfaces: from blood proteins and polymeric surfaces to partially disordered peptides and biomembranes	53
Christoph Bernhard, Daria Maltseva, Kristin N. Bauer, Steven J. Roeters, Tina Berger, Benedikt Goretzki, Kerstin Viet, Charlotte Guhl, Tobias Weidner, Mischa Bonn, Frederik R. Wurm, Ute A. Hellmich, <u>Grazia Gonella</u>	
Predissociation of N_2^+ isotopologues studied by TPEPICO imaging spectrometry	55
Helgi R. Hrodmarsson, Roland Thissen, Danielle Doweck, Gustavo A. Garcia, Laurent Nahon and <u>Thomas R. Govers</u>	
Theoretical simulations of non-adiabatic H atom scattering from tungsten	58
<u>Nils Hertl</u> , Oihana Galparsoro, Raidel Martin-Barrios, Alexander Kandratsenka, Pascal Larrégaray, Alec Wodtke	
Precision measurements in H_2 and H_2^+ using nonpenetrating Rydberg states	59
<u>Nicolas Hölsch</u> , Maximilian Beyer, Kjeld S. E. Eikema, Wim Ubachs, Christian Jungen and Frédéric Merkt	
Creating and controlling cryogenically-cooled beams of shock-frozen, isolated, biological and artificial nanoparticles	60
A. K. Samanta, M. Amin, A. Estillore, N. Roth, L. Worbs, D. A. Horke, <u>J. Küpper</u>	
Creating, imaging, and controlling chiral molecules with electric fields	61
Andrey Yachmenev, Emil Zak, Jolijn Onvlee, Alec Owens, Cem Saribal, <u>Jochen Küpper</u>	
Study of oxygen reactions on polymer surfaces previously treated by ozone	62
<u>Vera Mazankova</u> , David Trunec, Anezka Krzyzankova, Frantisek Krcma	
Tip-enhanced raman spectroscopy on two-dimensional polymers	66
<u>Timo S.G. Niepel</u> , Wei Wang, A. Dieter Schlüter, Renato Zenobi	
Plasmonically enhanced raman spectroscopy of surface bound molecular electrocatalyst	67
<u>Yashashwa Pandey</u> , Laurent Sévery, Guillaume Goubert, Jacek Szczerbinski, Timo S. G. Niepel, S. David Tilley, Renato Zenobi	

Electronic structure of copper formate clusters probed by UV/Vis spectroscopy <u>Tobias F. Pascher</u> , Milan Ončák, Christian van der Linde, Martin K. Beyer	68
Sputtering from a Beryllium surface: Neural-network based molecular dynamics simulations without empirical parameters Lei Chen, Ivan Sukuba, <u>Michael Probst</u> , Alexander Kaiser	69
Ultrafast spectroscopy at the ELI Beamlines facility: available capabilities for applications in molecular, biomedical and materials science <u>Mateusz Rebarz</u> , Shirley Espinoza, Jakob Andreasson	73
New high-density radical source for investigating conformational and state-specific effects in chemical reactions <u>P. Stranak</u> , L. Ploenes, H. Gao, F. Stienkemeier, K. Dulitz, J. Küpper, S. Willitsch	75
Plasma polymerized oxazoline based thin films for biomedical applications Pavel Stahel, Vera Mazankova, Klara Tomeckova, Antonin Brablec, Lubomir Prokes, Jana Jurmanova, Marian Lehocky, Petr Humpolicek, Kadir Ozaltin, <u>David Trunec</u>	77
Chirality transfer in a non-covalent molecular network <u>Jan Voigt</u> , Milos Baljovic, Christian Wäckerlin, Kévin Martin, Narcis Avarvari, Karl-Heinz Ernst	81
Electronic transport through 1D coordination polymers <u>Christian Wäckerlin</u> , Oleksander Stetsovych, Santhini Vijai Meena, Aleš Cahlík, Simon Pascal, Martin Švec, Jesús Mendieta, Pingo Mutombo, Olivier Siri, Pavel Jelínek	82
A study of small iron clusters on Cu(111) by atomic force microscopy <u>Franz J. Giessibl</u>	83
Molecular nanostructures on metals vs. graphene Brian Baker, Mihaela Enache, Stefano Gottardi, Remco W. A. Havenith, Anna K. H. Hirsch, Jun Li, Leticia Monjas, Juan Carlos Moreno Lopez, Nico Schmidt, <u>Meike Stöhr</u>	84
Structural changes of buckybowl via selective on-surface hydrogenation Christian Wäckerlin, Aurelio Gallardo, Anaïs Mairena, <u>Milos Baljovic</u> , Aleš Cahlík, Pavel Jelínek, Karl-Heinz Ernst	86
Low-energy stereodynamics in merged beams <u>Andreas Osterwalder</u>	87
Vibrational energy pooling studied by mid-infrared laser induced fluorescence with a superconducting nanowire single photon detector <u>Alec M. Wodtke</u>	88
Single-molecule motion at surfaces <u>Leonhard Grill</u>	89
Quantum non-demolition state detection and spectroscopy of single trapped molecules <u>Mudit Sinhal</u> , Ziv Meir, Aleksandr Shlykov, Stefan Willitsch	90

Nucleophilic substitution and ligand exchange dynamics in bimolecular collisions with microhydrated anions	92
<u>Björn Bastian</u> , Tim Michaelson, Jennifer Meyer, Atilay Ayasli, Roland Wester	
Reaction kinetics of trapped molecular ions with conformer- and isomer-selected neutral molecules	93
<u>Ardita Kilaj</u> , Hong Gao, Daniel Rösch, Uxia Rivero, Jochen Küpper, Stefan Willitsch	
Photochemistry and spectroscopy of molecules at surfaces: Insights from ab initio molecular dynamics	94
M. Alducin, G. Floss, G. Füchsel, J.I. Juaristi, S. Lindner, I. Lončarić, G. Melani, Y. Nagata, R. Scholz, E. Titov, <u>Peter Saalfrank</u>	
Quantum mechanics for intramolecular reactions and conformational space exploration of organic molecules on metallic surfaces	95
<u>Mariana Rossi</u>	
Simultaneous detection of polycyclic aromatic hydrocarbons and inorganic ions in on-line single aerosol particle laser mass spectrometry using molecular as well as atomic resonances	96
<u>R. Zimmermann</u> , J. Passig, J. Schade, R. Irsig, S. Ehlert, M. Sklorz, T. Adam, C. Li, Y. Rudich	
Precision tests of nuclear spin symmetry and parity conservation in polyatomic molecules	100
Eduard Miloglyadov, <u>Martin Quack</u> , Georg Seyfang, Gunther Wichmann	
Electron-induced processes in novel dielectric gases	104
<u>Juraj Fedor</u>	
Unravelling isomers of reactive ionic intermediates	105
<u>Sandra Brünken</u>	
Combining ultrahigh-resolution ion mobility with cryogenic ion vibrational spectroscopy for the analysis of glycans	107
Stephan Warnke, Ahmed Ben Faleh, Ali Abi Khodr, Priyanka Bansal, Eduardo Carrascosa, Irina Dyukova, Robert P. Pellegrinelli, Natalia Yalovenko, Vasy Yatsyna, Lei Yue, <u>Thomas R. Rizzo</u>	
Gas-phase dications: Creation, coincidences, charges and chemistry	108
<u>Lilian Ellis-Gibbings</u> , Sam Armenta Butt, Eleanor Smith, Will Fortune, Stephen D. Price	
Recent advancements in surface science instrumentation	110
Markus Maier, <u>Eleni Anargirou</u>	
ZnO: Ultrafast generation and decay of a surface metal	111
Lukas Gierster, Sesha Vempati, <u>Julia Stähler</u>	
Nanoscale insights into surface electrochemistry - Au oxidation revisited	112
Jonas H.K. Pfisterer, Masoud Baghernejad, Giovanni Giuzio, Ulmas Zhumaev, Manuel Breiner, Juan M. Feliu, <u>Katrin F. Domke</u>	

Molecules in interaction with nanoparticles grown on alumina film : the benefits of combined SFG spectroscopy and STM microscopy Natalia Alyabyeva, A. Ghalgaoui, Aimeric Ouvrard, Serge Carrez, Wanquan Zheng, <u>Bernard Bourguignon</u>	113
Thiolate-protected metal clusters: Chirality and dynamic nature <u>Thomas Bürgi</u>	114
Spin excitations and interactions on superconductors – probed and manipulated by scanning tunneling microscopy Michael Ruby, Benjamin W. Heinrich, Yang Peng, Felix von Oppen, <u>Katharina Franke</u>	115
Carbon nanoconduits: 2D materials for water purification and osmosis <u>Armin Götzhäuser</u>	116
Interstellar organic molecules and (anti-)masers <u>Alexandre Faure</u> , François Lique, Antony J. Remijan, Brett A. McGuire	117
Electroreduction of water and CO₂: competition or synergism on Mo₂C film electrodes? Eva-Maria Wernig, Daniel Winkler, Christoph Griesser, Niuscha Shakibi Nia, <u>Julia Kunze-Liebhäuser</u>	119
Neutralization dynamics of highly charged ions in 2D materials <u>Friedrich Aumayr</u>	120
Small chiral molecules: Progress in synthesis and beyond <u>Jürgen Stohner</u>	123
Ion-molecule reactions below 1 K V. Zhelyazkova, F. B. V. Martins, M. Zesko, K. Höveler, J. Deiglmayr, <u>F. Merkt</u>	125



Instruments for Advanced Science

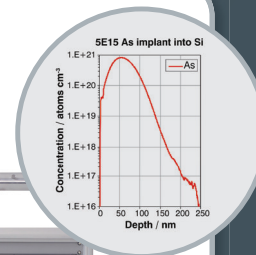
Residual Gas Analysis

- ▶ RGA at UHV/XHV
- ▶ High pressure RGA
- ▶ Molecular beams
- ▶ High mass RGA
- ▶ Temperature programmed desorption
- ▶ Electron/photon stimulated desorption



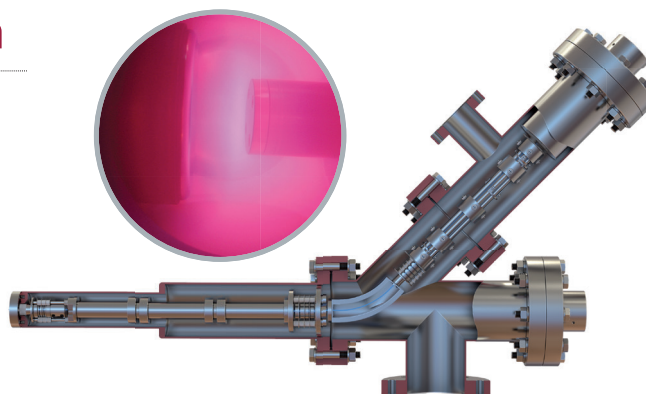
Thin Film Surface Analysis

- ▶ Static and dynamic SIMS
- ▶ Chemical composition & depth profiling
- ▶ SIMS for FIB including bolt-on modules & integrated SIMS-on-a-Flange
- ▶ Choice of primary ions
- ▶ Complete SIMS workstations



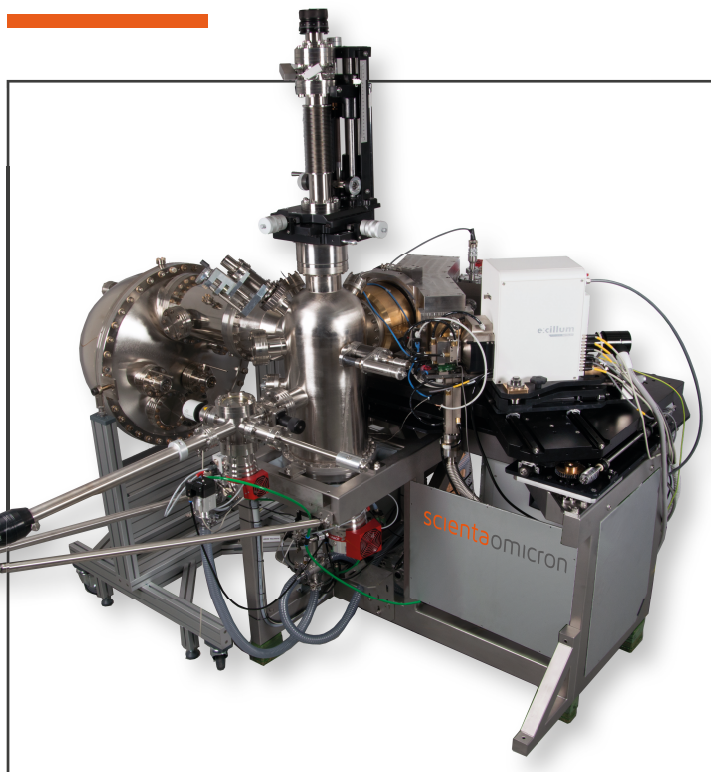
Plasma Characterization

- ▶ EQP ion mass and energy analyzer
- ▶ RF, DC, ECR and pulsed plasma
- ▶ Neutrals and neutral radicals
- ▶ Time resolved analysis
- ▶ HPR-60 extends analyses to atmospheric pressure processes



HAXPES Lab

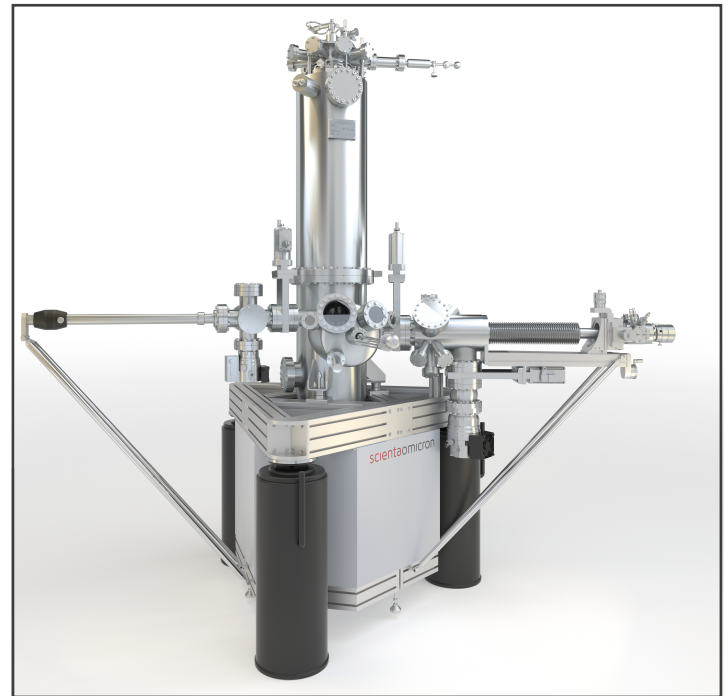
A window to the bulk



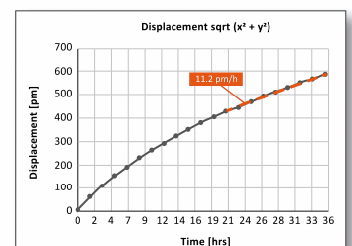
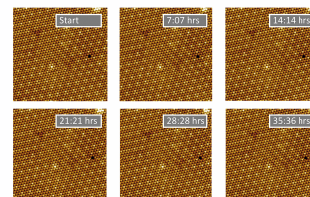
- Robust laboratory based HAXPES solution
- Time scales comparable to synchrotron experiments
- Five times higher information depth than AlK α X-Rays
- High flux monochromated Hard X-rays at 9.25 keV
- Access to deep core levels
- Non-destructive measurements of buried interfaces
- Bulk sensitive photoemission spectroscopy

TESLA JT SPM

Low temperatures & variable magnetic fields



- > 5 days uninterrupted measurement time in varying magnetic fields with only 11 L LHe
- Temperatures down to 1 K with 4He
- Ultra low thermal drift
- Magnetic fields $B_Z > 3$ T
- Optical access
- STM and QPlus AFM



Exceptionally low thermal drift at T=1 K. 36 hours total acquisition time showing a thermal drift stabilising at 11.2 pm/h.

For further questions please contact us:
info@scientaomicron.com

CONTRIBUTIONS

"Molecular Switches and Motors at Interfaces"

Ben L. Feringa

Stratingh Institute for Chemistry, University of Groningen

Nijenborgh 4, 9747 AG Groningen, The Netherlands

b.l.feringa@rug.nl

Summary. The fascinating molecular motors and machines that sustain life offer a great source of inspiration to the molecular explorer at the nanoscale. Among the major challenges ahead in the design of complex artificial molecular systems is the control over dynamic functions and responsive far-from-equilibrium behaviour. Chemical systems ultimately require integration of structure, organization and function of multi-component dynamic molecular assemblies at different hierarchical levels. A major goal is to achieve and exploit translational and rotary motion at different length scales and at interfaces.

In this presentation the focus is on the assembly, organization and dynamics of responsive molecular systems with a focus on interface phenomena. We design switches and motors in which molecular motion is coupled to specific functions. Responsive behaviour will be illustrated in self-assembly, at interfaces and in 2d and 3D confined space. The design, synthesis and functioning of rotary molecular motors and machines will also be presented with a prospect toward future dynamic molecular systems

Information on <http://www.benferinga.com>

Strong-field physics in the molecular frame and the recording of the molecular movie

Jochen Küpper

Center for Free-Electron Laser Science, Deutsches Elektronen-Synchrotron DESY, Hamburg, Germany

Department of Physics, Universität Hamburg, Hamburg, Germany

Department of Chemistry, Universität Hamburg, Hamburg, Germany

Center for Ultrafast Imaging, Universität Hamburg, Hamburg, Germany

Email: jochen.kuepper@cfel.de,

Observing molecules in action through the recording of “molecular movies”, i. e., their spatiotemporal evolution during chemical dynamics, at atomic spatial and temporal resolution could revolutionize our understanding of the molecular sciences. I’ll outline approaches to prepare highly controlled samples that enable advanced imaging methods of individual molecular species and directly in the molecular frame and discuss their application in a self-imaging approach to record such movies with few-picometer and few-femtosecond resolution. This so-called laser-induced electron diffraction is based on the interaction of strong laser fields with matter, which intrinsically provides powerful tools to image transient dynamics with an extremely high spatiotemporal resolution.

Besides the presentation of first images, I will discuss some important aspects of the corresponding electron-dynamics in the molecular frame: In strong-field physics, the initial conditions of the laser-molecule interaction are generally considered a weak perturbation. We investigated strong-field ionization of state-selected and strongly laser-aligned molecules and unraveled a full real-time picture of the photoelectron dynamics in the presence of the laser field and the molecular interaction. We demonstrated that the molecular potential defines the initial conditions of the photoelectron at birth and has a dramatic impact on the overall strong-field recollision dynamics. This result represents a new benchmark for the seminal statements of molecular-frame strong-field physics. Our findings have strong impact on the interpretation of self-diffraction experiments, where the photoelectron momentum distribution is used to retrieve molecular structures. Furthermore, the resulting encoding of the time-energy relation in molecular-frame photoelectron distributions shows the way of accessing a deeper understanding of electron transport during strong-field interactions and probing the molecular potential in real-time.

Insulin and other proteins at interfaces – from amyloidosis to fabric stains

Jamaica-Marie Bucag, Xinyang Li, Alice Mason, Jack Quayle, Heike Arnolds

*Department of Chemistry, University of Liverpool, Crown Street, Liverpool L9 7ZD, UK
(corresponding author: Heike Arnolds, e-mail: Heike.Arnolds@liverpool.ac.uk)*

Human Insulin is a relatively small peptide (51 amino acids) which plays a major role in controlling glycemia in the human body. It is also a model protein for understanding protein unfolding and aggregation into fibril-like structures called amyloid which are the hallmark of many degenerative diseases such as diabetes, Alzheimer's and Parkinson's, but also occur during purification, storage and delivery of protein-based drugs.

Amyloids are frequently formed at interfaces, ranging from cell membranes to syringes, in particular if those interfaces are hydrophobic. The main driver for adsorption at hydrophobic interfaces is the entropy gain from excluding water at the interface. The handwaving explanation of why proteins unfold suggests that this adsorption makes it more favourable for hydrophobic amino acid side chains that are normally buried inside the protein structure to attach to the surface which causes unfolding.

Using a range of vibrational spectroscopies, we made the surprising discovery that hydrophobic interfaces can actually stabilise the native structure of insulin at both air-water and water-solid interfaces [1,2] and that unfolding only occurs well above room temperature. We suggested that the interface inhibits fibril formation because it protects the aggregation-prone hydrophobic domains on the insulin monomer by adsorption on the hydrophobic surface. We have since found that this stabilisation of the native structure occurs on a large variety of interfaces, ranging from model functionalised silicon wafers, to porous functionalised silica beads used in reverse phase liquid chromatography and fabrics such as cotton and polyester.

In this talk I focus on how this protection mechanism depends on the precise chemical nature of the interface (hydrophobicity, aromaticity, charge) and whether we can use surface chemistry to control protein aggregation at interfaces.

- [1] S. Mauri, T. Weidner, H. Arnolds, "The structure of insulin at the air/water interfaces: monomers or dimers?" *Phys. Chem. Chem. Phys.* 16 (2014) 26722
- [2] S. Mauri, M. Volk, S. Byard, H. Berchtold, H. Arnolds, "Stabilization of Insulin by Adsorption on a Hydrophobic Silane Self- Assembled Monolayer" *Langmuir* 2015, 31, 8892

On-surface synthesis of low-dimensional carbon-based nanostructures

Sabine Maier

*Friedrich-Alexander-Universität Erlangen-Nürnberg, Department of Physics,
91052 Erlangen, Germany*

(corresponding author: S. Maier, e-mail: sabine.maier@fau.de)

2D porous molecular networks have become subject of intense interest because the surface-confined pores in the networks can accommodate guest molecules and tune the electronic band structure of the carbon-based networks. Hence, porous carbon-based networks are exiting materials for prospective applications in nanoscale electronics, sensor and energy storage devices, and other fields. The stability and intermolecular charge transport are significantly improved in covalent molecular 2D networks compared to traditional non-covalent self-assemblies. However, the fabrication of covalent networks via on-surface synthesis often lacks structural control owing to the irreversible nature of the newly formed covalent bonds.

In my presentation, I will focus on recent high-resolution scanning probe microscopy experiments in combination with density-functional theory about the bottom-up fabrication and electronic properties of atomically precise one- and two-dimensional covalent molecular nanostructures.[1-5] The influence of the symmetry of the precursor molecules, as well as the templating effect of adsorbed Br and metal adatoms on the structure formation of covalently-linked molecular structures, will be discussed. In particular, it will be outlined how well-ordered nanoporous 1D and 2D covalent molecular structures can be fabricated.

Support by the German Science Foundation (DFG) and the ERC Starting Grant SURFLINK (contract No. 637831) is gratefully acknowledged.

- [1] C. Steiner et al. Nature Communications 2017, 8, 14765.
- [2] M. Ammon, T. Sander, S. Maier, J. Am. Chem. Soc., 2017 139 (37), 12976–12984.
- [3] Z. Yang et al. Nanoscale, 2018, 10, 3769-3776.
- [4] M. Ammon et al. ChemPhysChem, 2019, doi:10.1002/cphc.201900347.
- [5] X. Zhang et al., ACS Nano, 2019, 13 (2), 1385–1393.

Nitrophobia of size selected iron clusters under cryo isolation

A. Steiner¹, S. Dillinger¹, Jennifer Mohrbach¹, Christopher Wiehn¹,
M. P. Klein¹, D. V. Fries¹, P. B. Armentrout², and G. Niedner-Schatteburg¹

¹*Fachbereich Chemie and Forschungszentrum OPTIMAS, Technische Universität
Kaiserslautern, 67663 Kaiserslautern, Germany*

²*Department of Chemistry, University of Utah, Salt Lake City, Utah 84112, USA*

We strive to characterize the adsorption and activation of N₂ by isolated transition metal cluster surfaces under cryo conditions. We utilize tandem cryo ion trapping in conjunction with Fourier Transform Ion Cyclotron Resonance Mass Spectrometry (FT-ICR MS). Our setup combines a RF hexapole cryo ion trap for kinetic studies with a consecutive cryo FT-ICR cell for IR-photo dissociation studies and for mass analysis. Both ion traps are cryogenically cooled to temperatures below 11 K. With this tandem cryo trap instrument we have investigated before the N₂ adsorption on Co_n⁺, Ni_n⁺, Rh_n⁺ [1-5] and the co-adsorption of N₂ and H₂ on Ru₈⁺ [6].

In continuation of this previous work, we conduct a long term investigation of N₂ adsorption on Fe_n⁺ clusters. From the recorded kinetics, we deduce otherwise unpredictable cluster size effects, such as e.g. a very slow N₂ adsorption on Fe₁₇⁺, and an isomerism of the Fe₁₈⁺ cluster. The deduced N₂ uptake limits are in line with icosahedral cluster structures, except for the clusters Fe₁₄₋₁₇⁺ which are somewhat reluctant to take up N₂.

Gas phase IR spectra of isolated Fe_n(N₂)_m⁺ cluster adsorbate complexes help to elucidate. They reveal complex spectral variations by (n,m). Varying numbers of IR active N₂ stretching bands reveal varying red shifts with respect to the IR inactive stretching mode of free N₂ (2330 cm⁻¹). We compare in detail the stepwise nitrogen adsorption by the “normal” Fe₁₃⁺ cluster with that of the “nitrophobic” Fe₁₇⁺ cluster. Exploratory DFT studies support our quest for cluster morphologies and for N₂ activities on the Fe_n⁺ cluster surfaces.

Our studies receive support from the DFG in the framework of the transregional collaborative research center 3MET.de

- [1] S. Dillinger, J. Mohrbach, J. Hower, M. Gaffga, G. Niedner-Schatteburg, *Phys. Chem. Chem. Phys.* **17** 10358 (2015).
- [2] J. Mohrbach, S. Dillinger, G. Niedner-Schatteburg, *J. Phys. Chem. C* **121**, 10907 (2017).
- [3] J. Mohrbach, S. Dillinger, G. Niedner-Schatteburg, *J. Chem. Phys.* **147**, 184304 (2017).
- [4] S. Dillinger, J. Mohrbach, G. Niedner-Schatteburg, *J. Chem. Phys.* **147**, 184305 (2017).
- [5] M. P. Klein, A. A. Ehrhard, J. Mohrbach, S. Dillinger, G. Niedner-Schatteburg, *Top. Catal.* **61**, 106 (2018).
- [6] S. Dillinger, M. P. Klein, A. Steiner, D. C. McDonald, M. A. Duncan, M. M. Kappes, G. Niedner-Schatteburg, *J. Phys. Chem. Lett.* **9**, 914 (2018).

Methane Chemisorption on Stepped Ni and Pt Surfaces Studied by Vibrational Spectroscopy

Rainer D. Beck

Ecole Polytechnique Fédérale de Lausanne

CH-1015 Lausanne, Switzerland

rainer.beck@epfl.ch

Methane dissociation is the rate limiting step in the steam reforming process used by the chemical industry to convert natural gas into a mixture of H₂ and CO known as synthesis gas. To better understand the microscopic mechanism and reaction dynamics of methane chemisorption, we use vibrational spectroscopies and infrared lasers for quantum state-resolved studies of methane dissociation and state-to-state scattering on Ni and Pt surfaces [1]. Our experiments prepare surface incident methane molecules in specific ro-vibrational quantum states by state-selective infrared laser excitation via rapid adiabatic passage in a molecular beam. The state prepared molecules then collide with a clean single crystal transition metal surface in ultrahigh vacuum and both reactive and non-reactive processes are monitored by infrared spectroscopic techniques.

Surface bound methyl species as products of the dissociative chemisorption of methane are detected on the platinum surface by Reflection Absorption Infrared Spectroscopy (RAIRS). RAIRS allows for real-time and in-situ monitoring of the uptake of chemisorbed methyl species enabling quantum state-resolved measurements of reactive sticking coefficients. RAIRS is also used to study the vibrationally bond selective dissociation of partially deuterated methane demonstrating that a single quantum of C-H stretch excitation of the incident methane is sufficient to achieve bond-selective chemisorption. Furthermore, RAIRS allows for site specific detection of reaction products used to measure separately the dissociation probability of methane on steps, terraces, and kink sites on Pt(211) and Pt(210) [2-4].

Our state-resolved experiments provide clear evidence for mode- and bond-specificity as well as steric effects in chemisorption reactions and show that methane dissociation cannot be described by statistical rate theory but requires a dynamical treatment including all internal vibrational and rotational degrees of freedom of the dissociating molecule. The detailed reactivity and state-to-state scattering data from our measurements are used as stringent tests in the development of a predictive understanding by first principles theory [5-6] of these industrially important gas/surface reactions.

References

- [1] H.J. Chadwick and R.D. Beck, *Chem. Soc. Rev.* **2016**, 45, 3576-3594.
- [2] H.J. Chadwick, H. Guo, A. Gutiérrez Gonzáles; J.P. Menzel, B. Jackson, and R.D. Beck, *J. Chem. Phys.* **2018**, 148, 1470.
- [3] A. Gutiérrez Gonzáles, F.F. Crim, R.D. Beck, *J. Chem. Phys.* **2018**, 149, 74701.
- [4] H.J. Chadwick, A. Gutiérrez Gonzáles, R.D. Beck, and G-J. Kroes, *J. Phys. Chem. C.* **2019**, 123, 14530-14539.
- [5] P.M. Hundt, B. Jiang, M.E. Van Reijzen, H. Guo, and R.D. Beck, *Science*, **2014**, 344, 504.
- [6] P.M. Hundt, M.E. Van Reijzen, R.D. Beck, H. Guo, and B. Jackson, *J. Chem Phys.*, **2017**, 146, 54701.

Vibrations and dielectric properties at perovskite surfaces

Florian O. Schumann, Krassimir L. Kostov¹, Veronica Goian², Jonas Pantzer, Wolf Widdra

Institute of Physics, Martin-Luther-Universität Halle-Wittenberg, Halle, Germany
(corresponding author: W. Widdra, e-mail: wolf.widdra@physik.uni-halle.de)

¹ *Institute of General and Inorganic Chemistry, Bulgarian Academy of Sciences, 1113 Sofia, Bulgaria*

² *Institute of Physics, Czech Academy of Sciences, 182 21 Prague, Czech Republic*

Vibrations, either localized as within molecules or delocalized as in lattice vibrations and surface phonons, are fundamental low-energy excitations that are typically excited at room temperature. For ionic crystals, optical phonons couple with electromagnetic waves to the so-called phonon-polaritons as new quasiparticles. The latter are central for the dielectric properties of the host material.

In this presentation, the vibrational properties of ultrathin oxide films and oxide surfaces in the range from 1 to 50 THz (4 - 200 meV) will be discussed. Surface vibrational spectroscopy based on high-resolution electron energy loss spectroscopy (HREELS) reveals the quantitative surface response with respect to surface phonons, surface plasmons, and their corresponding phonon-polaritons and plasmon-polaritons. For the binary oxide BaO grown epitaxially on Pt(001), we find fully unstrained BaO(001) ultrathin films due to an ideal matching of oxide and substrate lattice constants [1]. Thickness-dependent HREEL spectra exhibit surface phonon-polariton shifts which will be compared with the known response for strained oxide films in the case of NiO(001) [2]. For the perovskite SrTiO₃(001) and BaTiO₃(001) surfaces, three surface phonon-polariton modes are present that are fully describable by the surface-mediated coupling between bulk-like phonons and surface electromagnetic waves [3].

For doped oxides, the electron-phonon coupling turns out to be important and might even lead to superconductivity. The electron-phonon coupling at perovskite surfaces will be discussed for homogeneously doped SrTiO₃(001) crystals and for SrTiO₃(001) samples, which form a two-dimensional electron gas at the surface [4].

Support by the Sonderforschungsbereich SFB-762 “Functional oxide interfaces” is gratefully acknowledged.

- [1] V. Goian, F. O. Schumann, and W. Widdra, *Journal of Physics: Condensed Matter* **30**, 095001(2018).
- [2] K. L. Kostov, F. O. Schumann, S. Polzin, D. Sander, and W. Widdra, *Phys. Rev. B* **94**, 075438(2016).
- [3] J. Premper, F. O. Schumann, A. Dhaka, S. Polzin, K. L. Kostov, V. Goian, D. Sander, and W. Widdra, *phys. stat. sol.* (submitted).
- [4] A. F. Santander-Syro et al., *Nature* **469**, 189-93(2011).

Ionic Liquid Adsorption and Ion Exchange Processes at Single Crystal Surfaces

Hans-Peter Steinrück

Lehrstuhl für Physikalische Chemie II, Friedrich-Alexander-Universität Erlangen-Nürnberg,
Egerlandstr. 3, 91058 Erlangen, Germany

Thin films of ionic liquids (ILs) have been in the focus of ultra-high vacuum (UHV) surface science in the past ten years as they provide a powerful route for molecular level studies of liquid/solid interfaces in general. The detailed knowledge of the structure and the formation of the IL/solid interface enables a more complete description and control of the interface properties and the system's overall stability and performance in applications where ILs are in contact with solid surfaces, such as catalysis. In this contribution, we summarize recent results on ultrathin IL films, which have been prepared by *in situ* physical vapor deposition. We particularly concentrate on processes that occur in mixtures of two different ILs, which were successively deposited on Ag(111) as model support. By temperature-dependent angle-resolved X-ray photoelectron spectroscopy, we found pronounced surface and interface enrichment effects due to rapid ion exchange processes. We propose that the phenomena observed in these films are driven by the interplay of interface adsorption energy at the liquid/solid interface and the surface free energy at the liquid/vacuum interface.

Supported by the European Research Council (ERC) through an Advanced Investigator Grant to HPS (No. 693398-ILID).

Kinetics and Dynamics of CO Oxidation on atomically stepped Pd Surfaces

Dmitry Borodin¹, Michael Schwarzer¹, Jannis Neugebohren¹, Barratt G. Park¹, Alec M. Wodtke¹ and Theofanis. N. Kitsopoulos^{1,2}

*Max Planck Institute for Biophysical Chemistry, 37073 Göttingen, Germany
(corresponding author: T.N. Kitsopoulos, e-mail: tkitsop@mpibpc.mpg.de)*

¹*Georg August University, 37073 Göttingen, Germany*

²*University of Crete, 71110 Heraklion, Greece*

Our new experimental approach, velocity resolved kinetics, combines surface science techniques, such as ultra-high-vacuum and single crystal surfaces, with slice imaging [1] of reaction products to measure the reaction dynamics and kinetics of catalytic reactions at surfaces simultaneously. A well-chosen arrangement of the ion imaging detector [2] offers a straightforward way to map out the in-plane velocity distribution, while velocity-resolved kinetics (product flux as a function of reaction time) is measured in a Pump-Probe type experiment. With this approach, we have recently determined the site-specific oxidation mechanism for CO on platinum surfaces, which could explain the results of 40 years of research on this system [3]. In this work we investigate the kinetics and dynamics of CO

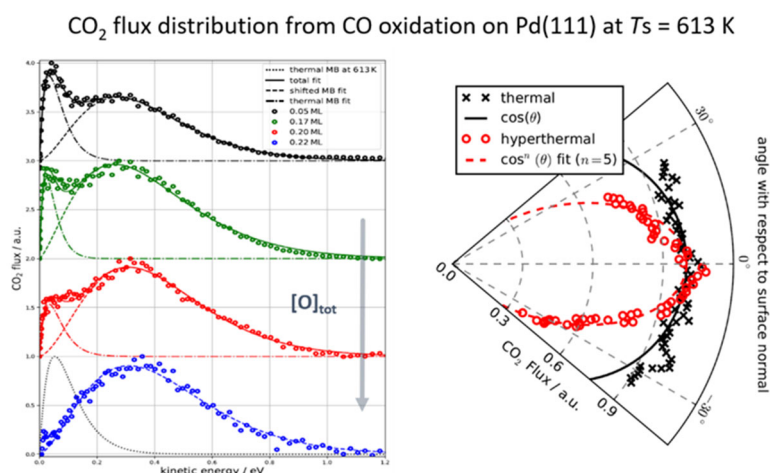


Figure 1 Speed and angular distributions of CO₂ products from the oxidation of CO on Pd(111)

oxidation on Pd(111), which show similarities but marked differences from Pt(111). CO₂ shows two distinct channels: a hyperthermal CO₂ formed on terraces, showing large translational energies and an angular distribution peaked along the surface normal; a thermal CO₂ channel formed at atomic steps of the crystal and has thermal speed distributions with cos(θ)-angular distributions. We show that the combination of reaction dynamics and kinetics

can determine and quantify the underlying kinetic mechanism even though the adsorbates are exchanging between the active sites.

Support by the European Research Council (grant agreement No. [833404]) is gratefully acknowledged.

[1] C. Gebhardt et al. *Rev. Sci. Instrum.* **72**, 3848, (2001).

[2] D. Harding et al. *J. Chem. Phys.* **147**, 013939, (2017).

[3] J. Neugeboren et al. *Nature* **558**, 280, (2018).

Vibrational spectroscopy and non-equilibrium dynamics at aqueous metal oxide interfaces

Giacomo Melani^{1,4}, Yuki Nagata², R. Kramer Campen³, Peter Saalfrank¹

¹*Institut für Chemie, Universität Potsdam, Karl-Liebknecht-Strasse 24/25,
D-14476 Potsdam-Golm, Germany*

²*Max-Planck-Institut für Polymerforschung, Ackermannweg 10, 55128 Mainz, Germany*

³*Fritz-Haber-Institut der Max-Planck-Gesellschaft, Faradayweg 4-6, D-14195 Berlin, Germany*

⁴*Institut für Chemie, Universität Zürich, Winterthurerstrasse 190, 8057 Zürich, Switzerland
(corresponding author: G. Melani, e-mail: giacomo.melani@chem.uzh.ch)*

Atomistic description of water adsorption on metal oxide surfaces like $\alpha\text{-Al}_2\text{O}_3$ is of crucial importance for many research areas, from geochemistry to heterogeneous catalysis [1]. In particular, water can adsorb molecularly or dissociatively onto different sites of metal oxide surfaces [2]. These adsorption sites can be disentangled using surface-sensitive vibrational spectroscopy, as Vibrational Sum Frequency (VSF) generation [3]. The spectroscopic assignment is often corroborated by theoretical calculation of vibrational frequencies, which, in many cases is limited to static Normal Mode Analysis (NMA). To go beyond this approach, classical time-correlation functions [4] obtained from Ab Initio Molecular Dynamics are the perfect tools to include anharmonicity, line broadening, surface thermal motion and spectroscopic selection rules.

Here, using an efficient scheme based on velocity-velocity autocorrelation functions from DFT-based AIMD trajectories [5], we report vibrational signatures of water on $\alpha\text{-Al}_2\text{O}_3(0001)$ surface: from Vibrational Density Of States (VDOS) curves, to InfraRed (IR) and VSF spectra. We consider two representative cases for low and medium coverage regimes: first, describing deuterated water dissociative adsorption on the thermodynamically most stable Al-terminated surface [6] and then simulating a reconstructed, O-terminated hydroxylated surface, with or without additional water. While the first example allows for analysis of dissociated OD species at sub-monolayer coverages and comparison with experimental VSF spectra in UHV, the second corresponds to a stable situation in environmental conditions, towards the description of a solid / liquid interface [7]. For the hydroxylated surface model, we highlight high-frequency vibrations of interfacial OH bonds, disentangling their spectral features in terms of their local hydrogen bonding environment and their average orientation. Both cases are directly tested against previous experiments [2, 8, 9] with an overall good agreement.

While sampling of equilibrium trajectories provides information about vibrational frequencies and spectra, a non-equilibrium picture is required to describe adsorbate-surface couplings and

energy transfer at the interface. Together with pump-probe VSF experiments, non-equilibrium AIMD simulations are employed considering a water-covered hydroxylated (0001) surface model. Our aim is to reproduce the dynamics of vibrationally excited OH bonds and to follow their behaviour upon IR-light absorption. The corresponding trajectories are then analyzed either by looking at the kinetic energy decay of selected OH bonds or by calculating transient VDOS spectra, in order to extract vibrational lifetimes which are also determined experimentally. Overall, we find that interfacial OH groups with stretching frequencies above 3700 cm^{-1} decay with a timescale between 2 and 4 ps. This observation is in good agreement with experiments, especially for vibrational lifetimes obtained for the air/ α -alumina and the liquid/ α -alumina interfaces. Moreover, we can also dissect pathways for vibrational energy redistribution, where the adsorbed water layer and hydrogen-bonded surface OH groups play the most prominent role.

References

- [1] Olle Björneholm et al, *Chem. Rev.*, 116(13):7698, 2016.
- [2] Harald Kirsch et al, *J. Phys. Chem. C*, 118(25):13623, 2014.
- [3] Paul A. Covert et al, *Ann. Rev. Phys. Chem.*, 67(1):233, 2016.
- [4] B. J. Berne et al, *Adv. Chem. Phys.*, 27:64, 1970.
- [5] Tatsuhiko Ohto et al, *J. Chem. Phys.*, 143(12):124702, 2015.
- [6] Giacomo Melani et al, *J. Chem. Phys.*, 150, 244701, 2019.
- [7] Giacomo Melani et al, *J. Chem. Phys.*, 149, 014707, 2018.
- [8] Luning Zhang et al, *J. Am. Chem. Soc.*, 130(24):7686, 2008.
- [9] Yujin Tong et al, *J. Chem. Phys.*, 144(12):054704, 2015.

Highly Charged Helium Nanodroplets: a Cool Tool for Well-Defined Cluster Formation

Felix Laimer,¹ Lorenz Kranabetter,¹ Lukas Tiefenthaler,¹ Simon Albertini,¹ Fabio Zappa,^{1,2} Andrew M. Ellis,³ Michael Gatchell,^{1,4} and Paul Scheier¹

¹*Institut für Ionenphysik und Angewandte Physik, Universität Innsbruck, Technikerstr. 25, A-6020 Innsbruck, Austria*

(corresponding author: Lukas Tiefenthaler, e-mail: Lukas.tiefenthaler@uibk.ac.at)

²*Departamento de Física-ICE, Universidade Federal de Juiz de Fora, Campus Universitário, 36036-900, Juiz de Fora, MG, Brazil*

³*Department of Chemistry, University of Leicester, University Road, Leicester, LE1 7RH, United Kingdom*

⁴*Department of Physics, Stockholm University, 106 91 Stockholm, Sweden*

Super fluid helium nanodroplets (HNDs) are frequently used in experiments as super cold matrices for the analysis of molecules and atoms [1]. In recent experiments, we discovered and studied stable, highly charged HNDs [2].

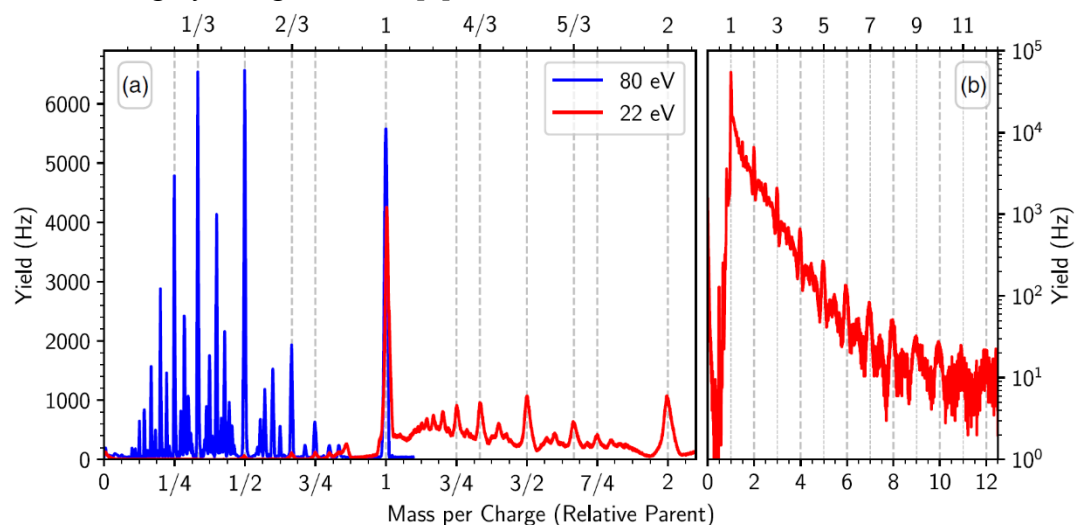


Figure 1: Mass per charge selected HNDs containing about 4 million He atoms per charge (relative parent = 1) are ionized a second time. blue: positively charged precursor droplets are further ionized which leads to narrow peaks at integer fractions smaller than one; red: positively charged precursor droplets are neutralized producing signal at integer fractions above one [2].

The HNDs are produced in a free jet expansion through a 5 μm nozzle at temperatures as low as 4.2 K and pressures between 20 bar and 25 bar. Electron bombardment in a Nier-type, electron impact ion source leads to high charge states utilizing high electron currents. The large geometric cross section of HNDs with a diameter of up to several μm and their low velocity of about 150 to 250 m/s when passing the electron beam leads to multiple electron collisions. The droplets are mass-per-charge selected by a spherical electrostatic sector. The HNDs are then ionized again in a second, identical ion source before passing through another mass per charge filter. Charged droplets are finally detected by a channel electron multiplier.

Using this setup, the second ion source can be used to increase the charge state of the ionized droplets (decrease of the mass per charge ratio, blue line in figure 1) or reduce it (increase of mass per charge ratio, red line in figure 1). This way we can safely assume, that the highly charged droplets formed in the first ion source, are indeed stable in the microsecond time scale. Droplets with up to 55 charges are found and the appearance size of highly-charged HNDs is measured as a function of their charge state. Excess energy deposited by the ionization events into the HNDs as well as Coulomb explosion for highly-charged droplets below their critical size leads to the ejection 1600 He atoms per eV vibrational energy and of small charged clusters with sizes with no more than a few percent of the droplet mass, respectively. According to our results, symmetric Coulomb explosion can be ruled out. Coulomb repulsion between the charge centers leads to minimum energy configurations where the charges are located close to the surface of the droplet forming a two-dimensional Wigner crystal.

Pickup of dopants into highly-charged HNDs leads to a homogeneous breeding of charged dopant clusters or nanoparticles with the charge centers acting as seeds for the cluster growth. Deposition of highly-charged HNDs doped with gold atoms onto a transmission electron microscopy (TEM) grid leads to stable patterns of nanoparticles that can be visualized in a TEM. Under extreme conditions (4.25K, 20bar and intense ionization) droplets with an average size of $> 10^{10}$ He [3] atoms can be deflected by sector field with a mass per charge ratio of 10^7 He atoms per charge. More than thousand charge centers in these HNDs lead to equally many charged gold nanoparticles that can cover homogeneously a TEM grid within seconds with more than 50 nanoparticles per μm^2 .

We designed a new instrument where we combine a source for highly-charged HNDs with a mass spectrometer system (see Figure 1) with the aim to produce intense beams of mass selected cluster ions.

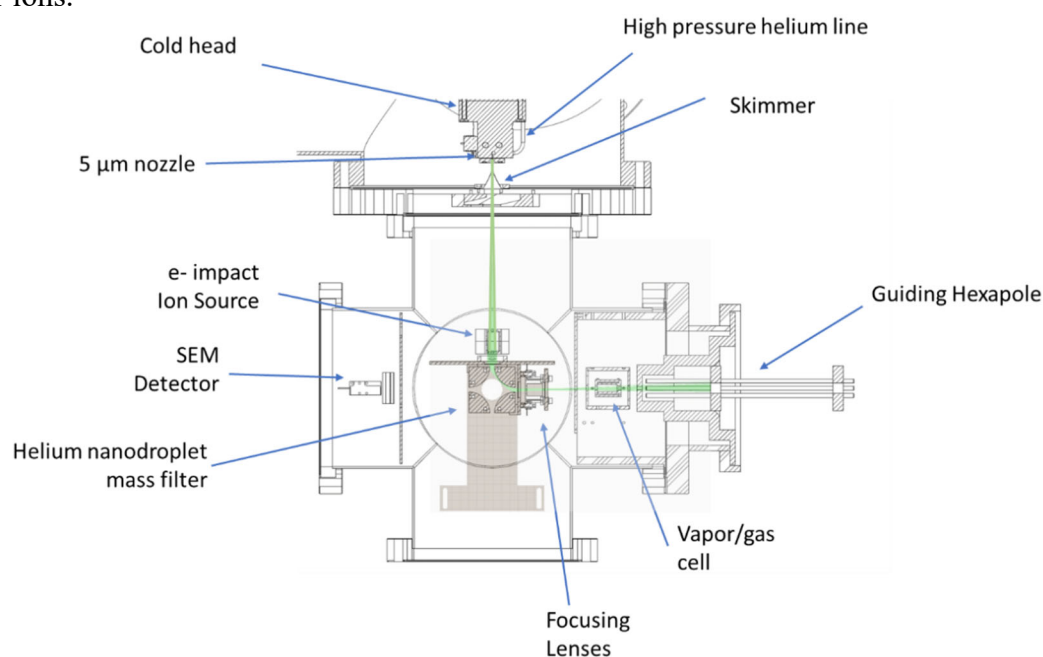


Figure 2: Schematic of the newly designed instrument that utilizes highly charged HNDs to produce intense beams of charged cluster ions. The green lines are simulated trajectories of HNDs

In order to liberate the dopant cluster ions from the large HNDs, multiple collisions with room temperature He in a RF-hexapole is used. By this method much higher cluster ion yields can be achieved than by using a conventional, neutral pickup source. The size distribution of the sample clusters produced is also found to be much narrower than in neutral pickup experiments. Furthermore, the center of the sample cluster size distribution can be varied by choosing different mass per charge ratios of the HNDs. The pickup with charged HNDs also has other benefits like ultra-cold cluster ions as well as very efficient helium tagging of the charged dopant clusters. The latter is especially interesting for messenger type spectroscopy.

Acknowledgement

This work was supported by the EU commission, EFRE K-Regio FAENOMENAL EFRE 2016-4, the Austrian Science Fund FWF (P31149 and W1259) and the Swedish Research Council (Contract No. 2016-06625). F. Z. acknowledges support from Brazilian agency CNPq

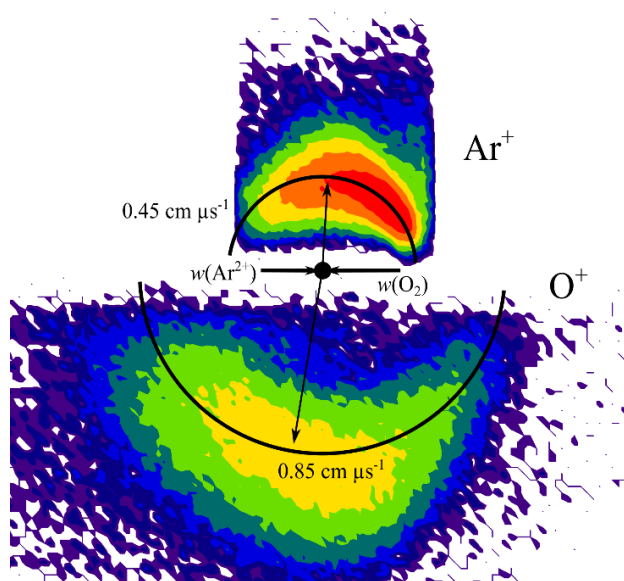
References

- [1] A. Mauracher, O. Echt, A.M. Ellis, S. Yang, D.K. Bohme, J. Postler, A. Kaiser, S. Denifl, P. Scheier, Cold Physics and Chemistry: Collisions, Ionization and Reactions inside Helium Nanodroplets Close to Zero K, *Phys. Rep.*, 751 (2018) 1-90.
- [2] F. Laimer, L. Kranabetter, L. Tiefenthaler, S. Albertini, F. Zappa, A.M. Ellis, M. Gatchell, P. Scheier, Highly charged droplets of superfluid helium, *Phys. Rev. Lett.*, 123 (2019) 165301.
- [3] L.F. Gomez, E. Loginov, R. Sliter, A.F. Vilesov, Sizes of large He droplets, *J. Chem. Phys.*, 135 (2011) 154201.

The dynamics of the reactions of Ar^{2+} with small molecules: complexation and bond formation

Sam Armenta Butt, Stephen D. Price

*Department of Chemistry, University College London, 20 Gordon Street, London WC1H 0AJ, UK
(corresponding author: S. Armenta Butt, e-mail: sam.butt.16@ucl.ac.uk)*



Molecular and atomic species in the ionosphere (a region of the upper atmosphere) can be ionised by UV radiation from the sun or by other collisional processes. This ionisation leads to the formation of monocations and dications (doubly-charged cations), as well as other species. The relatively low gas pressure in the ionosphere also reduces the rate of collisional de-excitation of monocations. This low rate results in a higher probability for the sequential ionisation of a neutral species to form a dication.¹ Computational modelling suggests that dications can be present in ionospheres with abundances comparable to chemically relevant monocations.² Indeed, dications have been directly detected in the atmospheres of Earth,^{3,4} Venus⁵ and Io,^{6,7} whilst dications are also predicted to be present in the ionospheres of Mars and Titan.^{8,9}

Dications were first detected during the development of mass spectrometry in the 1930s,¹⁰ however, their involvement in chemical processes is often overlooked. Dications can display unusual reactivity, such as an ability to form bonds involving the noble gases, for example HCCAr^{2+} .¹¹ Despite their high reactivity, atomic dications are stable in a collision free environment and many molecular dications have metastable states with lifetimes long enough to allow encounters with other species at ionospheric pressures.¹² During these encounters, chemical reactions can take place, with their products influencing the environments where dications are present. With a significant relative abundance and high reactivity, dications can therefore play a role in ionospheric chemistry. Dications can aid in the formation of complex molecules:² they can be involved in reactions that increase the complexity of organic molecules, for example carbon-carbon coupling reactions with methane or ethyne.^{13,14} However, dications are often not considered in ionospheric processes, partly due to the difficulty in detecting them unambiguously using mass spectrometry.¹⁵ A database of reactions involving dications and neutral species, especially those in which bond-forming steps are present, should be developed in order to help us understand the chemistry of ionospheres and potentially explain the presence of complex molecules in these environments.

In this submission we present a study of the reactions resulting from the collisions between $\text{Ar}^{2+} + \text{O}_2$ and $\text{Ar}^{2+} + \text{N}_2$. Our experimental technique involves the use of position-sensitive coincidence mass spectrometry, detecting pairs of product cations from Ar^{2+} reactions, revealing detailed information on the dynamics and energetics of the different reaction channels. In the $\text{Ar}^{2+} + \text{O}_2$ and $\text{Ar}^{2+} + \text{N}_2$ systems, four reaction channels were observed: (i) non-dissociative single electron transfer (SET), involving the transfer of an electron from the neutral species to the Ar^{2+} ; (ii) dissociative single electron transfer (DSET), involving the dissociation of the nascent O_2^+ or N_2^+ monocation after an initial single electron

transfer; (iii) dissociative double electron transfer, forming $O^+ + O^+$ and $N^+ + N^+$ via O_2^{2+} and N_2^{2+} respectively; (iv) chemical bond formation, with the production of ArO^+ and ArN^+ . Despite displaying the same general classes of reaction pathways, the reactions of Ar^{2+} with O_2 and N_2 proceed by different mechanisms. For example, the SET reaction with O_2 proceeds via a conventional, long range, direct mechanism, whereas in the reaction with N_2 , the dynamics and exoergicities are markedly different. The DSET reactions with O_2 and N_2 both display evidence for the formation of an intermediate collision complex (see Figure). The chemical bond formation channels in both systems appear to proceed via direct mechanisms, implying the long-range abstraction of O^- or N^- , from the neutral molecule, by Ar^{2+} . This varied reactivity demonstrates the mechanistic complexity involved in what are seemingly quite simple systems. As in other dicationic collision systems, our observation of complex formation, complexes with high potential energies, and bond-formation involving rare gas species, demonstrates the range and richness of the chemistry accessible to dications.

References

- 1 D. Smith and P. Spanel, *Mass Spectrom. Rev.*, 1995, **14**, 255–278.
- 2 R. Thissen, O. Witasse, O. Dutuit, C. S. Wedlund, G. Gronoff and J. Lilensten, *Phys. Chem. Chem. Phys.*, 2011, **13**, 18264–18287.
- 3 O. Witasse, T. Slanger and R. Thissen, *Ann. Geophys.*, 2011, **29**, 2235–2238.
- 4 J. H. Hoffman, C. Y. Johnson, J. C. Holmes and J. M. Young, *J. Geophys. Res.*, 1969, **74**, 6281–6290.
- 5 S. Ghosh, K. K. Mahajan, J. M. Grebowsky and N. Nath, *J. Geophys. Res.*, 1995, **100**, 23983–23991.
- 6 L. A. Frank, W. R. Paterson, K. L. Ackerson, V. M. Vasyliunas, F. V Coroniti and S. J. Bolton, *Science*, 1996, **274**, 394–395.
- 7 D. E. Shemansky and G. R. Smith, *J. Geophys. Res.*, 1981, **86**, 9179–9192.
- 8 J. Lilensten, O. Witasse, C. Simon, H. Soldi-Lose, O. Dutuit, R. Thissen and C. Alcaraz, *Geophys. Res. Lett.*, 2005, **32**, L03203.
- 9 C. Simon, J. Lilensten, O. Dutuit, R. Thissen, O. Witasse, C. Alcaraz and H. Soldi-Lose, *Ann. Geophys.*, 2005, **23**, 781–797.
- 10 A. L. Vaughan, *Phys. Rev.*, 1931, **38**, 1687–1695.
- 11 D. Ascenzi, P. Tosi, J. Roithová, C. L. Ricketts, D. Schröder, J. F. Lockyear, M. A. Parkes and S. D. Price, *Phys. Chem. Chem. Phys.*, 2008, **10**, 7121–7128.
- 12 D. Mathur, L. H. Andersen, P. Hvelplund, D. Kella and C. P. Safvan, *J. Phys. B At. Mol. Opt. Phys.*, 1995, **28**, 3415–3426.
- 13 C. L. Ricketts, D. Schröder, C. Alcaraz and J. Roithová, *Chem. - A Eur. J.*, 2008, **14**, 4779–4783.
- 14 E.-L. Zins and D. Schröder, *J. Phys. Chem. A*, 2010, **114**, 5989–5996.
- 15 J. D. Fletcher, M. A. Parkes and S. D. Price, *Int. J. Mass Spectrom.*, 2015, **377**, 101–108.

Lack of Chirality Induced Spin Selectivity (CISS) in molecular layers of helicenes

Milos Baljozovic, Anaïs Mairena, Benito Arnoldi¹, André Luis Fernandes Cauduro², Eduardo Bonini Guedes³, Christian Wäckerlin, Jan Voigt, Bahaaeddin Irziqat, Jan Hugo Dill³, Benjamin Stadtmüller¹, Andreas Schmid², Karl-Heinz Ernst

Empa, Swiss Federal Laboratories for Materials Science and Technology, 8600 Dübendorf, Switzerland (corresponding author: M. Baljozovic, e-mail: milos.baljozovic@empa.ch)

¹ *Department of Physics, Technical University Kaiserslautern, 67663 Kaiserslautern, Germany*

² *The Molecular Foundry, Lawrence Berkeley National Laboratory, CA 94720 Berkeley, USA*

³ *Swiss Light Source, Paul Scherrer Institute, 5232 Villigen PSI, Switzerland*

Chirality Induced Spin Selectivity (CISS) stands for an effect of chirality dependent transmission of electrons through the molecules.[1] It was demonstrated that up and down electron spins would differently interact with the chiral molecules leading to the certain spin asymmetries in the outgoing electron beam. In addition, a significant dependence on the energy of the incoming electrons was established..[2] Recently, the CISS has drawn significant attention to helical layers on surfaces as a consequence of a demonstration of spin asymmetries up to 60% in the photoemission experiments performed on DNA layers at room temperature.[3] Layers of prototypical helical molecules, the helicenes, have also exhibited the CISS effect, both in photoemission [4] and the spin-polarized tunneling experiments [5]. Although the proof-of-concept experiments performed with helicenes showed promising results, they lack angular and/or energy resolution that is necessary to glimpse into the mechanism of this phenomenon. Our experimental attempts to energy and/or angle resolve the CISS effect in layers of various helicenes in both photoemission and electron reflectivity experiments were so far in vain. Throughout the large energy and angle range, there is no chirality induced spin asymmetry observed.

Financial support by the Swiss National Science Foundation is acknowledged.

[1] D. M. Campbell *et al.*, *J. Phys. B: At. Mol. Phys.*, vol. 20, no. 19, pp. 5133–5143, Oct. 1987.

[2] S. Mayer *et al.*, *Phys. Rev. Lett.*, vol. 74, no. 24, pp. 4803–4806, Jun. 1995.

[3] B. Göhler *et al.*, *Science*, vol. 331, no. 6019, pp. 894–897, Feb. 2011.

[4] M. Kettner *et al.*, *J. Phys. Chem. Lett.*, vol. 9, no. 8, pp. 2025–2030, Apr. 2018.

[5] V. Kiran *et al.*, *Advanced Materials*, vol. 28, no. 10, pp. 1957–1962, 2016.

Diastereoselective on-surface synthesis of bisheptahelicene, their (cyclo)dehydrogenation and consequent HBr desorption

Milos Baljozovic, Anaïs Mairena, Maciej Kawecki, Konstantin Grenader¹, Martin Wienke², Kévin Martin³, Laetitia Bernard, Narcis Avarvari³, Andreas Terfort¹, Karl-Heinz Ernst, Christian Wäckerlin

Empa, Swiss Federal Laboratories for Materials Science and Technology, 8600 Dübendorf, Switzerland (corresponding author: M. Baljozovic, e-mail: milos.baljozovic@empa.ch)

¹ *Department of Chemistry, Institute of Inorganic and Analytical Chemistry, Goethe-University, 60438 Frankfurt, Germany*

² *Department of Chemistry, University of Hamburg, 20146 Hamburg, Germany*

³ *Laboratoire Moltech-Anjou, CNRS-Université d'Angers, 49045 Angers, France*

Ullmann and Scholl coupling reactions are among numerous surface reactions by far the most successful in the creation of C-C bonds at surfaces.[1] The fate of halogens and hydrogen originating as side products in these reactions have been long disputed. Here, step-wise Ullmann coupling of 9-bromoheptahelicene (Br-[7]H) to bis-heptahelices (bis[7]H), its dehydrogenation as well as the desorption of HBr is investigated on Au(111). As evidenced by the STM, successful Ullmann coupling of racemic Br-[7]H results in a diastereomeric excess of 50% of the heterochiral (M,P) bis[7]H with respect to the homochiral (M,M and P,P) form due to a topochemical effect. [2] Further on, the synthesized bis[7]H is modified by (cyclo)dehydrogenation, as identified by the in-situ ToF-SIMS. The bromine present on the surface desorbs then as HBr that is detected by TPDS. In the absence of molecules bromine desorbs at much higher temperatures. Finally, the evolution of H₂ sets in only once all of the Br is desorbed. This leads to a very characteristic TPD spectrum. Such behavior is determined by the reaction order of HBr and H₂ desorption and is fully reproduced by kinetic modelling. By the comparison with different molecules containing sterically overcrowded hydrogen atoms, we established that the desorption temperature of HBr is linked to the dehydrogenation temperature of these molecules as a direct consequence of their structure. In-situ ToF-SIMS arises to be a very powerful tool that complements the “common” surface-analytical methods such as XPS, TPDS and STM in shedding light on the role of transiently produced hydrogen and halogens in on-surface reactions. [3]

Financial support by the Swiss National Science Foundation, the Competence Centre for Materials, the French National Centre for Scientific Research, the University of Angers and the Région Pays de la Loire through the RFI LUMOMAT is acknowledged.

[1] J. Björk *et al.*, *Chemistry - A European Journal*, vol. 20, no. 4, pp. 928–934, Jan. 2014.

[2] A. Mairena *et al.*, *Journal of the American Chemical Society*, vol. 140, no. 45, pp. 15186–15189, Nov. 2018.

[3] A. Mairena *et al.*, *Chem. Sci.*, vol. 10, no. 10, pp. 2998–3004, Mar. 2019.

Chiral recognition in the self-assembly of trioxa[11]helicene molecules on metal surfaces

Bahaaeddin Irziqat¹, Jan Berger¹, Jesus Mendieta², Shyam Sundar³, Ashutosh Bedekar³, Pavel Jelinek², and Karl-Heinz Ernst^{1,4}

¹*Empa, Swiss Federal Laboratories for Materials Science and Technology, 8600 Dübendorf, Switzerland*

(corresponding author: J. Berger, e-mail: jan.berger@empa.ch)

²*Institute of Physics, Czech Academy of Sciences, Cukrovarnická 10, 162 00 Prague 6, Czech Republic*

³*Department of Chemistry, Faculty of Science, M.S. University of Baroda, Vadodara 390 002, India*

⁴*Department of Chemistry, University of Zurich, 8057 Zurich, Switzerland*

Besides its interest for the production of devices based on organic materials, such as molecular-spin filters, chiral molecular recognition is of paramount importance in the chemical world, as well as in many aspects of physics, biology, and material science. However, why racemic chiral compounds resolve into their pure enantiomers via crystallization, like in Pasteur's case, or crystallize as racemic crystals containing both enantiomers, is still not understood. It is thus worthwhile to study manageable model systems, such as two-dimensional (2D) crystallization of chiral polyaromatic hydrocarbon molecules on surfaces of single crystals using scanning-probe microscopy techniques and theoretical molecular modeling for unveiling the fundamental principles of intermolecular chiral recognition (1).

In this frame, the 2D-crystallization of enantiopure and racemic of the helical aromatic hydrocarbon 7,12,17-trioxa[11]helicene (TO[11]H) on the single crystalline (100) surfaces of silver and copper has been studied. In similarity to previously observed 2D-crystallization of heptahelicene ([7]H) on Ag(100) and Cu(100) (1, 2), the racemic TO[11]H molecules on Ag(100) form islands that are comprised of heterochiral domains with non-alternating enantiomer sequence in the principal lattice directions of the crystal. Whereas on Cu(100) and under identical conditions, homochiral domains, forming a 2D conglomerate structure are favoured.

[1] J. Seibel et al., J. Am. Chem. Soc. **137**, 7970-7973 (2015).

[2] J. Seibel et al., Chem. Commun. **50**, 8751 (2014).

Fusion relevant reactive ion surface collision investigation using the SurfTOF tandem mass spectrometer

Felix Duensing, Lorenz Ballauf, Faro Hechenberger, Paul Scheier

*Institut für Ionenphysik und angewandte Physik, Universität Innsbruck,
6020 Innsbruck, Austria*

(corresponding author: F. Duensing, e-mail: felix.duensing@uibk.ac.at)

In nuclear fusion reactors, the plasma facing material suffers from a continuous bombardment of highly energetic atoms and neutrons. Some of its compounds are very hazardous like molecules containing tritium, the radioactive isotope of hydrogen. Utilizing a newly commissioned apparatus, the formation of hydrogen containing molecular species under fusion relevant conditions will be investigated. In a preparatory study, we observed efficient formation of metal hydrides that can be sputtered as molecular ions from beryllium as well as tungsten surfaces. Non-radioactive deuterium is used as a surrogate for tritium in the proposed studies. We will present ongoing investigations of codeposition, sputtering inhibition by scavengers, sputtering analysis of neutrals, and molecule formation with adsorbates layers. These systems are measured on the new tandem mass spectrometer SurfTOF, which is perfectly suitable.

Support by the Commission for the Coordination of Fusion Research in Austria is gratefully acknowledged.

On the density of racemic and homochiral crystals: Wallach, Liebisch and Sommerfeld in Göttingen

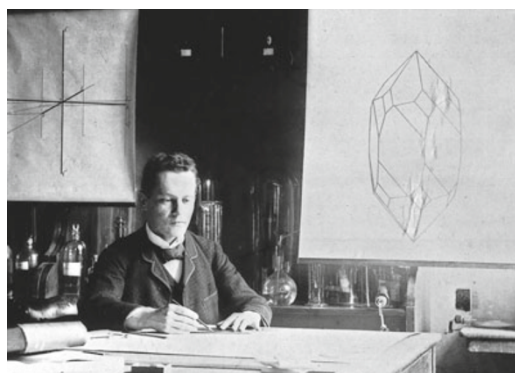
Karl-Heinz Ernst

*Empa, Swiss Federal Laboratories for Materials Science and Technology, 8600 Dübendorf,
Switzerland*

(e-mail: karl-heinz.ernst@empa.ch)

*Department of Chemistry, University of Zurich, Winterthurerstrasse 190, CH-8057 Zürich,
Switzerland*

Alfred Werner (1866–1919) is the undisputed founder of coordination chemistry, but many years passed before his stereochemical insights were accepted. Only after he proved conclusively that metal complexes can be chiral did his model become accepted and earn him the nickname “Inorganic Kekulé” and the Nobel Prize in Chemistry in 1913. But it took more than ten years from the time he predicted chirality in coordination compounds for his group to succeed in separating enantiomers. During the 1980s, reports appeared stating that some of the compounds originally prepared by one of Werner’s students, Edith Humphrey, resolve spontaneously into the enantiomers during crystallization. This led to the claim that Werner could have proven his theory much earlier if he had only tested a single crystal for optical activity. However, our re-examination of the original samples, which are stored in the Werner collection at the University of Zurich, and perusal of the corresponding doctoral theses of Werner’s students, reveals new aspects of conglomerate crystallization in the old samples [1].



Arnold Sommerfeld as post doc of mineralogy in Göttingen in 1894.

The first comparison of densities of heterochiral crystals with their homochiral counterparts was given by Otto Wallach (Nobel Prize in Chemistry 1910) in an account on carvone bromide crystals in 1895 in *Liebigs Annalen der Chemie*. Although the well-known mineralogist Theodor Liebisch, professor in Göttingen from 1887 to 1908, wrote the last four pages of that *Annalen* paper, his colleague from chemistry, Wallach served as sole author. The tedious density measurements in Liebisch’s laboratory were performed by one of the

fathers of theoretical physics, Arnold Sommerfeld! We discuss whether Wallach or Liebisch had the idea of a comparative study of crystal densities of racemates and their homochiral analogues and who of the two should be credited [2].

[1] K.-H. Ernst et al. *Angew. Chem. Int. Ed.* **50** (2011) 10780

[2] K.-H. Ernst, *Isr. J. Chem.* **57** (2017) 24

A Versatile Experimental Platform for Ultrafast Time-Resolved Ellipsometry from VUV to NIR

Shirly Espinoza

ELI Beamlines. Institute of Physics. Czech Academy of Science. Za Radnicí 835, 252 41 Dolní Břežany. Czech Republic

(corresponding author: S. Espinoza, e-mail: shirly.espinoza@eli-beams.eu)

Employment of ultrashort pulses of different energies in ellipsometry enables insight in a variety of ultrafast processes inaccessible by other experimental techniques. The charge carriers and phonons generated upon external electromagnetic stimulus in bulk and on the surface can scatter, diffuse and recombine in a very short time scale affecting the temporal and local changes of dielectric and optical constants of the material. Therefore a deep understanding of such processes is indispensable for further progress in operational parameters of electronic and optoelectronic devices.

Time-resolved absorption, reflectivity and ellipsometry are widely used tools for this purpose. However, some spectral regions like vacuum ultra-violet (VUV) have been excluded from this type of measurement because of lacking the reliable ultrashort pulse sources. The current advancement in femtosecond lasers and laser-driven secondary sources has opened a new perspective for spectroscopic measurements. In the VUV spectral region, these techniques can provide information about processes in dielectrics and wide-bandgap semiconductors. Nevertheless, the propagation and detection of ultrashort and ultra-broadband pulses in the setup require a special care and thoughtful choice of all optical components; VUV pulses are particularly demanding in this matter because such radiation is highly absorbed in quartz and even air.



Fig. 1. UHV chamber for the VUV experiments

Here, we present a versatile experimental platform, located in ELI Beamlines facility in Czech Republic, dedicated to ultrafast pump-probe ellipsometry with time resolution about 100 fs. The platform comprises two independent ellipsometers optimized for different spectral regions. The first instrument, shown in figure 1 and explained in reference [1], is dedicated to experiments with VUV radiation. It is based on a 15 fs

30 mJ, 1 kHz, in-house-developed laser with central wavelength 830 nm [2]. The VUV instrument is enclosed in an ultrahigh vacuum chamber (UHV) equipped with reflective polarizing optics and uses the beam produced by High Harmonic Generation laser-driven source in a range 5-120 nm [3]. This setup is equipped with a cryostat that allows for the measurements at temperatures from 20 K to 350 K. The upcoming upgrade with switchable Helmholtz coils will enable the experiments in magnetic field up to 1.5 T at 1 kHz.

The second setup instrument is devoted to UV-VIS-NIR spectral range. It is based on 1 kHz Ti:Saph laser which produces fundamental ultrashort (35 fs) NIR (800 nm) pulses subsequently transformed into desired pump and probe beams. The broadband probe pulses obtained by super-continuum generation cover 350-1300 nm region. The narrowband pump pulses are produced by optical parametric amplification and can be tuned from 190 nm to 20 μm . [4,5]

We present the experimental details of this cutting edge ellipsometric platform and discuss the possibilities that external scientists have to carry on their measurements on it.

Support by the projects Structural dynamics of biomolecular systems (CZ.02.1.01/0.0/0.0/15-003/0000447) and Advanced research using high intensity laser produced photons and particles (CZ.02.1.01/0.0/0.0/16-019/0000789) from the European Regional Development Fund is gratefully acknowledged.

- [1] S. Espinoza et al., Appl. Surf. Sci. **421**, 378-382 (2017).
- [2] F. Batysta et al, Opt. Express **24**, 17843–17848 (2016).
- [3] O. Hort et al., Opt. express **27**, 8871–8883 (2019).
- [4] S. Espinoza et al., Appl. Phys. Lett. **115**, 052105 (2019).
- [5] S. Richter. ArXiv:1902.05832 (2019),

Spontaneously electrical solids: how ammonia misbehaves

David Field, Andrew Cassidy, Rachel James¹

*Department of Physics and Astronomy, Aarhus University, Langelandsgade Aarhus DK8000 C,
Denmark*

(corresponding author: D.Field, e-mail: dfield@phys.au.dk)

¹ *Open University, School of Physical Sciences, Walton Hall, Milton Keynes, MK7 6AA, UK*

Deposit gas phase polar molecules onto a suitably cold substrate and, without any other intervention, a film is formed which may contain electric fields of up to 10^8 Vm^{-1} [1,2,3]. This so-called ‘spontelectric effect’ has been established using electron beams, Kelvin probes, [4] infrared spectroscopy [5] and most recently VUV spectroscopy [6,7]. Using VUV spectroscopy, we have shown that Wannier-Mott excitons form in solid CO, N₂O and, in very recent work, recorded here using the ASTRID2 storage ring at Aarhus University, also in ammonia. This is a preliminary report, since results were obtained in late October 2019, at the time of writing.

In the spontelectric state, electric fields are established through spontaneous dipole orientation in molecular films. The strength of the field is strongly dependent on the temperature of deposition of the material. With reference to the VUV spectroscopy of solids films, fields act to change the several nm separation of the hole and electron in Wannier-Mott excitons, and therefore change the absorption energy of the solid. Spectra accordingly show a marked dependence on the temperature of deposition [6,7], an effect well-known in the literature but previously unexplained before the detailed description of the spontelectric effect. [8,9]

Examples of spectra of solid state ammonia deposited at 60K and 80K are shown in Figure 1, for the G←X region around 120 nm, adopting gas phase assignments. The upper blue line refers to a film deposited at 60K and shows an absorption maximum at 121.37 nm. The lower orange line is for a film deposited at 80K and shows an absorption maximum at 123.48 nm, a shift of 1408 cm^{-1} or 175 meV. Note that the stability of the ASTRID2 source is essential for the very high S/N necessary for the successful prosecution of these experiments.

The spontelectric effect is the result of an order-disorder competition between dipole orientation and temperature. Thus one would expect that the electric field should always decrease with increasing temperature of deposition. This is indeed observed in numerous cases, e.g. for N₂O, toluene, CF₂Cl₂ etc.[3] However this is not the case in *cis*-methyl formate, [2, 3, 10] which shows a marked increase in electric field at deposition temperatures above 78K. It now turns out that ammonia may also demonstrate this remarkable behaviour. We have previously shown [3] that this anomaly is predicted by our model for spontelectrics. This behaviour is based squarely upon the unexpected mathematical properties of this model, described in detail in [3].

The evaluation of the spontelectric fields, in solid ammonia, may be performed using data for spectral shifts, for a variety of deposition temperatures between 20K and 80K, such as those shown in Fig. 1. A simple electrostatic model has been described in [6,7] in which the spontelectric field modifies the separation of the hole and electron in the exciton. The field causes the electron-hole separation to grow for higher fields. We have shown in [7] that the energy shift between temperatures T_i and T_j is given, in atomic units, by

$$\Delta\epsilon_{ij} = 2r\{(1-2E_i/\epsilon r^2)^{-1/2} E_i - (1-2E_j/\epsilon r^2)^{-1/2} E_j - (E_i - E_j)\} \quad (1)$$

where ϵ is the permittivity of the bulk material. Here 'r' is the electron-hole separation in the absence of any spontelectric field. The value of r may be determined experimentally from data taken for films prepared at 84K, where the field is unstable with time and decays to zero, or from extrapolation of data to zero layer thickness. [3] In eq. 1, E_k is the spontelectric field at temperature T_k . Analysis yields the spontelectric fields as a function of temperature. We may then show that parameters, governing the observed temperature dependence, places them in the regime in which, above deposition temperatures of 80K, the electric field in solid ammonia should begin to *increase* with increasing deposition temperature, as noted above. Details of this analysis will be presented elsewhere.

Perhaps even more remarkably, we also find that we can observe the formation of an exciton in ammonia in real-time, with an absorption peak, in the A \leftarrow X band, growing before our eyes on the thousands of seconds timescale. Data, to be described elsewhere, also show that the rate of peak growth depends both on temperature of film deposition and on film thickness, the latter illustrating the non-local nature of interactions within thin films.

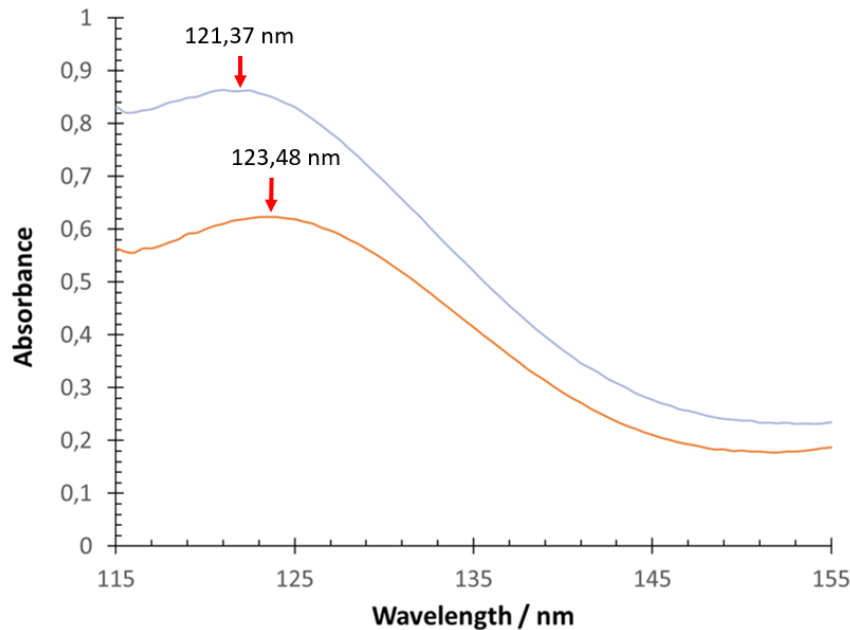


Figure 1: Absorption spectra of solid ammonia at for films prepared at 60K (blue line) and 80K (orange line) in the G \leftarrow X region around 120 nm. Films are of thickness of ~7 nm or 28 ML. Wavelengths of maxima are also shown.

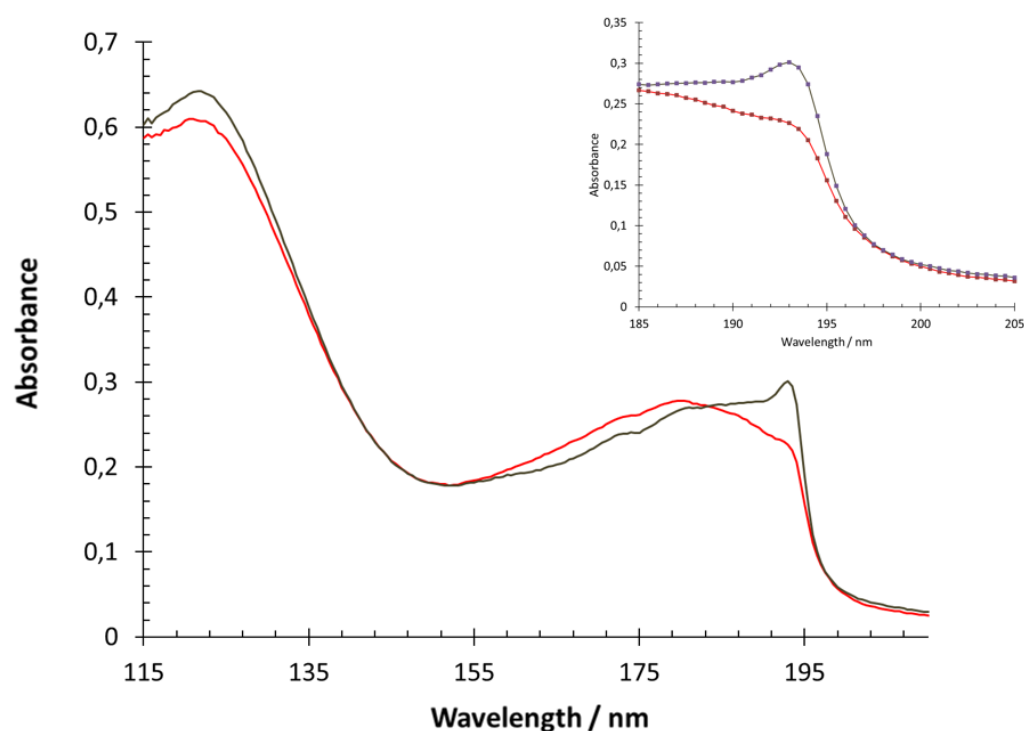


Figure 2: Absorption spectra of solid ammonia for a film prepared at 50K in the A \leftarrow X region around 195 nm. Red line: spectra taken at time zero. Black line: spectrum taken after a delay of 5400 seconds. Note the growth of the exciton peak on this timescale. Films are of thickness of ~ 7 nm or ca. 28 ML, as in Fig.1.

We should like to acknowledge the Centre for Storage Ring Facilities at Aarhus (ISA) for granting access to the AU-UV beamline on the ASTRID2 storage ring and the staff at ASTRID2 for their technical assistance in performing our experiments, with special thanks to Nykola Jones. The research leading to results presented here has been supported by the project CALIPSOplus under the Grant Agreement 730872 from the EU Framework Programme for Research and Innovation HORIZON 2020.

¹ R. Balog, et al. *Phys. Rev. Lett.*, 2009, **102**, 2

² O. Plekan et al. *EJPD . Eur. Phys. J. D*, 2017, **71**, 162

³ D. Field et al., *Int.Rev.Phys.Chem.* 2013, **32**, 345

⁴ A.Pilidi et al. *J.Phys.Chem.B* 2019, **123**, 8505

⁵ J.Lasne et al. *PCCP*, 2015, **17**, 20971

⁶ Y-J Chen et al. *Phys.Rev.Lett.* 2017, **119**, 157703

⁷ A.Cassidy et al. *PCCP*, 2019, **21**, 1190

⁸ A. Dawes et al. *J. Chem. Phys.* 2007, **126**, 244711

⁹ G.M.Munoz-Caro et al., *Astron. Astrophys.* 2016, **A19**, 589

¹⁰ M. Roman et al. *PCCP*, 2018, **20**, 5112

Interaction of Biomolecules with Soft Surfaces: from Blood Proteins and Polymeric Surfaces to Partially Disordered Peptides and Biomembranes

Christoph Bernhard, Daria Maltseva, Kristin N. Bauer, Steven J. Roeters¹, Tina Berger^{2,3}, Benedikt Goretzki^{2,3}, Kerstin Viet^{2,3}, Charlotte Guhl^{2,3}, Tobias Weidner¹, Mischa Bonn, Frederik R. Wurm, Ute A. Hellmich^{2,3}, Grazia Gonella

*Max Planck Institute for Polymer Research,
Ackermannweg 10, 55128 Mainz, Germany
(corresponding author: G. Gonella, e-mail: gonella@mpip-mainz.mpg.de)*

¹Department of Chemistry, Aarhus University, 8000 Aarhus C, Denmark

*²Institute for Pharmacy and Biochemistry, Johannes Gutenberg-Universität Mainz,
55128 Mainz, Germany*

*³Center for Biomolecular Magnetic Resonance (BMRZ), Goethe-Universität,
60438 Frankfurt am Main, Germany*

Nanoparticles and liposomes are used as versatile drug nanocarriers. Upon injection into the bloodstream a protein layer will immediately coat the nanocarrier surface forming the so-called protein corona. By far the most widely used protein repelling polymer is poly(ethylene glycol) (PEG), but new and more biodegradable non-fouling polymers such as polyphosphoesters (PPEs) have been recently proposed.

We use monolayers at the air/water interface as model systems for differently functionalized nanocarrier surfaces. We study polymer/water and the protein/polymer interactions by a combination of complimentary surface science techniques. Our results on PEG and PPEs suggest that, for certain proteins, PEG and members of the PPEs family not only influence the amount of adsorbed protein but also the ordering at the surface [1-3] while for other new non-fouling polymers the interactions seem altogether more complex [2].

The N-terminus of the transient receptor potential mucolipin 1 (TRPML1) ion channel is partly disordered and usually not reported in the available TRPML1 cryo-EM structures [4]. It contains binding sites for PI(4,5)P₂ (plasma membrane lipid) and PI(3,5)P₂ (lysosomal lipid) [5]. We test the influence of negatively-charged phospholipids on the secondary structure formation of the N-terminus by forming monolayers at the air/buffered aqueous solution interface. The data suggest a predominantly α -helical structure and orientation at the interface which is enhanced in presence of negatively charged lipids. We also obtain information on the effect of

the peptide binding on the order in the phospholipid monolayer and observe that the adsorption of the peptides also clearly affects the phospholipid headgroup and only slightly the tails [6].

- [1] C. Bernhard, et al., PCCP 19, 28182 (2017).
- [2] C. Bernhard, et al., ACS Applied Mater. Interfaces 11, 1624 (2019).
- [3] C. Bernhard, et al., Langmuir 35, 14092 (2019).
- [4] P. Schmiede, et al. Nature **550**, 366 (2017).
- [5] X.-P. Dong, et al., Nature Comm. **1**, 1 (2010)
- [6] T. Berger, et al., In preparation

Predissociation of N_2^+ isotopologues studied by TPEPICO imaging spectrometry

Helgi R. Hrodmarsson*, Roland Thissen¹, Danielle Dowek²,

Gustavo A. Garcia, Laurent Nahon and Thomas R. Govers³

Synchrotron SOLEIL, L'Orme des Merisiers, St. Aubin BP 48, 91192 Gif sur Yvette, France

(corresponding author: T. Govers, thomas.govers@wanadoo.fr)

¹ *Laboratoire de Chimie Physique, Bâtiment 350, Université Paris-Sud, Orsay, France* ; ² *Institut des Sciences Moléculaires, Bâtiment 520, Université Paris-Sud, Orsay, France* ; ³ *59 rue de Prony, Paris, France*

At SASP 2016, one of us re-examined the excitation and decay of N_2^+ states populated by charge transfer between (near-)thermal He^+ ions and $^{14}\text{N}_2$ or $^{15}\text{N}_2$. Isotope effects on the rate constants for production of N_2^+ and N^+ were compared to those pertaining to the specific transfer into the $\text{C}^2\Sigma_u^+(v')$ levels [1]. For $v' \geq 3$, the latter can decay either by $\text{C} \rightarrow \text{X}$ emission forming N_2^+ in its electronic ground state, or by predissociation into ground-state $\text{N}^+ + \text{N}$.

The competition between these two C-state decay modes varies with v' , and is subject to an unusually strong isotope effect. It was initially quantified by measuring $\text{C}(v') \rightarrow \text{X}(v'')$ emission rates observed when fast electrons or -ions impact a static room-temperature nitrogen target, and comparing these intensities with those expected in the absence of predissociation [2]. It was suggested that the assumptions made in the analysis of these fluorescence experiments could be avoided by using (T)PEPICO imaging spectrometry to directly measure the decay of vibrationally selected C-state levels into either N_2^+ or N^+ [1].

Reference [3] reports the results of such experiments carried out at the SOLEIL synchrotron in Saclay, using the SAFIRS end station installed on the DESIRS VUV beamline. The photon bandwidth was 2.5 meV fwhm, and the mass selected photoions were measured in coincidence with threshold electrons having energies between 0 and 5 meV. The branching ratios $\text{I}(\text{N}_2^+)/[\text{I}(\text{N}_2^+) + \text{I}(\text{N}^+)]$ thus obtained are summarised in Tables 1 and 2 for $^{14}\text{N}_2$ and $^{15}\text{N}_2$, respectively, together with the results of fluorescence measurements.

Reference	$^{14}\text{N}_2^+ (\text{C}, v') v' =$	2	3	4	5	6	7	8
3	$\text{BR}(^{14}\text{N}_2^+) \text{ TPEPICO}$	100%	$3.0 \pm 0.8\%$	$1.8 \pm 0.9\%$	$\leq 0.3\%$	$\leq 0.3\%$	NM	NM
2b	$\text{BR}(^{14}\text{N}_2^+) \text{ ion impact fluoresc.}$	100%	$9.3 \pm 1.2\%$	$5.3 \pm 1.0\%$	$2.9 \pm 0.4\%$	$1.9 \pm 0.5\%$	$1.7 \pm 0.5\%$	$0.26 \pm 0.06\%$
4	$\text{BR}(^{14}\text{N}_2^+) \text{ Auger fluorescence}$	100%	9.1%	5.2%	2.6%	1.6%	NM	NM

Table 1: Branching ratios, $^{14}\text{N}_2^+ / (^{14}\text{N}_2^+ + ^{14}\text{N}^+)$, for unimolecular decay of the $^{14}\text{N}_2^+$ C-state vibrational levels, v' , as indicated.

Reference	$^{15}\text{N}_2^+ (\text{C}, v') v' =$	2	3	4	5	6	7	8
3	$\text{BR}(^{15}\text{N}_2^+) \text{ TPEPICO}$	100%	$37 \pm 3\%$	$24 \pm 0.7\%$	$12 \pm 0.6\%$	$2.1 \pm 0.2\%$	$4.9 \pm 0.3\%$	$\leq 4\%$
2b	$\text{BR}(^{15}\text{N}_2^+) \text{ ion impact fluoresc.}$	100%	$51 \pm 3.0\%$	$39.6 \pm 1.8\%$	$23.9 \pm 1.3\%$	$5.4 (4.6 \text{ to } 6.6)\%$	$7.1 (6.1 \text{ to } 8.5)\%$	$2.9 (2.3 \text{ to } 4.6)\%$

Table 2: Branching ratios, $^{15}\text{N}_2^+ / (^{15}\text{N}_2^+ + ^{15}\text{N}^+)$, for unimolecular decay of the $^{15}\text{N}_2^+$ C-state vibrational levels, v' , as indicated.

For $^{15}\text{N}_2^+$ the TPEPICO branching ratios are typically half as large as those obtained from the fluorescence experiments, and for $^{14}\text{N}_2^+$ the difference is even more pronounced. It was verified that there is no significant mass effect on the ion detection efficiency in the TPEPICO experiments. The fluorescence data, on the other hand, are substantiated by the excellent agreement between results of ref. [2] and those obtained in Auger fluorescence experiments by Ehresmann et al. [4]. It was therefore concluded that the substantial difference between the two sets of data results from the difference in the target characteristics: in the TPEPICO experiments it is a supersonic beam with a rotational “temperature” between 30 and 50 K, while the fluorescence experiments were conducted with a room-temperature static N_2 target. Given a propensity for small changes in rotational quantum number upon ionisation, the fluorescence data can be considered as pertaining to a rotational distribution close to room-temperature, while the TPEPICO results characterise the competition between emission and predissociation of rotationally “cold” $\text{N}_2^+(\text{C}, v')$ ions.

The $\text{C} \rightarrow \text{X}$ emission rates, $A_{\text{em}}(v')$, are not expected to vary strongly with rotational or vibrational quantum number, or from one isotopologue to the other. The variations in the branching ratios summarised in tables 1 and 2 therefore result mainly from changes in the rates of predissociation, $A_{\text{pred}}(v')$:

$$A_{\text{pred}}(v') = A_{\text{em}}(v') * [1 - \text{BR}(v', \text{N}_2^+)] / \text{BR}(v', \text{N}_2^+).$$

The emission rate $A_{\text{em}}(v')$, the inverse of the “radiative lifetime”, can be obtained from the experimental lifetimes of non-predissociated levels, $v' \leq 2$. For $^{14}\text{N}_2^+$, Erman measured a lifetime $\tau(v')$ of 77 ns for $v'=1$ and of 79 ns for $v'=2$ [5]. Collins et al. computed radiative lifetimes which decrease slowly from 60 ns for $v'=0$ to 49 ns for $v'=5$ [6]. To illustrate the variations in the predissociation rates implied by the branching ratios of Tables 1 and 2, we report in Tables 3 and 4 the predissociation rates obtained assuming the radiative lifetime to be constant and equal to the average of the above values, 62.26 ns, i.e. $A_{\text{em}}(v') = 1.61\text{E}+07 \text{ s}^{-1}$.

Reference	$^{14}\text{N}_2^+ (\text{C}, v') v' =$	2	3	4	5	6	7	8
3	From TPEPICO	0	5.19E+08	8.76E+08	$\geq 5.34\text{E}+09$	$\geq 5.34\text{E}+09$	NM	NM
2b	From ion impact fluorescence	0	1.57E+08	2.87E+08	5.38E+08	8.29E+08	9.29E+08	6.16E+09
4	From Auger fluorescence	0	1.60E+08	2.93E+08	6.02E+08	9.88E+08	NM	NM

Table 3: Predissociation rates, $A_{\text{pred}}(v')$, in s^{-1} , deduced from the data of table 1, assuming a constant emission rate $A_{\text{em}}(v')$ of $1.61\text{E}+07 \text{ s}^{-1}$.

Reference	$^{15}\text{N}_2^+ (\text{C}, v') v' =$	2	3	4	5	6	7	8
3	From TPEPICO	0	2.73E+07	5.09E+07	1.18E+08	7.49E+08	3.12E+08	$\geq 3.85\text{E}+08$
2b	From ion impact fluorescence	0	1.54E+07	2.45E+07	5.11E+07	2.81E+08	2.10E+08	5.38E+08

Table 4: Predissociation rates, $A_{\text{pred}}(v')$, in s^{-1} , deduced from the data of table 2, assuming a constant emission rate $A_{\text{em}}(v')$ of $1.61\text{E}+07 \text{ s}^{-1}$.

For $^{15}\text{N}_2^+$, the predissociation rates deduced from the TPEPICO measurements are typically twice as high as those obtained from the fluorescence experiments. For $^{14}\text{N}_2^+$, the predissociation rates increase by a factor ranging from 3 to 10. Our interpretation is that the lower rotational levels predissociate considerably faster than do those populated at room temperature, and that the effect is stronger for $^{14}\text{N}_2^+$ than for $^{15}\text{N}_2^+$.

The effect of rotation on the C-state predissociation rates has been examined by Roche and Tellinghuisen [7] within the frame of a model which attributes the predissociation to the coupling, by the nuclear kinetic energy operator, of the C-state levels with the dissociation continuum of the $B^2\Sigma_u^+$ state [8]. The theoretical results do reproduce the vibrational- and isotopic variations of the predissociation rates. But they indicate a very weak dependence on rotation in the case of $^{14}\text{N}_2^+$, and a strong dependence for $^{15}\text{N}_2^+$, contrary to what is found in Tables 3 and 4.

To verify our interpretation of the differences between the TPEPICO data and the fluorescence measurements, we have requested additional beamtime at the SOLEIL synchrotron with the aim of repeating the coincidence experiments with a static nitrogen target. These additional data, if obtained in time, will be reported at the conference. If the rotational effect is confirmed, it will provide a further test of the theoretical description of the C-state predissociation, and possibly discriminate between the accidental mechanism first proposed by Lorquet and Desouter [9] and the direct homogeneous predissociation put forward by Tellinghuisen and Albritton [8].

A rotational dependence of the C-state predissociation rates will also affect the kinetics of (near-)thermal charge transfer between He^+ and N_2 . A low rotational temperature of the neutral molecule, if at least partially preserved upon population of the C-state, will enhance the production of N^+ through predissociation, while “hot” rotation may favour the final N_2^+ product channel. Admittedly, it will also complicate the quantitative interpretation of the $\text{C} \rightarrow \text{X}$ emission spectra, especially at low collision energies where rotational excitation cannot be excluded. In their flowing afterglow study of the $\text{He}^+ + \text{N}_2$ charge transfer reaction, Tsuji et al., for instance, found that the emission from $\text{C}, v'=3$ could be characterised by a rotational temperature of 1200 K, while that from $\text{C}, v'=4$ was fitted with a rotational temperature of 850 K [10]. A significant rotational dependence of the predissociation probabilities will indeed make it difficult to establish whether this rotational excitation reflects the dynamics of the initial charge transfer collision, or whether it results from the preferential depletion of the low rotational levels by C-state predissociation.

*Present Address: Sackler Laboratory for Astrophysics, Leiden Observatory, Leiden University, PO Box 9513, NL 2300 RA Leiden, The Netherlands

References:

- [1] T.R.Govers, XXth Symposium on Atomic, Cluster and Surface Physics, SASP 2016, Davos, Switzerland, February 7-12, 2016. Book of Abstracts, J. Stohner and C. Yernetzian Eds., Innsbruck University Press, 2016, pp.133 – 136.
- [2] a) C.A. van de Runstraat, F.J. de Heer, and T.R. Govers, *Chemical Physics* **3**, 431 (1974)
b) T.R. Govers, C.A. van de Runstraat, and F.J. de Heer, F.J., *Chemical Physics* **9**, 285 (1975)
- [3] H. R. Hrodmarsson et al., *Frontiers Chemistry* **7**, article 222 (2019); doi.org/10.3389/fchem.2019.00222
- [4] A. Ehresmann et al., *J. Phys. B At. Mol. Opt. Phys.* **39**, L119 (2006); doi: 10.1088/0953-4075/39/6/L03
- [5] P. Erman, *Physica Scripta* **14**, 51 (1976)
- [6] L.A. Collins et al., *J. Phys. B: Atom. Molec. Phys.* **13**, L613 (1980)
- [7] A.L. Roche and J. Tellinghuisen, *Molec. Phys.* **38**, 129 (1979); doi: 10.1080/00268977900101561
- [8] J. Tellinghuisen and D.L. Albritton, *Chem. Phys. Letters* **31**, 91 (1975)
- [9] J.C. Lorquet and M. Desouter, *Chem. Phys. Letters* **16**, 136 (1972)
- [10] M. Tsuji et al., *J. Chem. Phys.* **115**, 6811 (2001)

Theoretical simulations of non-adiabatic H atom scattering from tungsten.

^{1,2}Nils Hertl, ^{1,2}Oihana Galparsoro, ³⁻⁵Raidel Martin-Barrios, ^{1,2}Alexander Kandratsenka,
^{3,4}Pascal Larrégaray, ^{1,2}Alec Wodtke

¹*Max-Planck-Institut für Biophysikalische Chemie, Am Faßberg 11, 37077 Göttingen, Germany*

²*Georg-August-University Göttingen, Tammanstraße 6, 37077 Göttingen, Germany*

(corresponding author: N. Hertl, e-mail: nils.hertl@mpibpc.mpg.de)

³*Université de Bordeaux, 351 Cours de la Libération, 33405 Talence, France*

⁴*CRNS, 351 Cours de la Libération, 33405 Talence, France*

⁵*Universidad de La Habana, San Lazaro y L, CP 10400 La Habana, Cuba*

Recently, detailed theoretical and experimental investigations of energy transfer between hydrogen atoms and late *fcc* transition metal (111) surfaces have been made and on the basis of these experiments, it was possible to clarify the role of electron-hole pair excitation during the scattering process. [1-4] However, those investigative efforts excluded metals that crystallise in other crystal structures, because the theoretical methods in those investigations are based on Effective Medium Theory (EMT) [5], a theory that has been formulated to describe *fcc* metals and their alloys. Here, I present my first efforts to extend the EMT formalism to describe H atoms interacting with *bcc* metal surfaces. The obtained energy formula is fitted to DFT energies for H atoms at W(111). The obtained global EMT-PES is used to perform molecular dynamics simulations to investigate of how the scattering dynamics between H atom and metal surface is affected by the crystal structure and surface facet and surface temperature.

- [1] O. Bünermann et. al., *Science*, **350**, 1346 (2015).
- [2] S. M. Janke et. al., *J. Chem. Phys.*, **143**, 124708 (2015).
- [3] M. Kammler et. al., *Chem. Phys. Lett.*, **683**, 286 (2017).
- [4] Y. Dorenkamp et. al., *J. Chem. Phys.*, **148**, 034706 (2018).
- [5] K. W. Jacobsen et. al., *Surf. Sci.*, **366**, 394-402 (1996).

Precision measurements in H_2 and H_2^+ using nonpenetrating Rydberg states

Nicolas Hölsch¹, Maximilian Beyer², Kjeld S. E. Eikema³, Wim Ubachs³, Christian Jungen⁴ and Frédéric Merkt¹

¹*Laboratorium für Physikalische Chemie, ETH Zürich, Zurich, Switzerland*

²*Department of Physics, Yale University, New Haven, USA*

³*LaserLaB, Vrije Universiteit, Amsterdam, The Netherlands*

⁴*Department of Physics and Astronomy, University College London, London, UK*

H_2 is the simplest molecule displaying all features of a chemical bond and its ion H_2^+ is the simplest three-body system. As such, they are important systems for the development of molecular quantum mechanics and precise measurements of their ground state properties present benchmark quantities for ab initio calculations. As an example, the latest nonadiabatic calculations, which include relativistic and QED corrections, have reached a precision of better than 1 MHz for the dissociation energy of H_2 [1], which is of the same order of magnitude as the shifts resulting from the finite size of the proton.

Our studies combine high-resolution spectroscopy of high- n Rydberg states in H_2 and Rydberg series extrapolation using multichannel quantum defect theory (MQDT) [2]. We access nonpenetrating ($l=3$) Rydberg states which form regular series and are hardly subject to autoionization or predissociation but which are sensitive to stray electric fields.

We shall present the determination of the ionization energy of para H_2 , which is obtained as a sum of three intervals, the first between the ground state and a selected low- n ($n=2,3$) Rydberg state, the second between the selected state and high- n ($n=50-70$) Rydberg states, and the third being the binding energy of the high- n states. The experiments are carried out using slow supersonic beams generated by cryogenic pulsed valves and frequency-comb-calibrated lasers. From the ionization energies of ortho H_2 [3] and para H_2 , we extract their dissociation energies using a thermochemical cycle and determine the energy interval separating the ground states of ortho and para H_2 for the first time, at a precision of 1.5 MHz [4].

We will also present a measurement of the hyperfine structure of the ground state of ortho H_2^+ , combining hyperfine-resolved millimeter-wave measurements of Rydberg states with Rydberg series extrapolation by MQDT [5]. Compensating stray electric fields in three dimensions to better than 0.1 mV/cm, we have measured hyperfine intervals in H_2^+ with a precision of about 100 kHz.

[1] M. Puchalski, J. Komasa, P. Czachorowski and K. Pachucki, *PRL*, submitted.

[2] D. Sprecher, Ch. Jungen and F. Merkt, *J. Chem. Phys.* 140, 104303:1-18 (2014).

[3] N. Hölsch, M. Beyer, E. Salumbides, K. Eikema, W. Ubachs, Ch. Jungen and F. Merkt, *Phys. Rev. Lett.* 122(10), 103002 (2019).

[4] M. Beyer, N. Hölsch, J. Hussels, C-F Cheng, E. Salumbides, K. Eikema, W. Ubachs, Ch. Jungen and F. Merkt, *Phys. Rev. Lett.* 123(16), 163002 (2019).

[5] A. Osterwalder, A. Wüest, F. Merkt and Ch. Jungen, *J. Chem. Phys.* 121, 11810 (2004).

Creating and controlling cryogenically-cooled beams of shock-frozen, isolated, biological and artificial nanoparticles

A. K. Samanta, M. Amin, A. Estillore, N. Roth, L. Worbs, D. A. Horke, J. Küpper

Center for Free-Electron Laser Science, Deutsches Elektronen-Synchrotron DESY, Hamburg, Germany

Department of Physics, Universität Hamburg, Hamburg, Germany

Department of Chemistry, Universität Hamburg, Hamburg, Germany

Center for Ultrafast Imaging, Universität Hamburg, Hamburg, Germany

Email: jochen.kuepper@cfel.de,

Single-particle diffractive imaging (SPI) is emerging as a new technique for the three-dimensional atomic-resolution imaging of aerosolized nanoparticles at x-ray free-electron lasers (XFELs). However, one of the primary bottlenecks in realizing SPI is the efficient delivery of isolated, reproducible target particles into the x-ray focus. Here, we present novel approaches for the production of cold and high-density beams [1] of a broad variety of biological nanoparticles, ranging from single-domain proteins, including membrane proteins, to multi-subunit protein complexes and molecular machines, designed for use in XFEL experiments. This will also enable us to gain a better understanding of the ultrafast dynamics across extended biological systems. Fast freezing from ambient temperature to 10 K in less than 10 μ s will help freezing room-temperature equilibrium state distribution and even trapping reaction intermediates.

Furthermore, we have developed a numerical simulation infrastructure that allows quantitative simulation of isolated particle trajectories throughout the setup [2]. This allowed us to improve injection geometries and build aerosol- injection systems optimized for specific particle sizes in order to produce the highest-density particle beams. We propose an optimized setup with cooling rates of 10^6 K/s, shockfreezing few-nanometers particles and molecules within nanoseconds. The produced beams of shockfrozen isolated nanoparticles provide a paradigm shift in sample delivery, e.g., for diffractive imaging and microscopy or low-temperature nanoscience. The nanoparticle beams can subsequently be further manipulated and controlled using acoustic [3], electric [4] or optical fields [5].

References

- [1] A. K. Samanta, M. Amin, A. D. Estillore, N. Roth, L. Worbs, D. A. Horke, and J. Küpper, submitted (2019), arXiv:1910.12606 [physics].
- [2] N. Roth, S. Awel, D. A. Horke, and J. Küpper, *J. Aerosol. Sci.* **124**, 17 (2018), arXiv:1712.01795 [physics].
- [3] Z. Li, L. Shi, L. Cao, Z. Liu, and J. Küpper, *Phys. Rev. Appl.* **11**, 064036 (2019), arXiv:1803.07472 [physics].
- [4] Y.-P. Chang, D. A. Horke, S. Trippel, and J. Küpper, *Int. Rev. Phys. Chem.* **34**, 557 (2015), arXiv:1505.05632 [physics].
- [5] N. Eckerskorn, R. Bowman, R. A. Kirian, S. Awel, M. Wiedorn, J. Küpper, M. J. Padgett, H. N. Chapman, and A. V. Rode, *Phys. Rev. Appl.* **4**, 064001 (2015).

Creating, imaging, and controlling chiral molecules with electric fields

Andrey Yachmenev, Emil Zak, Jolijn Onvlee, Alec Owens, Cem Saribal, Jochen Küpper

Center for Free-Electron Laser Science, Deutsches Elektronen-Synchrotron DESY, Hamburg, Germany

Department of Physics, Universität Hamburg, Hamburg, Germany

Department of Chemistry, Universität Hamburg, Hamburg, Germany

Center for Ultrafast Imaging, Universität Hamburg, Hamburg, Germany

Email: jochen.kuepper@cfel.de,

Chirality is an important concept in physics, chemistry, and biology as well as pharmacology. Its importance is emphasized by the fact that life on earth is based on chiral biomolecules all naturally selected with a single handedness. Chirality is a fundamental and important property of molecules and materials leading to very interesting optical-activity effects in linear and nonlinear optics. Accurate experimental characterization of the enantiomeric excess and absolute handedness in mixtures of chiral molecules as well as efficient chiral purification and discrimination remain very challenging and highly demanding tasks for a broad scope of applications. Recently, a number of novel experiments have been developed for measuring the enantiomeric excess or absolute handedness.

We will present novel robust techniques devised in our group for the detection of the enantiomeric excess [1], the efficient spatial separation of chiral molecules [2], and the generation of dynamically chiral molecules from samples of statically achiral molecules [3]. These results are based on robust and highly accurate variational simulations of molecular ro-vibrational dynamics in the presence of electric fields. We will also present challenges and perspectives for experimental realizations of the proposed techniques.

References

- [1] A. Yachmenev and S. N. Yurchenko, Phys. Rev. Lett. **117**, 033001 (2016).
- [2] A. Yachmenev, J. Onvlee, E. Zak, A. Owens, and J. Küpper, Phys. Rev. Lett. (2019), in press, arXiv:1905.07166 [physics].
- [3] A. Owens, A. Yachmenev, S. N. Yurchenko, and J. Küpper, Phys. Rev. Lett. **121**, 193201 (2018), arXiv:1802.07803 [physics].

Study of oxygen reactions on polymer surfaces previously treated by ozone

Vera Mazankova^{1,2}, David Trunec³, Anezka Krzyzankova², Frantisek Krcma²

¹*Department of Mathematics and Physics, Faculty of Military Technology, University of Defence in Brno, Kounicova 65, 662 10 Brno, Czech Republic*

²*Institute of Physical and Applied Chemistry, Faculty of Chemistry, Brno University of Technology, Purkynova 118, 612 00 Brno, Czech Republic*

³*Department of Physical Electronics, Faculty of Science, Masaryk University, Kotlarska 2, 611 37 Brno, Czech Republic*

(corresponding author: V. Mazankova, e-mail: vera.mazankova@unob.cz)

1. Introduction

Ozone is a strong oxidizing agent and it plays an important role in many applications, e.g. in wastewater treatment [1], air pollution abatement [2], chemical etching [3], biomedical applications [4], agriculture [5] and others. The ozone is mainly produced in dielectric barrier discharges (DBD). The plasma surface interactions are of considerable importance for a wealth of discharge phenomena. It has been also observed that the ozone concentration in high purity (99.99995%) oxygen-fed ozonizers decreases from the initial level to almost zero during several hours. This phenomenon is known as Ozone Zero Phenomenon [6]. This phenomenon is probably caused by surface processes at ozonizer electrodes. Explanation of this phenomenon can bring deeper insight into surface processes in ozonizer and it is also important for the models of ozone production in dielectric barrier discharges.

On the other hand, ozone formation on the surface was also observed. The surface recombination of oxygen atoms in O₂ plasma was studied by Lopaev et al. [7]. Marinov et al. [8] also directly observed ozone formation on SiO₂ surfaces in oxygen discharges. In this study, the ozone concentration also decreased in latter times, which has to be attributed also to surface destruction of ozone.

In our recent studies [9, 10] the ozone creation and destruction on electrode surface previously treated in oxygen DBD at atmospheric pressure were studied. In this paper, we show that the treatment of surfaces by ozone only (without any discharge) is sufficient to observe subsequent creation and destruction of ozone by surface reactions.

2. Experimental setup

Experimental setup used for this study is shown in Fig. 1. Extremely high-grade oxygen of 99.9999% purity was led through the molecular sieve and the mass flow controller into the cylindrical ozonizer, which was used for ozone generation. The high voltage power supply operating at frequency 20 kHz and voltage amplitude of 4.5 kV was used to generate DBD in

the ozonizer. The ozone concentration generated at these conditions was $3.3 \times 10^{20} \text{ cm}^{-3}$. The ozone generated in ozonizer was led in the samples, inside which the surface reactions were studied. The samples were made of silicone rubber. The silicone rubber tube was 180 mm long with inner diameter of 3.6 mm. The input and output of samples could be closed by valves and then the gas flow bypassed the sample. Finally, the gas was led through the quartz absorption cell, where the ozone concentration was measured by absorption spectroscopy with time step of 0.1 s. For blowing out of ozone from the sample oxygen or argon could be used.

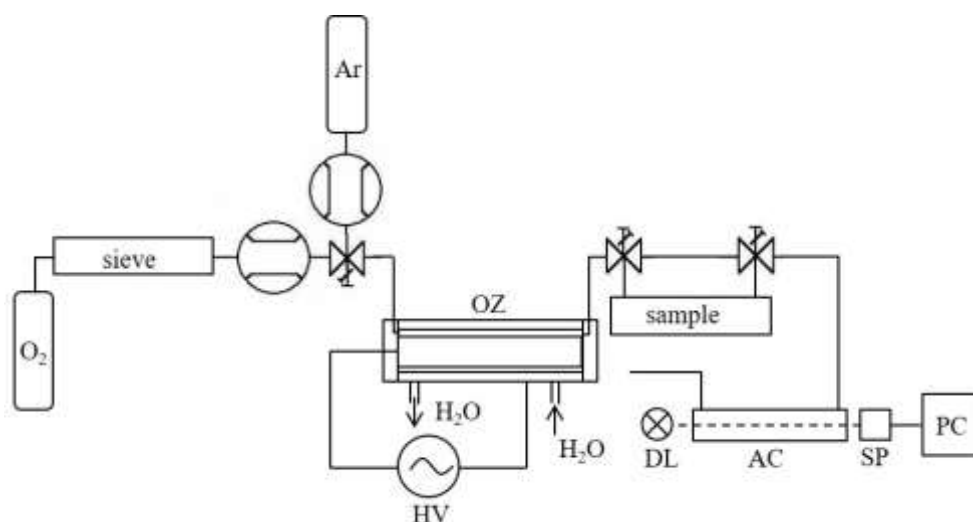


Fig. 1 Experimental setup. HV-high voltage power supply, OZ-ozonizer, DL-deuterium lamp, AC-absorption cell, SP-spectrometer, PC-computer.

3. Results

The procedure for this set of experiments was as follows: a) the ozone was flowing through the sample with the flow rate of 2 slm for 5 min; b) the ozone flow was switch off and the sample was flowing by pure oxygen for 15 s (after this time all ozone was removed from the inside of the sample and no ozone was detected by absorption measurement); c) pure oxygen was closed inside the sample by valves for given reaction time t_r ; d) after elapsing the reaction time the sample was blown through by pure oxygen with flow rate of 2 slm and the ozone concentration was measured by absorption spectroscopy. Thereafter the whole procedure was repeated for different reaction time t_r . The experiment was also performed for blowing out the created ozone by argon. The dependence of ozone amount on reaction time t_r for blowing out by oxygen or by argon is shown in Fig. 2. Blowing out of ozone was for flow rate of 2 slm. The time dependences of ozone concentration measured in the absorption cell (item d) in above described procedure are shown in Fig. 3. The total amount of ozone was then determined from the time dependence of ozone concentration by integration. It follows from Fig. 2 that ozone is created at short reaction times (up to 5 min) and then at longer reaction times the destruction of ozone prevails. This dependence is similar to the dependence measured by Marinov et al. [8]. The explanation of these results is as follows. When the

surface is brought into contact with ozone, the surface is quickly covered by atomic oxygen species through dissociative adsorption of ozone. Then the Eley–Rideal reaction of a gaseous oxygen molecule with adsorbed atomic oxygen leads to formation of gaseous ozone molecule



where O_S is the oxygen atom adsorbed at the surface.

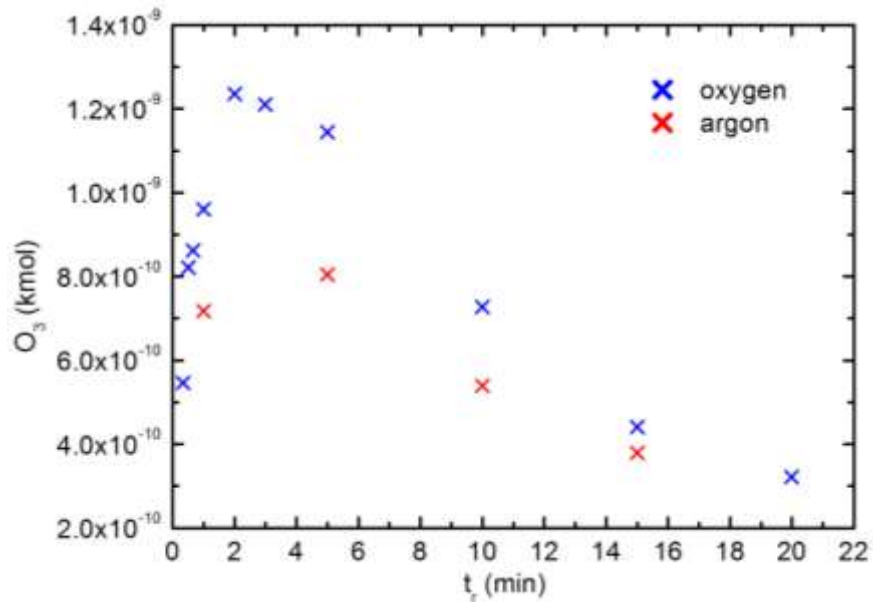


Fig. 2 The dependence of ozone amount on reaction time t_r . Blowing out of ozone with oxygen or argon with flow rate 2 slm.

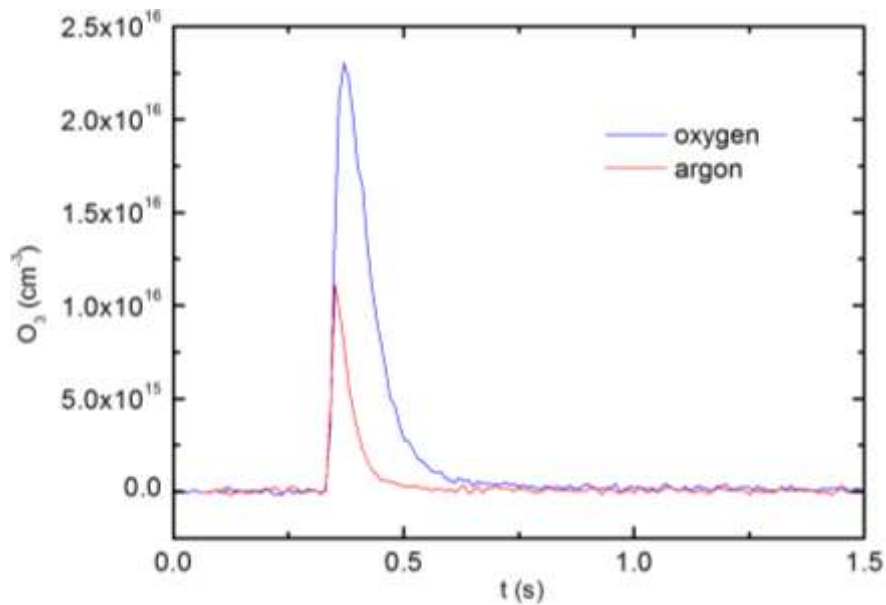
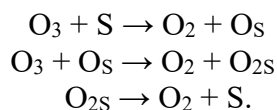


Fig. 3 The time dependence of ozone concentration. Blowing out of ozone with oxygen or argon with flow rate 2 slm. The reaction time t_r was 3 min.

The ozone can be decomposed as follows



The experiments proved the creation and destruction of ozone on polymer surfaces which were treated by ozone. The measured time dependence of produced amount of ozone shows a steep increase of ozone concentration in first tens of seconds, which is due to fast ozone formation on surface. The ozone is created in the reaction of molecular oxygen in gas phase with oxygen atom adsorbed on surface. In later time the ozone is destroyed in reactions with free active site or adsorbed atomic oxygen.

4. Acknowledgement

The present work has been supported by institutional support for the research organization development awarded by the Ministry of Defence of the Czech Republic.

5. References

- [1] S. Ognie et al., Plasma Chem. Plasma Process 29, 261 (2009).
- [2] C. Ayraul et al., Catal. Today 89, 75 (2004).
- [3] S. Collin et al., Polymer 44, 2403 (2003).
- [4] U. Cvelbar et al., J. Appl. Phys. 106, 103303 (2009).
- [5] J. Pawlat et al., Plasma Process. Polym. 15, e1700064 (2018).
- [6] M. Taguchi et al., HAKONE XII Proceedings, 291 (2009).
- [7] D. V. Lopaev et al., J. Phys. D: Appl. Phys., 44, 015202 (2011).
- [8] D. Marinov et al., J. Phys. D: Appl. Phys., 46, 032001 (2013).
- [9] D. Trunec et al., HAKONE XV Proceedings, 213 (2016).
- [10] V. Mazankova et al., ELMECO & AoS Proceedings, 1 (2017).

Tip-enhanced Raman Spectroscopy on Two-Dimensional Polymers

Timo S.G. Niepel, Wei Wang¹, A. Dieter Schlüter¹, Renato Zenobi*

*ETH Zurich, Swiss Federal Institute of Technology in Zurich, Laboratory of Organic Chemistry,
Vladimir-Prelog-Weg 3, 8093 Zurich, Switzerland
(corresponding author: R. Zenobi, e-mail: zenobi@org.chem.ethz.ch)*

¹*ETH Zurich, Institute for Polymers, Vladimir-Prelog-Weg 5, 8093 Zurich, Switzerland*

Tip-enhanced Raman spectroscopy (TERS) is a high-resolution nanoscopy method, which has been continuously developed since its invention in our research group at ETH Zurich. [1] Its spatial resolution below the limit of diffraction as well as its chemical specificity nowadays qualify TERS imaging as the analytical method of choice for investigations on structured surfaces and thin films. [2] Out of these, two-dimensional polymers are of particular interest to us, since they are crystalline in two directions while being molecularly thin. Their particularly uniform pore size distribution and high mechanical stability make them promising candidates for applications as nanomembranes in separation science. [3] However, the membrane's performance is negatively impacted by defect sites.

In this work, we have synthesized large areas of these novel materials on the air-water interface of a Langmuir-Blodgett trough and spectroscopically quantified such defects using TERS. Polymerization is induced with a photochemical [2 + 2]-cycloaddition of the trifunctional monomers. The Raman shift of optical phonons is validated with an LCAO-CO density functional theoretical normal coordinate analysis under diperiodic boundary conditions. Factor group analysis of the 2D-polymer's symmorphic layer group $p6$ (ITE L73) is employed to explain the Raman activity of these experimentally observed vibrational modes near the center of the Brillouin zone. Scarce residual monomer and unreacted olefinic sites (< 5%) are discerned through their characteristic spectral features in the fingerprint region, *e.g.* the symmetric backbone vibration $26A_1$ at about 1240 cm^{-1} . This study rigorously assesses the validity of solid-state Raman selection rules at the nanoscale with gap-mode TERS.

This project has received funding from the European Research Council (ERC) under the European Union's Horizon 2020 research and innovation programme under grant agreement No 741431 (2DNanoSpec).

[1] a) R.M. Stöckle, Y.D. Suh, V. Deckert, R. Zenobi, Chem. Phys. Lett. **318**, 131 (2000); b) M.S. Anderson, Appl. Phys. Lett. **76**, 3130 (2000); c) N. Hayazawa, Y. Inouye, Z. Sekkat, S. Kawata, Opt. Commun. **183**, 333 (2000); d) B. Pettinger, G. Picardi, R. Schuster, G. Ertl, Electrochemistry (Tokyo, Jpn.) **68**, 942 (2000).

[2] a) J. Stadler, T. Schmid, L. Opilik, P. Kuhn, P.S. Dittrich, R. Zenobi, Beilstein J. Nanotechnol. **2**, 509 (2011); b) L. Opilik, P. Payamyar, J. Szczerbiński, A.P. Schütz, M. Servalli, T. Hungerland, A.D. Schlüter, R. Zenobi, ACS Nano **7**, 4252 (2013); c) W. Wang, A.D. Schlüter, Macromol. Rapid Commun. **40**, 1800719 (2019); d) F. Shao, R. Zenobi, Anal. Bioanal. Chem. **411**, 37 (2019).

[3] T.S.G. Niepel, Y. Pandey, R. Zenobi, Chimia **73**, 493 (2019).

Plasmonically Enhanced Raman Spectroscopy of Surface Bound Molecular Electrocatalyst

Yashashwa Pandey¹, Laurent Sévery², Guillaume Goubert¹, Jacek Szczerbinski¹, Timo S. G. Niepel¹, S. David Tilley², Renato Zenobi¹

(corresponding author: Y. Pandey, e-mail: yashashwa.pandey@org.chem.ethz.ch)

1. ETH Zurich, D-CHAB, Vladimir-Prelog-Weg 3, 8093 Zurich, Switzerland

2. Department of Chemistry, University of Zurich, Zurich, Switzerland

Molecular Water Oxidation Catalysts (WOCs) are promising candidates for efficient solar fuel production, owing to their high activity and tunability. By binding the electrocatalyst molecule to the electrode surface we can simplify the reaction system, easily isolate the products, reduce side reactions and achieve faster electron transfer rates. However, the stability of the anchored species and the operating mechanism of such catalysts is not fully known [1]. We are using plasmonically enhanced and surface specific Raman spectroscopic techniques, namely Tip-Enhanced Raman Spectroscopy (TERS) and Shell-Isolated Nanoparticles Enhanced Raman Spectroscopy (SHINERS) [2], to answer these questions.

TERS is an advanced analytical technique that combines the high spatial resolution of Scanning Probe Microscopy with spectroscopic information provided by the Raman Spectroscopy. It is well suited to study 2-dimensional systems. Similar to Surface-Enhanced Raman Scattering (SERS), it relies on the enhancement of the Raman signal in presence of a strong electromagnetic field between a plasmonic tip and the sample [3]. In this study, we used an ambient TERS system to study attachment of an Iridium based molecular WOC bound to Indium Tin Oxide (ITO) sputtered onto a gold substrate and embedded in a thin TiO₂ layer. We have also performed SHINERS at ambient conditions as well as *in situ* to study the changes in the structure of the catalyst and its attachment to the ITO surface upon activation in electrochemical conditions.

The authors would like to thank European Research Council (ERC) Advanced Grant (2DNanoSpec), Swiss National Science Foundation (SNSF), AP Energy Grant # PYAPP2 and University of Zurich Research Priority Program (URPP) Light-CheC for their generous financial support.

[1] L. Sévery et al., *Inorganics* **6**, 105 (2018).

[2] J. F. Li et al., *Nature* **464**, 392 (2010).

[3] R. M. Stöckle et al., *Chem. Phys. Lett.* **318**, 131 (2000).

Electronic structure of copper formate clusters probed by UV/Vis spectroscopy

Tobias F. Pascher, Milan Ončák, Christian van der Linde, Martin K. Beyer

*Institut für Ionenphysik und Angewandte Physik, Universität Innsbruck
6020 Innsbruck, Austria*

(corresponding author: T. F. Pascher, e-mail: tobias.pascher@uibk.ac.at)

Copper-based catalysts are widely investigated for carboxylation reactions and hydrogen storage applications. They are already applied in industrial catalysis, e.g. in methanol synthesis [1]. The formation of formate is regarded as a crucial step in the activation and transformation of carbon dioxide to methanol or formic acid [2]. It was shown in the gas phase that copper hydride clusters can react with carbon dioxide barrierlessly to copper formate species [3,4]. We have recently shown that the formation of formic acid is a key step in the decomposition of small Cu(II) formate clusters [5].

In this contribution, well-defined gas phase systems are used to investigate the electronic structure of copper formate clusters by means of UV/Vis spectroscopy in an FT-ICR mass spectrometer. The clusters are excited electronically using a tunable laser system while the decomposition products are detected. The experiments are supported by quantum chemical calculations.

The observed electronic transitions hereby mainly depend on the oxidation state of the copper centers along with the orientation of the formate ligands. However, no copper-copper bonding interaction is observed. For Cu(I) centers, Cu(*d*) to Cu(*s/p*) transitions are observed while Cu(II) centers exhibit Cu(*d*)-Cu(*d*) transitions along with charge transfer from ligand to metal. The decomposition products depend on the photon energy. Most of these products are similar to the ones observed in IRMPD experiments, pointing towards accessible conical intersections. However, a few additional channels, e.g. loss of a HCOO radical, point towards additional photochemical pathways following a ligand-to-metal charge transfer transition.

- [1] J. Cai et al., *Nature* **466**, 470 (2010).
- [1] M. Behrens et al., *Sci.* **336**, 893 (2012).
- [2] A. Álvarez et al., *Chem. Rev.* **117**, 9804 (2017).
- [3] A. Zarvas et al., *Inorg. Chem.* **56**, 2387 (2017).
- [4] Y.-Z. Liu et al., *J. Phys. Chem C* **122**, 19379 (2018)
- [5] T. F. Pascher et al., *ChemPhysChem* **20**, 1420 (2019)

Sputtering from a Beryllium Surface: Neural-Network based Molecular Dynamics Simulations without Empirical Parameters

Lei Chen, Ivan Sukuba¹, Michael Probst, Alexander Kaiser*

University of Innsbruck, Institute of Ion Physics and Applied Physics, 6020 Innsbruck, Austria

**corresponding author: alexander.kaiser@uibk.ac.at*

¹Department of Nuclear Physics and Biophysics, Comenius University, SK-84248 Bratislava, Slovakia

Modelling surface sputtering on an atomistic basis is difficult for a variety of reasons: (1) Molecular Dynamics simulations are the obvious choice to model the process but standard simulation packages are not well suited for such completely non-equilibrium situations. (2) Sputtering yields are often low and long simulation times (in case of cumulative sputtering) or many repeated simulation runs (repeated sputtering on pristine surfaces) are necessary. (3) Sputtering means that bonds are broken and others are possibly formed. Both is difficult to describe accurately with analytical energy expressions. (4) On the other side, methods like Car-Parrinello [1] would be suitable but are severely restricted in times and system sizes that can be studied. (5) Even in simple cases surface orientation, surface temperature, kinetic projectile energy and angle of incident open up a multidimensional parameter space that cannot be covered unless very fast modelling techniques are available.

We tried to alleviate the obstacles described in (3) and (4) by employing a machine-learning technique combined with molecular dynamics to simulate surface sputtering. While the technique is not new, several details have to be taken into account to make it working. In molecular dynamics simulations the total potential energy function of the system is the main input, together with the initial coordinates and velocities of the particles. Cartesian forces are the quantities being integrated but they are readily available from the energy. Quantum chemical methods, either wave-function or electron density based, are a natural choice to obtain this total energy. They do not provide an analytical expression but numerical by means of a computationally expensive iterative algorithm. As long as molecular simulation techniques exist, such quantum chemical energies were used to fit analytical energy expressions which were in turn then employed in the simulations. Such a hierarchical approach allows large-scale simulations over long times, nowadays up to microseconds. The fitting to obtain analytical potential energy expressions is not easy. It works well for systems where the pair approximation is valid and where a posteriori adjustments of the potential energy function to experimental quantities are possible. A good example is the multitude of models that describe bulk water [2]. For the important domain of systems where chemical reactions with bond breaking and bond formation is possible, it was never completely successful. Ingenious efforts

like bond order potentials [3] are used successfully but need tremendous effort to create new potential energy functions.

It is here where machine learning can play a role. Most often neural networks [NNs] model all or several terms of the potential energy surface. Several methods have been tried: The Behler-Parrinello [4] method and the Gaussian Approximation Potentials [5] approach are frequently used. There exist also methods where NNs mimic the kinetic and potential energy on the level of the electron density, thus providing a quantum chemical treatment without the cost of self-consistency and evaluation of the kinetic energy operator [6]. On another level, machine learning algorithms are especially well suited to improve the potential energy expression ‘on the fly’ [7] during a simulation and we exploit this feature as well (see below).

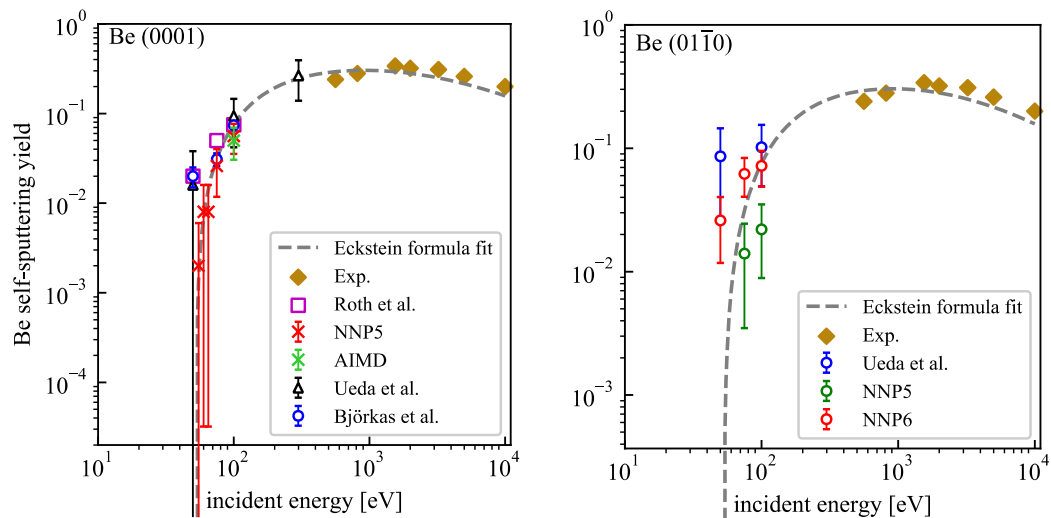
Our example deals with sputtering from Be(0001) and Be(0110) surfaces by incoming Be atoms. By means of molecular dynamics simulations we generate sample trajectories caused by incident energies from 50 to 100eV. They are obtained by numerical integration from interparticle forces stored in atom-based NNs with parameters obtained from density functional calculations. This system is technologically very relevant because Beryllium sheets have been chosen as armor material in the first wall of the ITER reactor currently being constructed. Experiments of Beryllium sputtering are complicated due to regulations to avoid Be poisoning. It is also impossible to reach the same conditions that will be present in ITER while – with the possible exception of the flux – they can be simulated. The method used here is easily transferable to more complicated systems and indeed we intend to further exploit it to increase our knowledge of fusion-relevant plasma-wall interactions involving multiple species.

We choose the Behler-Parrinello [4] approach for the potential energy. In this approach one does not simply express usual potential energy functions by a NN to gain flexibility but one starts from the concept that it is the atoms that are responsible for the total energy of the system. The energy of each atom is determined by its surroundings and the total energy is the sum of the energies of all atoms. Each atom type – normally each element - has its own neural network that stores the information how the energy depends on its surroundings. In some sense this is an extension of the idea of a directionally modified ‘local density’ which has been firstly used in the Sutton-Chen potentials [8] in a non-directional way and then in the Brenner-type potential functionals [9] where directional terms are present. Both of these approaches have opened up the possibility of reactive potential energy functions but were largely empirical. The Behler-Parrinello approach requires the input to the NN to be invariant to permutations of the same atoms and to translation and rotation. This seemingly simple requirement is in fact difficult to fulfill rigorously. It is approximated by converting the coordinates into symmetrized basis functions that are then input to the neural network.

In our case, each atom owns a feedforward $53 \times 30 \times 30 \times 1$ NN with identical parameters. The training was performed using configurations randomly extracted from 500 ab initio MD sputtering trajectories on a rather small Be(0001) surface slab with 96 atoms.

Since neural networks cannot extrapolate, this training is not sufficient, however, to reproduce ab initio energies of all possible configurations. Therefore, several NNs with different initial parameters were compared to each other with the first one being the ‘master’ determining the

trajectory. Large discrepancies of energies or forces between the networks indicate large distances from anchor points in the training set. They were iteratively included into the training set and the run was repeated with updated parameters. In this way the NN potential could accurately reproduce ab initio results as has been checked for a few cases. Several sputtering calculations were performed, both on Be(0001) and Be(100) surfaces. The plots below show some of the results, together with literature data [10,11].



It is important to note that for the Be(0110) surface training data from Be(0001) was not sufficient and new ab-initio data had to be fed into the networks.

At the end we would like to summarize possible or ongoing developments in the field:

(1) Atomistic simulations employing machine learning are a new subject and countless interesting aspects can be explored. The network architecture is never optimized but kept rigid or determined by trial and error. Indeed, it is doubtful that neural networks are the best choice in principle although the vast knowledge about them and their implementation in computer hardware make them possibly the best choice in practice. (2) For many systems the use of analytical expressions that contain the physical context together with NNs that take care of relatively small but difficult contributions that often arise will be a better choice than only NNs which are anyhow lacking long-range interactions. (3) It was crucial to use forces and not only energies in the NN training stage. It would be even better to use the Hessian matrix of second derivatives due to its even higher information content. This force matrix is available relatively cheap for a variety of quantum chemical methods. (4) The black box character of the NNs could be alleviated by implementing an analogue to the energy decomposition schemes common in quantum chemistry.

Acknowledgement:

This work was supported by the Austrian Science Fund (FWF): P28979-N27, the Tyrolean Science Fund (TWF): UNI-0404/2308 and the Kommission zur Koordination der Kernfusionsforschung der ÖAW (KKKÖ) and has been carried out within the framework of the EUROfusion Consortium. We have received funding from the Euratom research and training programme 2014-2018 and 2019-2020 under grant agreement No 633053. The views

and opinions expressed herein do not necessarily reflect those of the European Commission. The computational results have been obtained using the Vienna Scientific Cluster (VSC-3) and the HPC-infrastructure LEO of the University of Innsbruck.

- [1] Car, R.; Parrinello, M (1985). *Physical Review Letters*. 55 (22): 2471–2474.
- [2] Cisneros G, A, et al. (2016), *Chem. Rev.* 116, 13, 7501-7528
- [3] Tersoff, J. (1988), *Phys. Rev. B*. 37: 6991.
- [4] Behler, J.; Parrinello M. (2007) *Phys. Rev. Lett.* 98, 146401
- [5] Bartók, A. P.; Payne, M. C.; Kondor, R.; Csányi, G. (2010) *Phys. Rev. Lett.* 104, 136403.
- [6] Ryczko, K.; Strubbe, D.; Tamblyn, I. (2019) *Phys. Rev. A* 100, 022512
- [7] Li, Z.; Kermode, J. R.; De Vita, A. (2015) *Phys. Rev. Lett.* 114, 096405
- [8] Sutton, A. P.; Chen (1990) *Phil. Mag. Lett.* 61, 139
- [9] Brenner, D. W. (1990). *Phys. Rev. B*. 42 (15): 9458.
- [10] Ueda, S.; Ohsaka, T.; Kuwajima, S. (1998) *J. Nucl. Materials* 258-263, 713-718.
- [11] Björkas, C.; Juslin, N.; Timko, H.; Vörtler, K.; Nordlund, K.; Henriksson, K.; Erhart, P. (2009) *J. Phys.-Condens. Mat.* 21, 445002

Ultrafast spectroscopy at the ELI Beamlines facility: available capabilities for applications in molecular, biomedical and materials science

Mateusz Rebarz¹, Shirley Espinoza¹, Jakob Andreasson^{1,2}

*ELI Beamlines, Institute of Physics. Czech Academy of Science
Prague, Czech Republic*

(corresponding author: M. Rebarz, e-mail: mateusz.rebarz@eli-beams.eu)

¹ *ELI Beamlines. Institute of Physics. Czech Academy of Science
Za Radnicí 835, 252 41 Dolní Břežany. Czech Republic*

² *Condensed Matter Physics, Department of Physics, Chalmers University of Technology
SE-412 96 Gothenburg, Sweden*

Extreme Light Infrastructure (ELI) is a European Project forming a pan-European Laser facility to provide the most intense femtosecond lasers in the world for fundamental and applied research [1]. The ELI Beamlines (ELI BL) research center, located in Czech Republic, is a part of this project and its scientific activities are based on the utilization of four unique ultrashort pulse lasers with a unique combination of pulse profile, repetition rate and intensity. Important mission of ELI BL is to develop a new generation of laser driven light sources for ultrashort pulses covering the VUV to gamma-ray energy range based on plasma effects in gases and solids as well as relativistic electron acceleration. All sources have the potential to be used in combination with beams split off from their corresponding drive lasers for pump-probe experiments. In contrast to the situation at accelerator based light sources, like synchrotrons and FELs, the fact that the pump pulse can be split off from the same laser pulse that generates the X-ray pulse provides an intrinsic synchronization between the pump and the probe pulses.

Here we introduce the experimental capabilities and activities of one of the ELI BL research programs: Applications in Molecular, Biomedical and Materials (MBM) science. This program is focused on developing the complementary capabilities in optical, VUV and X-ray science in one location, with advanced sample preparation abilities. The complex ultrafast phenomena in physics, chemistry and biology can be studied utilizing pulsed lasers and laser driven X-ray sources such as a High Harmonics Generation (HHG) source and a Plasma X-ray Source (PXS) driven by high power kHz lasers [2,3].

The experimental stations include:

1. Atomic, Molecular and Optical (AMO) Science and Coherent Diffractive Imaging (CDI)

- 2: Soft X-ray Materials Science and time resolved magneto-optical ellipsometry [4]
- 3: Hard X-ray science, diffraction, spectroscopy and pulse radiolysis
- 4. Ultrafast UV-VIS-IR spectroscopy (fs ellipsometry [5], transient absorption [6], stimulated Raman, pulse shaping).

ELI is thought as a user facility open to all scientists. Details of how to submit a proposal to carry on experiments using ELI BL capabilities will be provided with examples of the results obtained by the first users.

Support by the projects Structural dynamics of biomolecular systems (CZ.02.1.01/0.0/0.0/15-003/0000447) and Advanced research using high intensity laser produced photons and particles (CZ.02.1.01/0.0/0.0/16-019/0000789) from the European Regional Development Fund is gratefully acknowledged.

- [1] G. Korn et al., CLEO 2013, OSA, Washington, D.C., p. CTu2D.7 (2013).
- [2] O. Hort et al., Opt. express **27**, 8871–8883 (2019).
- [3] J. Nejd et al., SPIE Proc.111110I (2019).
- [4] S Espinoza et al., Appl. Surf. Sci. **421**, 378-382 (2017).
- [5] S Espinoza et al., Appl. Phys. Lett. **15**, 052105 (2019).
- [6] V. Kuznetsova et al., BBA Bioenergetics **1861**, 148120 (2019).

New high-density radical source for investigating conformational and state-specific effects in chemical reactions

P. Stranak¹, L. Ploenes¹, H. Gao^{1,2}, F. Stienkemeier³, K. Dulitz³, J. Küpper^{4,5,6}
and S. Willitsch¹

¹*Department of Chemistry, University of Basel, Klingelbergstrasse 80,
4056 Basel, Switzerland
(corresponding author: P. Stranak, e-mail: patrik.stranak@unibas.ch)*

²*Present address: Beijing National Laboratory of Molecular Sciences, Institute of Chemistry,
Chinese Academy of Sciences, Beijing 100190, China*

³*Institute of Physics, University of Freiburg, Hermann-Herder-strasse 3,
79104 Freiburg, Germany*

⁴*Center for Free-Electron Laser Science, DESY, Notkestrasse 85, 22607 Hamburg, Germany*

⁵*Department of Physics and The Hamburg Center for Ultrafast Imaging, University of
Hamburg, Luruper Chaussee 149, 22761 Hamburg, Germany*

⁶*Department of Chemistry, University of Hamburg, Martin-Luther-King-Platz 6,
20146 Hamburg, Germany*

Despite their great importance, the influence of molecular conformations and individual quantum states on the mechanisms and dynamics of chemical reactions is still insufficiently characterized. Due to thermal interconversion, the isolation and control of individual conformers was for a long time a major obstacle in their experimental investigation. Recently, the successful spatial separation of conformers and rotational states of molecules entrained in a molecular beam was demonstrated using an electrostatic deflector.¹ The resulting molecular beams of state- and conformationally selected species provide the starting point to perform controlled, state- and conformer-selective reaction experiments.² Using this approach, studies of the conformation and state specific reaction dynamics have already been successfully performed in the investigation of reactive collisions of 3-aminophenol with a Coulomb crystal of Ca⁺ ions and, more recently, of the nuclear-spin isomers of water with sympathetically cooled N₂H⁺ ions.^{3,4}

Here, we present a new high-density, high-frequency pulsed molecular-beam source for fluorine atoms and other radicals. A supersonic beam of fluorine radicals is produced by means of a DC plate or dielectric-barrier discharges using a CRUCS valve⁵. The performance of these two discharge techniques for producing fluorine atoms and metastable species is characterized and compared. The high radical

densities achieved with this source in combination with good long-term stability over a broad range of working parameters at experimental repetition rates up to 200 Hz make the source an ideal tool for crossed beam studies.

The source is implemented in a crossed-molecular beam machine in which a beam of free radicals is crossed with a beam of spatially separated conformers or rotational-state selected molecules. Product detection is performed by a combination of time-of-flight mass spectrometry and velocity-map imaging⁶ enabling to obtain angle-, energy- and mass-resolved distributions of the reaction products. First target systems include the reactions of halogen radicals and metastable excited rare gas atoms with rotationally state-selected molecules, such as OCS and H₂O. In combination with a complementary setup for ion-molecule reactions^{2,3,4}, this experiment gives us the means to characterize the mechanistic details of conformationally and state selected reactions from the synergistic perspective of both, ionic and neutral reaction partners.

- [1] Y. P. Chang, et. al., *Int. Rev. in Phys. Chem.* **34**, 557-590 (2015).
- [2] S. Willitsch, *Adv. Chem. Phys.* **162**, 307 (2017).
- [3] Y. P. Chang, et. al., *Science* **342** (6154), 98-101 (2013).
- [4] A. Kilaj et. al., *Nat. Commun.* **9**, 2096 (2018).
- [5] J. Grzesiak et al., *Rev. Sci. Instrum.* **89**, 113103 (2018).
- [6] A. T. J. B. Eppink et. al., *Rev. Sci. Instrum.* **68**, 3477 (1997).

Plasma polymerized oxazoline based thin films for biomedical applications

Pavel Stahel, Vera Mazankova^{1,2}, Klara Tomeckova², Antonin Brablec, Lubomir Prokes,
Jana Jurmanova, Marian Lehocky³, Petr Humpolicek³,
Kadir Ozaltin³, David Trunec

*Department of Physical Electronics, Masaryk University,
Kotlarska 2, 611 37 Brno, Czech Republic
(corresponding author: D. Trunec, e-mail:trunec@physics.muni.cz)*

¹ *Department of Mathematics and Physics, Faculty of Military Technology, University of Defence in
Brno, Kounicova 65, 662 10 Brno, Czech Republic*

² *Institute of Physical and Applied Chemistry, Faculty of Chemistry, Brno University of Technology,
Purkynova 118, 612 00 Brno, Czech Republic*

³ *Centre of Polymer Systems, Tomas Bata University in Zlín, Trida Tomase Bati 5678, 760 01 Zlín,
Czech Republic*

1. Introduction

Polyoxazolines (POx) are a promising class of polymers that have attracted substantial attention recently due to their antibiofouling properties [1,2] and good biocompatibility [3]. Usually, POx are prepared by living-cationic ring opening polymerization, which is a lengthy wet process conducted in organic solvents. POx thin films are created in a subsequent step, which needs to be tailored for any particular types of substrates [4,5]. Other possible polymerization techniques are photocoupling [6] and grafting [7], and both techniques require the premodification of substrates. So, the formation of polyoxazoline coatings using conventional methods is slow and a complex multistep procedure, which can be conducted only on a limited range of substrates. The difficulties of these conventional methods can be overcome via plasma polymerization. Plasma polymerization is known to be a suitable method for the deposition of many biomaterial coating [8,9].

In this contribution, a new way to produce plasma polymerized oxazoline-based films with antibiofouling properties and good biocompatibility is presented. The films were created via the plasma deposition from 2-methyl-2-oxazoline vapours in nitrogen atmospheric pressure dielectric barrier discharge. Diverse film properties were achieved by increasing the substrate temperature at the deposition. The physical, chemical and biological properties of plasma polymerized polyoxazoline films were studied by SEM, EDX, FTIR, antibacterial and cytocompatibility tests. After tuning of the deposition parameters, films having the capacity to resist bacterial biofilm formation were achieved. Deposited films also promote cell viability.

2. Experimental

Plasma polymerization was performed in a custom build reactor (metallic chamber with dimensions 500 mm × 500 mm × 500 mm) with dielectric barrier discharge [10]. The discharge was generated between two planar metal electrodes. The bottom electrode with dimensions 150 mm × 55 mm could be heated using a heating spiral, and the electrode temperature was measured with a thermocouple. The upper electrode with dimensions 55 mm × 40 mm was covered with glass, 1.5 mm in thickness. A slit 2 mm wide in the centre of the upper electrode was used for the supply of working gas with the monomer to the discharge. The scheme of the electrode system can be found in a previous study [11], where also gas flow in the discharge gap was modelled. The glass substrates were cleaned in a mixture of cyclohexane and isopropylalcohol (1 : 1) and dried by airflow. Clean substrates were put into the reactor on the bottom electrode, which was then entirely covered by the substrate. The discharge gap between the substrate and the upper electrode was set to be 1.0 mm. Before starting the depositions, the discharge chamber was pumped down to a pressure of 100 Pa and then filled with nitrogen to a pressure of 101 kPa. Atmospheric pressure during the deposition was maintained by slight pumping. The nitrogen flow with flow rate of 100 sccm bubbled through the liquid 2-methyl-2-oxazoline monomer in a glass bottle container. This flow was then mixed with the main nitrogen flow with the flow rate of 500 sccm. The temperature of the monomer was kept constant and it was set to 20 °C. The monomer flow rate was determined by the weighing of monomer before and after the deposition, thus determined monomer flow rate was 20 mg s⁻¹. High voltage with the frequency 6 kHz was used for the generation of dielectric barrier discharge in the discharge gap. The discharge was burning in homogeneous atmospheric pressure Townsend like mode [11], which is suitable for the deposition of homogeneous thin films. The discharge mode was checked by current-voltage measurements using an oscilloscope. The input power to a high voltage source was set to 55 W and it was constant in all experiments presented in this contribution. The temperature of the bottom electrode was increased to a given value before the deposition. The upper electrode was periodically moving with a speed of 0.6 cm s⁻¹ above the substrate during the deposition in order to ensure even greater homogeneity of the deposited film. The deposition time was 23 min.

Deposited films were imaged with scanning electron microscope MIRA3 (TESCAN, Czech republic) equipped with secondary electron and back-scattered electron detectors as well as characteristic X-ray detector (EDX) analyser (Oxford Instruments, UK). The IR spectra of deposited films were measured by FTIR spectrometer Alpha (Bruker, USA) using a single reflection ATR module Platinum.

Antibacterial tests were performed according to the ISO 22196 procedure with modifications. For the determination of antibacterial performance, gram positive *Staphylococcus aureus* and gram negative *Escherichia coli* were used.

The mouse embryonic fibroblast continuous cell line (NIH/3T3, ATCC CRL-1658™, USA) was used for cytocompatibility test, according to the EN ISO 10993-5 standard, with modification.

3. Results

The POx films were deposited at substrate temperatures 60 °C, 90 °C, 120 °C and 150 °C and at nitrogen flow of 100 sccm through the monomer. It was found that the POx films deposited at substrate temperatures up to 90 °C can be washed by water from the substrate.

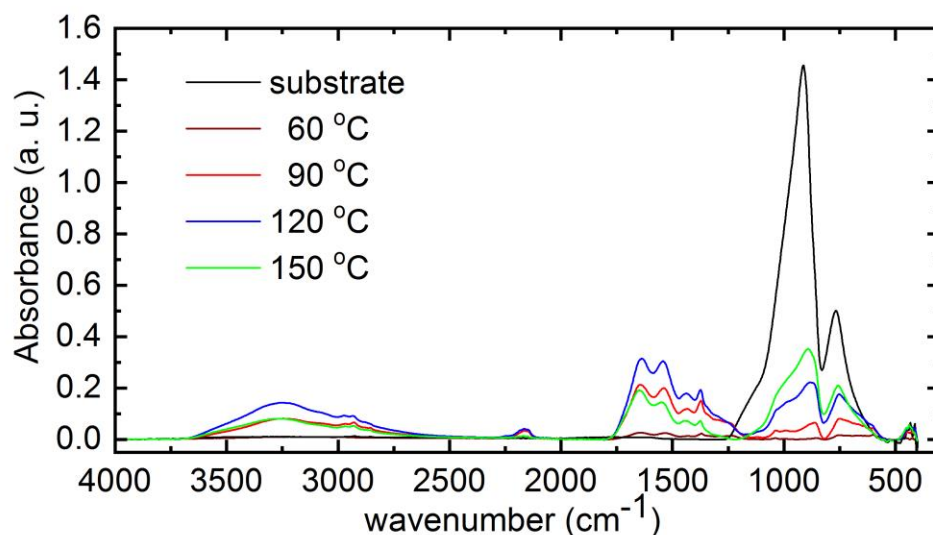


Fig 1. FTIR spectra of thin films deposited at different substrate temperatures.

The FTIR spectra of POx films are shown in Figure 1. Very low absorbance for the film deposited at substrate temperature of 60 °C was caused by small film thickness. Broad absorption band in the range 3000--3600 cm^{-1} consists of several peaks belonging to OH, NH and NH_2 groups. The bands at 2950 cm^{-1} , 1450 cm^{-1} and 1370 cm^{-1} are characteristic for vibrations of CH_3 and CH_2 groups. The band at 2170 cm^{-1} can be attributed to alkyne $\text{C}\equiv\text{C}$ and/or isocyanate $\text{O}=\text{C}=\text{N}$ and nitrile $\text{C}\equiv\text{N}$. Such chemical bonds are not present at traditional polymerization of oxazolines and they can be attributed to fragmentation and recombination of the oxazoline monomer during plasma polymerization. The band between 1790 cm^{-1} and 1590 cm^{-1} is characteristic for stretching vibration $\text{C}=\text{N}$ bond constituting the oxazoline ring. Its presence in IR spectrum indicates the presence of oxazoline rings in deposited films. The band around 1550 cm^{-1} belongs to N-H bonds. Finally, the bands below 1000 cm^{-1} belong to Si-O-Si or Si-O bonds from substrate glass.

The cytocompatibility tests showed that the films deposited at 60 °C and 90 °C exhibit almost identical cell viability as the blank substrate. However, in the case of the film deposited at 120 °C, the viability increased significantly when reaching the value of almost 180%. The highest fibroblasts cell viability was observed for the film deposited at 150 °C when the value was more than 270% what signifies an excellent compatibility to used cell substrate. The above mentioned results suggest that oxazoline based thin films are affecting cell behaviour, especially cell attachment. Moreover, with rising deposition temperature, the cell viability value is increasing.

Tab. 1. Antibacterial activity results of studied POx films.

Samples	<i>S. aureus</i> , N (CFU/cm ²)	<i>E. coli</i> , N (CFU/cm ²)
substrate	1.3×10^6	2.0×10^5
60 °C	<1	4.4
90 °C	<1	1.1
120 °C	<1	4.4
150 °C	1.6	5.4

Antibacterial activity against *S. Aureus* and *E. Coli* strains after 72 h of incubation time for the samples are listed in Table 1. The reference substrate glass was open to both gram positive and negative bacterial contamination and did not perform any antibacterial effect, as expected. Nevertheless, counted viable gram positive *S. aureus* level was found almost five times higher than the gram negative *E. coli* strain. The oxazoline based thin film deposited samples were highly active against both bacterial strains. The effect of the oxazoline based thin film against *S. aureus* was slightly higher compared to *E. coli*, but the differences were negligible. Among them, the sample deposited at 150 °C performed slightly lower antibacterial activity against both strains compared to other oxazoline based thin film deposited samples, probably due to its higher bonding performance. However, it is also negligible, since the difference is extremely low.

Based on results shown above it can be concluded that all deposited films exhibited excellent antibacterial properties against both bacterial strains used for antibacterial tests. The best cell viability results were found at films deposited at substrate temperatures of 120 °C and 150 °C. Lower cell viability on films deposited at substrate temperatures of 60 °C and 90 °C can be explained by their dissolvability in aqueous solvents. Deposited films could be used for wound healing or as the coatings with antibacterial and antibiofouling properties.

4. Acknowledgement

Support by the Ministry of Education, Youth and Sports of the Czech Republic is gratefully acknowledged.

5. References

- [1] M. C. Woodle et al., *Bioconjugate Chem.* **5**, 493 (1994).
- [2] S. Zalipsky et al., *J. Pharm. Sci.* **85**, 133 (1996).
- [3] P. Goddard et al., *J. Controlled Release* **10** 5 (1989).
- [4] R. Jordan et al., *J. Am. Chem. Soc.* **120**, 243 (1998).
- [5] P.J. M. Bouten et al., *Polym. Chem.* **6**, 514 (2015).
- [6] H. Wang et al., *ACS Appl. Mater. Interfaces* **3**, 3463 (2011).
- [7] B. Pidhatika et al., *Biointerphases* **7**, 110.1007/s13758-011-0001-y (2012).
- [8] K.Vasilev, *Plasma Chem. Plasma Process.* **34**, 545 (2014).
- [9] K.S.Siow et al., *Plasma Processes Polym.* **3**, 392 (2006).
- [10] D. Trunec et al., *J. Phys. D: Appl. Phys.* **43**, 225403 (2010).
- [11] A. Obrusnik et al., *Surface & Coatings Technology* **314**, 139 (2017).
- [12] D. Trunec et al., *J. Phys. D: Appl. Phys.* **37**, 2112 (2004).

Chirality transfer in a non-covalent molecular network

Jan Voigt, Milos Baljozovic, Christian Wäckerlin, Kévin Martin¹, Narcis Avarvari¹,
Karl-Heinz Ernst

*Empa, Swiss Federal Laboratories for Materials Science and Technology,
8600 Dübendorf, Switzerland
(corresponding author: K. Ernst, e-mail: Karl-Heinz.Ernst@empa.ch)*

¹*Université d'Angers, 40 Rue de Rennes, 49035 Angers, France*

Chirality is more than its own mirror. It is a multi-scale phenomenon [1], an indirect representative of the fundamental symmetries in nature [2] and a property with handy applications [3,4]. Studying the interdependence of microscopic and macroscopic chirality, i.e. the chiral crystallization process on single crystal templates, proved itself an important aspect of the field [5] from Pasteur's initial discovery towards modern surface science.

In this regard, the 2D crystallization of benzene – 1,3,5 – tris – tetrahelicene on the Ag(111) surface is studied with scanning tunneling microscopy. The molecule consists of three tetrahelicene sub-units attached to a central benzene ring via sigma bonds. With the respective building blocks, it exhibits an intrinsic chiral hierarchy and high configurational flexibility. Indeed, deposition on the sample kept at room temperature leads to self-assembled arrays of spiral shaped tris-helicenes. Above a critical coverage and temperature, a transfer of chirality from the single molecules to the self-assembled domain is observed. Topology and handedness of the supramolecular networks are linked to azimuthal orientation and handedness of single molecules.

Support by the Swiss National Science Foundation is gratefully acknowledged.

- [1] G. H. Wagnière, *On Chirality and the Universal Asymmetry: Reflections on Image and Mirror Image*. John Wiley & Sons, 2008.
- [2] M. Quack, "Molecular Parity Violation and Chirality: The Asymmetry of Life and the Symmetry Violations in Physics," in *Quantum Systems in Chemistry and Physics*, vol. 26, K. Nishikawa, J. Maruani, E. J. Brändas, G. Delgado-Barrio, and P. Piecuch, Eds. Dordrecht: Springer Netherlands, 2012, pp. 47–76.
- [3] R. Naaman and D. H. Waldeck, "Spintronics and Chirality: Spin Selectivity in Electron Transport Through Chiral Molecules," *Annu. Rev. Phys. Chem.*, vol. 66, no. 1, pp. 263–281, 2015.
- [4] M. Ortega Lorenzo, C. J. Baddeley, C. Muryn, and R. Raval, "Extended surface chirality from supramolecular assemblies of adsorbed chiral molecules," *Nature*, vol. 404, no. 6776, pp. 376–379, Mar. 2000.
- [5] S. Dutta and A. J. Gellman, "Enantiomer surface chemistry: conglomerate *versus* racemate formation on surfaces," *Chem. Soc. Rev.*, vol. 46, no. 24, pp. 7787–7839, 2017.

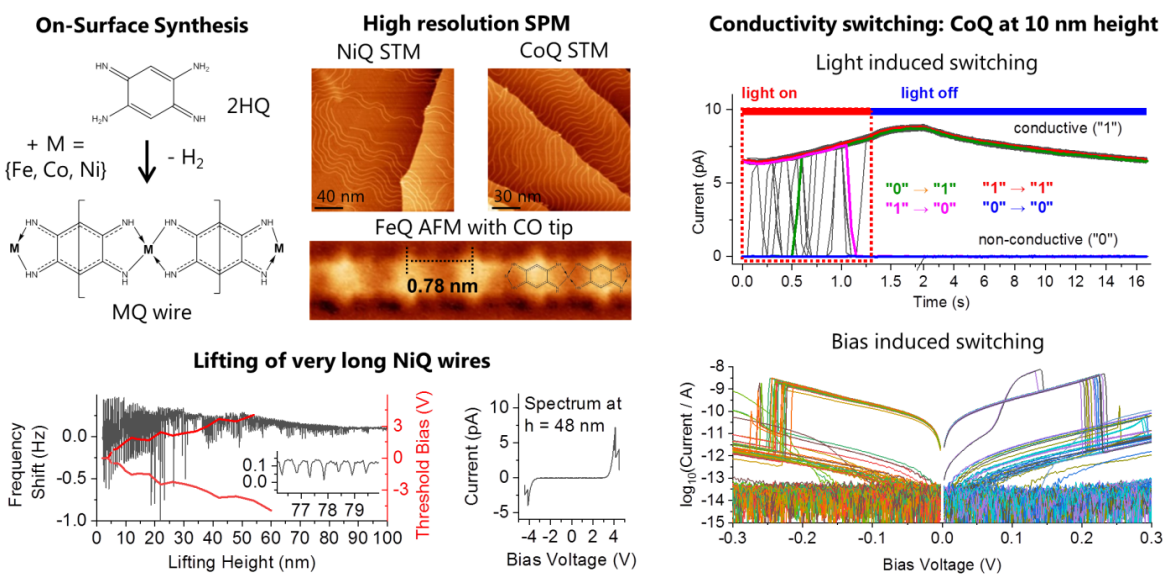
Electronic transport through 1D coordination polymers

*Christian Wäckerlin, Oleksander Stetsovych, Santhini Vijai Meena, Aleš Cahlik, Simon Pascal¹,
Martin Švec, Jesús Mendieta, Pingo Mutombo, Olivier Siri¹, Pavel Jelinek*

*Institute of Physics of the Czech Academy of Sciences, 162 00 Praha 6, Czech Republic
(corresponding author: C. Wäckerlin, e-mail: wackerlin@fzu.cz; christian@waeckerlin.com)*

¹*Aix Marseille Université, CNRS, CINaM UMR 7325, 13288, Marseille, France*

We report on the electric transport through transition metal based 1D coordination polymers (wires) suspended between the tip of a scanning probe microscope (SPM) and a Au(111) substrate. The wires are synthesized in-situ by co-deposition of the metal atoms and the quinonediimine (2,5-diamino-1,4-benzoquinone-diimine, 2HQ) ligand. Isostructural wires with lengths over 200 nm are obtained for Ni, Co and Fe. We are able to lift these wires quite far from the surface and to perform detailed transport measurements as a function of height and bias voltage.



The transition metal element contained in the organometallic wire has a profound impact on its transport properties: Fe and Ni wires exhibit a band gap at heights larger than 3 to 5 nm, but Co containing polymers are conductive without gap up to more than 12 nm. In addition, differential conductance measurements reveal pronounced steps at bias voltages of a few millivolts for Fe and Co wires but not for Ni ones. These conductance steps are attributed to spin excitations.

Finally, the conductivity of suspended CoQ wires can be switched by ~3 orders of magnitude by the electric bias and by irradiation with visible light. The switching by light is reversible (conductive \leftrightarrow non-conductive). Switching by bias occurs only in one way (conductive \rightarrow non-conductive) but the conductive state can be recovered by irradiation with light.

Support by the Swiss National Science Foundation is gratefully acknowledged.

A study of small iron clusters on Cu(111) by atomic force microscopy

Franz J. Giessibl

Institute of Experimental and Applied Physics, University of Regensburg, D-93053 Regensburg, Germany

e-mail: Franz.Giessibl@ur.de

Metal clusters on surfaces open exciting perspectives and show interesting features [1], ranging from their catalytic activity to magnetic properties [2]. Atomic force microscopy with CO terminated tips allows to resolve clusters at an unprecedented spatial resolution [3]. The clusters in Figure 1 had been created by thermal annealing, where a Cu(111) surface with adsorbed single Fe atoms was heated to about 15 K.

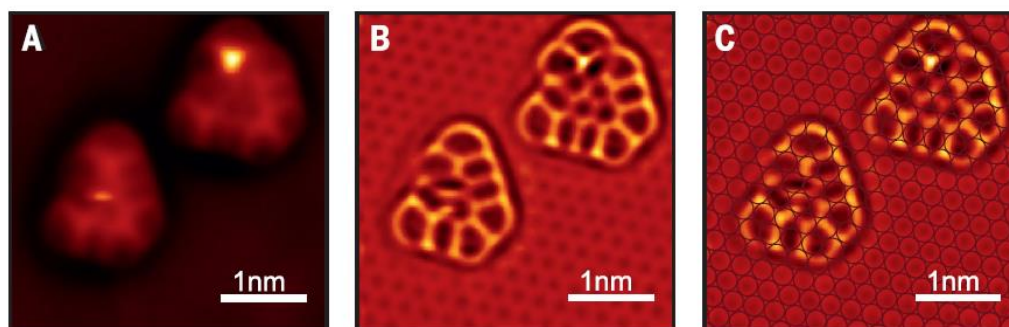


Fig. 1. AFM images of small metal clusters on Cu(111) using a CO terminated tip (Fig. 3 in [3]). **A** Frequency shift data. **B** Double Laplace filtered version of A, showing also the positions of the Cu substrate atoms. **C** Same as B with lattice overlay.

New measurements show that clusters from individual Fe atoms can be constructed in a controlled fashion by atomic assembly with CO terminated tips [4]. Ongoing studies investigate the chemical reactivity of these clusters as a function of the atomic position within the cluster [5].

Funded by the Deutsche Forschungsgemeinschaft (DFG, German Research Foundation) – Project-ID 314695032 – SFB 1277“.

- [1] Karl-Heinz Meiwes-Broer (Ed.), *Metal Clusters at Surfaces*, Springer 2000.
- [2] Alexander Ako Khajetoorians, Benjamin Baxevanis, Christoph Hübner, Tobias Schlenk, Stefan Krause, Tim Oliver Wehling, Samir Lounis, Alexander Lichtenstein, Daniela Pfannkuche, Jens Wiebe, Roland Wiesendanger, Current-driven spin dynamics of artificially constructed quantum magnets. *Science* **339**, 55 (2013).
- [3] Matthias Emmrich, Ferdinand Huber, Florian Pielmeier, Joachim Welker, Thomas Hofmann, Maximilian Schneiderbauer, Daniel Meuer, Svitlana Polesya, Sergiy Mankovsky, Diemo Ködderitzsch, Hubert Ebert, Franz J. Giessibl, Subatomic resolution force microscopy reveals internal structure and adsorption sites of small iron clusters, *Science* **348**, 308 (2015).
- [4] Julian Berwanger, Ferdinand Huber, Fabian Stilp, and Franz J. Giessibl, Lateral manipulation of single iron adatoms by means of combined atomic force and scanning tunneling microscopy using CO-terminated tips. *Phys. Rev. B* **98**, 195409 (2018).
- [5] Julian Berwanger et al., submitted.

Molecular nanostructures on metals vs. graphene

Brian Baker, Mihaela Enache, Stefano Gottardi, Remco W. A. Havenith, Anna K. H. Hirsch^{1,2}, Jun Li, Leticia Monjas¹, Juan Carlos Moreno Lopez, Nico Schmidt, Meike Stöhr

Zernike Institute for Advanced Materials, University of Groningen, Nijenborgh 4, 9747 AG Groningen, Netherlands (corresponding author: M. Stöhr, e-mail: m.a.stohr@rug.nl)

¹ *Stratingh Institute for Chemistry, University of Groningen, Nijenborgh 7, 9747 AG Groningen, The Netherlands*

² *Department of Pharmacy, Saarland University, 66123 Saarbrücken, Germany*

To preserve the (functional) properties of either individual adsorbates or well-ordered molecular assemblies upon adsorption on solid surfaces, the molecule substrate interactions have to be generally relatively weak. This can be achieved by introducing a decoupling layer between (metallic) surface and molecules. Among others, thin insulating layers of either NaCl or a single layer of hBN have been shown to be very useful to this end. The chemical inertness and the low density of states near the Fermi level also make graphene a good choice as a buffer layer to decouple adsorbed molecules from the underlying (metallic) substrate. Importantly, this holds the promise to preserve the intrinsic properties of the adsorbed species such as magnetic or catalytic properties. On the other hand, molecular self-assembly on graphene can be also employed as a promising method for tuning the electronic properties of graphene (doping or band gap opening) on a macroscopic scale while for this purpose, the molecule graphene interaction has to be larger than a mere physisorptive one.

Here we will discuss the structural and electronic properties for 1,3,5-benzenetribenzoic acid on graphene/Cu(111), for which different coverage dependent assemblies were observed. [1] We could demonstrate that the underlying Cu(111) surface influences the structural arrangement of the molecules. With respect to the electronic properties, angle-resolved photoemission spectroscopy measurements showed n-doping of graphene. For parahexaphenyl-dicarbonitrile (NC-Ph₆-CN) on graphene, we observed the arrangement of a close-packed structure with a peculiar shift of every 4th molecule independent of coverage. We concluded that the screening properties of graphene are responsible for this effect since such a shift was neither observed for the case of metallic substrates nor for the bulk phase. [2] Adding Cu adatoms to submonolayer coverage of NC-Ph₆-CN resulted in the formation of metal-organic coordination networks with varying arrangements in dependence of the stoichiometry between molecules and Cu atoms. With scanning tunneling spectroscopy we characterized the electronic properties and could identify differences between the different assembly structures. [3] On the basis of the self-assembly process of tetracyanophenyl porphyrins before and after coordination with Co-atoms on Au(111), the influence of molecular coverage on decoupling could be demonstrated [4].

Support by the Netherlands Organisation for Scientific Research and by the European Research Council is gratefully acknowledged.

- [1] J. Li et al., J. Phys. Chem. C **120**, 18093 (2016); N. Schmidt et al., in preparation.
- [2] N. Schmidt et al., Chem. Eur. J., **25**, 5065 (2019).
- [3] J. Li et al., J. Phys. Chem. C **123**, 12730 (2019).
- [4] B.D. Baker et al., J. Phys. Chem. C **123**, 19681 (2019).

Structural changes of buckybowls via selective on-surface hydrogenation

Christian Wäckerlin^{1,2}, Aurelio Gallardo^{2,3}, Anaïs Mairena¹, Milos Baljozovic¹, Aleš Cahlík², Pavel Jelínek², Karl-Heinz Ernst^{1,2,4}

¹ *Empa, Swiss Federal Laboratories for Materials Science and Technology, 8600 Dübendorf, Switzerland (corresponding author: M. Baljozovic, e-mail: milos.baljozovic@empa.ch)*

² *Institute of Physics of the Czech Academy of Sciences, Cukrovarnická 10, 162 00 Praha 6, Czech Republic*

³ *Faculty of Mathematics and Physics, Charles University, V Holešovičkách 2, 180 00 Prague, Czech Republic*

⁴ *Department of Chemistry, University of Zürich, 8057 Zürich, Switzerland*

Ullmann and Scholl coupling reactions are among numerous surface reactions by far the most successful in the creation of C-C bonds at surfaces.[1] Vast number of systems with peculiar properties such as bis/tris-helicenes [2], [3], graphene nanoribbons [4] and carbon nanotubes [5] can be thus reliably and predictably created in a bottom-up approach when the polycyclic aromatic hydrocarbons (PAHs) are used as precursors. The opposite process, namely unzipping of C60 into Nano-Graphenes occurs only at high temperatures and in hydrogen atmosphere. [6] Here, we demonstrate that the hydrogenation of buckybowl pentaindenocorannulene (PIC) on Cu(100) occurs in a step-wise manner at the temperatures significantly lower than previously reported. The hydrogen uptake is easily tracked by ToF-SIMS and showed that initially two hydrogens followed by another two are added to the molecules. This is most probably a consequence of specific adsorption of the "bowl up" molecules on Cu(100) substrate - DFT calculations and AFM height measurements strongly suggest that in this configuration the bowl is immersed into a 4-atom vacancy in the surface thus allowing access to the strained C-C bond between two indeno groups for hydrogenation/cleavage. Following this step, a C-C bond cleavage in the now exposed centered pentagonal ring is observed. The planarization of PIC molecules through hydrogenation is corroborated by HR-STM and nc-AFM. Moreover, both steps lead to the formation of non-Kekulé PAHs with an open shell electronic structure.

Financial support by the Swiss National Science Foundation (SNF) is gratefully acknowledged. CW thanks the SNF for a Mobility fellowship. KHE thanks the European Union for granting a Mobility Professorship. We thank Samuel Lampard and Jay Siegel for providing the PIC compound.

- [1] J. Björk *et al.*, *Chemistry - A European Journal*, vol. 20, no. 4, pp. 928–934, 2014.
- [2] J. Li *et al.*, *Chemical Communications*, vol. 54, no. 57, pp. 7948–7951, 2018.
- [3] A. Mairena *et al.*, *Journal of the American Chemical Society*, vol. 140, no. 45, pp. 15186–15189, 2018.
- [4] J. Cai *et al.*, *Nature*, vol. 466, p. 470, 2010.
- [5] J. R. Sanchez-Valencia *et al.*, *Nature*, vol. 512, p. 61, 2014.
- [6] A. V. Talyzin *et al.*, *J. Phys. Chem. C*, vol. 118, no. 12, pp. 6504–6513, 2014.

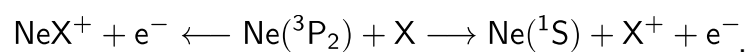
Low-energy stereodynamics in merged beams

Andreas Osterwalder

Institute for Chemistry and Chemical Engineering (ISIC), Ecole Polytechnique Fédérale de Lausanne (EPFL), Switzerland

andreas.osterwalder@epfl.ch

I will be presenting our recent experiments on stereodynamics in merged beams[1,2]. We studied sub-Kelvin stereodynamics in a prototypical energy transfer reaction, namely between metastable $\text{Ne}(^3\text{P}_2)$ and rare gas atoms [2,3] or diatomic molecules N_2 or CO [1,4]. Such reactions can proceed along two pathways according to



called Penning ionization (producing X^+) and associative ionization (producing NeX^+), respectively. At high energies the branching ratio between these channels can be controlled through the orientation of the $\text{Ne}(^3\text{P}_2)$ atom, but this ability is lost at low energies due to a reorientation of the reactants.

Secondary reactants like N_2 are particularly interesting because the vibrational structure of N_2^+ can be seen in associative ionisation as a new channel wherein the NeN_2^+ predissociates by transfer of vibrational energy from the N_2^+ moiety to the Ne-N_2^+ bond. Product vibrational state distributions were measured by velocity map imaging the electrons formed during the chemi-ionisation. The resulting information on the energy partitioning in the products is key to gain a full understanding of these reactions.

References

- [1] J. Zou, S.D.S. Gordon, S. Tanteri, and A. Osterwalder, *J. Chem. Phys.* **148**, 164310 (2018).
- [2] S.D.S. Gordon, J.J. Omiste, J. Zou, S. Tanteri, P. Brumer, and A. Osterwalder, *Nature Chemistry* **43**, 7279 (2018).
- [3] S.D.S. Gordon, J. Zou, S. Tanteri, J. Jankunas, and A. Osterwalder, *Phys. Rev. Lett.* **119**, 053001 (2017).
- [4] J. Zou, S.D.S. Gordon, and A. Osterwalder, *Phys. Rev. Lett.* **123**, 133401 (2019).

VIBRATIONAL ENERGY POOLING STUDIED BY MID-INFRARED LASER INDUCED FLUORESCENCE WITH A SUPERCONDUCTING NANOWIRE SINGLE PHOTON DETECTOR

Alec M. Wodtke

Max Planck Institute for Biophysical Chemistry, Göttingen Germany

Institute for Physical Chemistry, University of Göttingen, Germany

Using a mid-infrared emission spectrometer based on a superconducting nanowire single-photon detector (SNSPD), we observe the dynamics of vibrational energy pooling of CO adsorbed at the surface of a NaCl crystal. After laser-exciting a majority of the CO molecules to their first vibrationally excited state ($v=1$), we observe infrared emission from states up to $v=27$. Kinetic Monte Carlo simulations show that vibrational energy collects in a few CO molecules at the expense of those up to eight lattice sites away by selective excitation of NaCl's transverse phonons. The vibrating CO molecules behave like classical oscillating dipoles, losing their energy to NaCl lattice-vibrations via the electromagnetic near-field. This is a weak coupling limit where the anharmonic interatomic forces normally so important to energy flow can be completely neglected. SNSPDs enable novel laser induced fluorescence experiments with high temporal and spectral resolution with which we are able to observe interconversion from "the right-side up" to the "up-side down" orientational isomer of surface bound CO on NaCl. In its ground state, dipolar ($C^{\delta-}O^{\delta+}$) exhibits an electrostatic bond with the C atom adjacent to a Na^+ ion. Upon vibrational excitation, the dipole moment reverses sign ($C^{\delta+}O^{\delta-}$) causing rotation of the molecule and bringing the O atom close to the Na^+ ion. The binding strength of CO to NaCl arises predominantly from the interaction of molecule's quadrupole with the electric field gradient near the Na^+ ion, which is independent of orientation. Hence, the two orientational isomers exhibit similar stability. This remarkable system offers a unique opportunity to test modern theory's ability to describe quantum dynamical processes in the condensed phase.

Single-Molecule Motion at Surfaces

Leonhard Grill

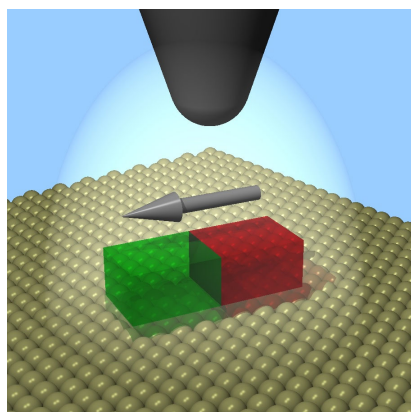
Single-Molecule Chemistry group

University of Graz, Austria

(www.nanograz.com; leonhard.grill@uni-graz.at)

Studying single-molecule motion at single-crystal surfaces holds various advantages: (i) highly defined potential landscapes of flat and stepped surfaces with specific chemical properties, (ii) directly visualization of single molecules and their pathways by scanning probe microscopy, (iii) manipulation to induce chemical processes (including motion) in a controlled way with the microscope tip, (iv) two-dimensional confinement of the motion and thus the possibility to follow single-molecule trajectories, and (v) identification of surface defects and thus control over the atomic-scale surroundings of each molecule.

In this presentation, various cases of mobile molecules at surfaces, studied by scanning tunneling microscopy (STM), will be discussed. The chemical structure of the molecule defines preferential orientations and directions of motion. Weak adsorption is advantageous for



efficient motion, which could be achieved by specific molecular side groups [1]. The same molecules can also be rotated with 100% directionality via an electric dipole in the molecule (as sketched in the figure) [2], even allowing to map the electric dipole of the molecule via the molecular response to the applied field. For azobenzene switching units in a tetrahedral arrangement not only reversible photo-isomerization for the upright standing unit is found, due to decoupling, but also isomer-dependent diffusion on the surface is observed [3]. On the other hand, by incorporating

isomerization-based molecular ‘Feringa’ motors, photo-enhanced and wavelength-sensitive translation of molecular machines is observed on a metal surface [4]. Importantly, the light does not change the *number* of moving molecules, but their lateral *displacement*. Beyond individual molecules, polymer chains can be moved with the microscope tip, both across and off the surface [5]. When pulling the wires off the surface, not only the electric current and forces can be measured and features can be assigned to specific structural defects in the molecule [6], but also various charge transport channels – with different chemical conjugations – can be identified in non-symmetrical molecular nodes [7].

- [1] G. J. Simpson et al., *Nature Nanotech.* 12, 604 (2017); [2] G. J. Simpson et al., *Nature Comm.* 10, 4631 (2019); [3] C. Nacci et al., *Angew. Chem. Int. Ed.* 57, 15034 (2018); [4] A. Saywell et al., *ACS Nano* 10, 10945 (2016); [5] L. Lafferentz et al., *Science* 323, 1193 (2009); [6] M. Koch et al., *Phys. Rev. Lett.* 121, 047701 (2018); [7] C. Nacci et al., *Angew. Chem. Int. Ed.* 55, 13724 (2016)

Quantum non-demolition state detection and spectroscopy of single trapped molecules

Mudit Sinhal, Ziv Meir, Aleksandr Shlykov and Stefan Willitsch

Department of Chemistry, University of Basel, Klingelbergstrasse 80, 4056 Basel, Switzerland

Trapped atoms and atomic ions are among the best controlled quantum systems which find widespread applications in quantum information, sensing and metrology. Owing to the complex energy level structure and the absence of optical cycling transitions in most molecular systems, quantum-state control, non-destructive state detection, state-and energy-controlled reactions and precision spectroscopic studies constitute a major challenge with molecules. Molecular ions trapped in radiofrequency ion traps which are sympathetically cooled by simultaneously trapped atomic ions [1, 2] have proven a promising route for overcoming these obstacles. In such experiments, quantum-logic protocols in which the atomic ions serve as probes for the molecular ions can be employed for achieving ultimate quantum control of molecular ions [3, 4].

We present a novel quantum-logic based quantum-non-demolition (QND) state-detection scheme of a single molecular nitrogen ion which is co-trapped with a single atomic calcium ion in an ion trap [3, 5]. Since N_2^+ is a homonuclear diatomic molecule with no permanent dipole moment, all rovibrational transitions are rendered dipole forbidden in its electronic ground state. Therefore, N_2^+ is an ideal testbed for precision spectroscopic studies [6], for tests of fundamental physics, for the realization of mid-IR frequency standards and clocks [7] and for the implementation of molecular qubits for quantum-information and computation applications [8].

Our state-detection protocol relies on coherent motional excitation of the $Ca^+ - N_2^+$ two-ion string [3-5, 9, 10] using an optical-dipole force (ODF). The magnitude of the excited motion is dependent on the molecular state and arises from a parametrically modulated ac-Stark shift experienced by the molecule due to off-resonant dispersive molecule-light interactions. Thus, we entangle the molecular state with the coherent motion of the two-ion crystal which is then read out on the Ca^+ ion without perturbing the N_2^+ ion, and hence preserving its state. We demonstrate state-detection fidelities above 99% for the ground rovibrational state of N_2^+ , limited only by the chosen bandwidth of the detection cycle.

As an application of our state-detection protocol, we demonstrate a type of “force” spectroscopy [3] which is used to study the $R_{11}(1/2)$ rovibronic component of the $A^2\Pi_u$ ($v' = 2$) $\leftarrow X^2\Sigma_g^+$ ($v'' = 0$) electronic-vibrational transition in N_2^+ . We perform the spectroscopy by measuring the excited coherent motion, and hence determining the ac-Stark shift experienced by the molecule at various laser detunings from the transition resonance. Our signal-to-noise ratio greatly exceeds previous destructive measurement schemes for trapped particles [11,

12]. We determine transition properties such as the line center and the Einstein-A coefficient which is validated against the results of previous studies using conventional and destructive spectroscopic methods.

Our QND scheme is universally applicable to both polar and apolar molecular ions. It represents a highly sensitive method to repeatedly and non-destructively read out the quantum state of a molecule and thus introduces a molecular counterpart to the state-dependent fluorescence on closed- cycling transitions which forms the basis of sensitive readout schemes in atomic systems [13]. It enables state-selected and coherent experiments with single trapped molecules with duty cycles several orders of magnitude higher than previous destructive state-detection schemes thus laying the foundations for vast improvements in the sensitivity and, therefore, precision of spectroscopic experiments on molecular ions. We are currently developing a precise, narrow-linewidth quantum-cascade laser to perform precision spectroscopy on a dipole-forbidden vibrational transition at 65 THz using the state detection scheme. We target a laser-limited relative measurement accuracy of the order 10^{-14} - 10^{-15} in the first attempt as compared to the present state-of-the-art of 10^{-9} [12, 14].

The possibility for efficient, non-destructive state readout also lays the foundation for the application of molecular ions in quantum-information, coherent-control experiments and realizing quantum memories. As another application, our scheme also enables studies of cold collisions and chemical reactions between ions and neutrals with state control on the single-molecule level and, therefore, offers prospects for the exploration of molecular collisions and chemical reaction mechanisms in exquisite detail.

- [1] K. Mølhave and M. Drewsen, *Phys. Rev. A* 62, 011401 (2000).
- [2] S. Willitsch, *Int. Rev. Phys. Chem.* 31, 175 (2012).
- [3] M. Sinhal, Z. Meir, K. Najafian, G. Hegi and S. Willitsch, arXiv preprint:1910.11600.
- [4] F. Wolf, Y. Wan, J. C. Heip, F. Gebert, C. Shi, and P.O. Schmidt, *Nature* 530, 457 (2016).
- [5] Z. Meir, G. Hegi, K. Najafian, M. Sinhal, and S. Willitsch, *Faraday Discuss.* 217, 561 (2019).
- [6] M. Kajita, *Phys. Rev. A* 92, 043423 (2015).
- [7] S. Schiller, D. Bakalov, and V. I. Korobov, *Phys. Rev. Lett.* 113, 023004 (2014).
- [8] S. Wehner, D. Elkouss, and R. Hanson, *Science* 362, eaam9288 (2018).
- [9] D. Hume, C. W. Chou, D. R. Leibbrandt, M. J. Thorpe, D. J. Wineland, and T. Rosenband, *Phys. Rev. Lett.* 107, 243902 (2011).
- [10] J. C. Koelemeij, B. Roth, and S. Schiller, *Phys. Rev. A* 76, 023413 (2007).
- [11] M. Germann, X. Tong, and S. Willitsch, *Nat. Phys.* 10, 820 (2014).
- [12] S. Alighanbari, M. G. Hansen, V. I. Korobov, and S. Schiller, *Nat. Phys.* 14, 555 (2018).
- [13] T. P. Harty, D. T. C. Allcock, C. J. Ballance, L. Guidoni, Janacek, N. M. Linke, D. N. Stacey, and D. M. Lucas, *Rev. Lett.* 113, 220501 (2014).
- [14] J. Biesheuvel, J. P. Karr, L. Hilico, K. S. E. Eikema, W. Ubachs, and J. C. J. Koelemeij, *Nat. Commun.* 7, 10385 (2016).

Nucleophilic substitution and ligand exchange dynamics in bimolecular collisions with microhydrated anions

Björn Bastian, Tim Michaelsen, Jennifer Meyer, Atilay Ayasli, Roland Wester

*Institut für Ionenphysik und Angewandte Physik,
6020 Innsbruck, Austria*

(corresponding author: R. Wester, e-mail: roland.wester@uibk.ac.at)

Reaction dynamics simulations and experimental findings on the gas phase $X^- + CH_3Y$ reactions have challenged the traditional view of nucleophilic substitution (S_N2) reactions with a multitude of involved stationary points and new mechanisms [1,2]. Microsolvation of the reactant anion offers a stepwise approach towards reaction dynamics in the liquid phase and adds further complexity. A previous study with $OH^-(H_2O) + CH_3I$ has shown that the first water molecule can steer the anion towards the C–I axis and enhance the Walden inversion mechanism in a flat entrance potential energy surface [3]. At the product side, the anion, neutral or none of them may be hydrated. The energetically favored formation of solvated products is typically suppressed and mechanisms such as association and ligand switching become important with increasing solvation [4]. For $F^-(H_2O)_n + CH_3I$ theory reports the early ejection of water molecules and nucleophilic substitution through a less solvated barrier [5].

Here we will present results on reactive collisions of $O_2^-(H_2O)_n$ ($n=1,2$), $Cl^-(H_2O)$ and $F^-(H_2O)$ with CH_3I from a crossed-beam imaging experiment. In case of direct mechanisms, the product angle distribution corresponds to the impact parameter and is linked to the opacity function. Isotropic distributions and low kinetic energies point to indirect pathways.

$F^-(H_2O)$ results at 0.32 eV collision energy agree with the predicted I^- to $I^-(H_2O)$ branching but do not confirm about 30 % of direct mechanisms [6]. Direct rebound is not observed below 1.5 eV collision energy. Monohydrated Cl^- and O_2^- show only indirect dynamics at low collision energy and only the latter gives rise to a small fraction of solvated I^- products. Further unexpected results were obtained for the ligand exchange mechanism with images evolving from isotropic via forward to dominant backward scattering with increasing energy.

- [1] J. Meyer, R. Wester, *Annu. Rev. Phys. Chem.* **68**, 333 (2017).
- [2] D. A. Tasi, Z. Fábián, G. Czakó, *Phys. Chem. Chem. Phys.* **21**, 7924 (2019).
- [3] R. Otto, J. Brox, M. Stei, S. Trippel, T. Best, R. Wester, *Nat. Chem.* **4**, 534 (2012).
- [4] J. V. Seeley, R. A. Morris, A. A. Viggiano, *J. Phys. Chem. A* **101**, 4598 (1997).
- [5] X. Liu, J. Xie, J. Zhang, L. Yang, W. L. Hase, *J. Phys. Chem. Lett.* **8**, 1885 (2017).
- [6] J. Zhang, L. Yang, L. Sheng, *J. Phys. Chem. A* **120**, 3613 (2016).

Reaction kinetics of trapped molecular ions with conformer- and isomer-selected neutral molecules

Ardita Kilaj¹, Hong Gao¹, Daniel Rösch¹, Uxia Rivero¹, Jochen Küpper^{2,3,4} and Stefan Willitsch¹

¹Department of Chemistry, University of Basel, 4056 Basel, Switzerland

²Center for Free-Electron Laser Science, DESY, 22607 Hamburg, Germany; ³Department of Physics and The Hamburg Center for Ultrafast Imaging, University of Hamburg, 22761 Hamburg, Germany; ⁴Department of Chemistry, University of Hamburg, 20146 Hamburg

(corresponding author: A. Kilaj, e-mail: ardit.kilaj@unibas.ch)

The experimental challenges in preparing pure samples of individual molecular isomers and conformers have thus far precluded a characterization of their distinct chemical behavior. Recent progress in manipulating polar molecules using electrostatic fields has made it possible to select and spatially separate different conformers and rotational states of molecules in supersonic molecular beams [1,2]. By combining this technology with a stationary reaction target of Coulomb-crystallized ions in a linear quadrupole ion trap [3] we have recently studied conformer selected molecule-ion reaction dynamics and observed that reaction-rate constants can strongly depend on molecular conformation [4,5]. More recently, we have extended this method to the separation of different nuclear-spin isomers for studies of ion-molecule reactions with control over the rotational and nuclear-spin state of the neutral reaction partner.

Water is one of the fundamental molecules in chemistry, biology and astrophysics. It exists as two distinct nuclear-spin isomers, *para*- and *ortho*-water, which do not interconvert in isolated molecules. We have successfully studied the proton-transfer reaction of the spatially separated ground states of *para*- and *ortho*-water with cold ionic diazenylium (N_2H^+), an important molecule in astrochemistry. We found a 23(9)% higher reactivity for the *para* nuclear-spin isomer which we attribute to the smaller degree of rotational averaging of the ion-dipole long-range interaction compared to the *ortho*-species [6]. This finding is in quantitative agreement with a modelling of the reaction kinetics using rotationally adiabatic capture theory [7] and highlights the ramifications of nuclear-spin symmetry on chemical reactivity.

Despite their significance in organic synthesis, the mechanistic details of Diels-Alder cycloadditions, in which a diene and a dienophile react to form a cyclic product, still remain an extensively discussed question. The ionic variant, polar cycloaddition, is a particularly efficient route to form cyclic compounds. Still, it has proven difficult to determine whether product formation only involves the *cis* conformer of the diene via a concerted mechanism or both *cis* and *trans* conformers in a stepwise mechanism [8]. In order to shed light on these questions we are currently investigating the polar cycloaddition reaction of 2,3-dibromo-1,3-butadiene with ionic propene. We have successfully verified the electrostatic separation of the two conformers using soft vacuum-ultraviolet ionization and are currently performing experiments that directly test the underlying mechanism of polar cycloadditions.

[1] D.A. Horke, Y.-P. Chang, K. Dlugolecki, J. Küpper, *Angew. Chem. Int. Ed.* **53**, 11965, (2014).

[2] Y.-P. Chang, D.A. Horke, S. Trippel, J. Küpper, *Int. Rev. in Phys. Chem.* **34**, 557, (2015).

[3] S. Willitsch, *Adv. Chem. Phys.* **162**, 307 (2017).

[4] Y.-P. Chang, K. Dlugolecki, J. Küpper, D. Rösch, D. Wild, S. Willitsch, *Science* **342**, 98, (2013).

[5] D. Rösch, S. Willitsch, Y.-P. Chang, J. Küpper, *J. Chem. Phys.* **140**, 124202, (2014).

[6] A. Kilaj, H. Gao, D. Rösch, U. Rivero, J. Küpper and S. Willitsch, *Nat. Commun.* **9**, 2096 (2018)

[7] D. Clary, *J. of Chem. Soc., Faraday Trans. 2*, **83**, 139, (1987).

[8] M. Eberlin, *Int. J. Mass. Spectrom.* **235**, 263 (2004).

Photochemistry and spectroscopy of molecules at surfaces: Insights from ab initio molecular dynamics

M. Alducin¹, G. Floss, G. Füchsel, J.I. Juaristi¹, S. Lindner, I. Lončarić², G. Melani, Y. Nagata³, R. Scholz, E. Titov, Peter Saalfrank

*Chemistry Department, University of Potsdam, 14476 Potsdam-Golm, Germany
(corresponding author: P. Saalfrank, e-mail: peter.saalfrank@uni-potsdam.de)*

¹*Centro de Fisica de Materiales (CFM) and Donostia International Physics Center (DIPC), 20018
Donostia-San Sebastián, Spain*

²*Institut Ruder Bošković, 10000 Zagreb, Croatia*

³*Max Planck Institute for Polymer Research, 55124 Mainz, Germany*

The interaction of adsorbates on solid surfaces with light is central to surface spectroscopy, surface photochemistry, and non-adiabatic surface science in general. In the present contribution, light-driven molecular adsorbates will be modelled by ab initio (in one example, semiempirical) molecular dynamics. Three examples will be highlighted:

First, we consider femtosecond laser (FL) pulse driven chemistry at metals, e.g., FL-induced, hot-electron mediated desorption or diffusion. We describe these processes by (Langevin) Ab Initio Molecular Dynamics with Electronic Friction (AIMDEF) based on Density Functional Theory (DFT), and random forces obtained from a two-temperature model. Our focus is on associative desorption of H₂ and isotopomers from Ru(0001) and its “dynamical promotion” [1], as well as on desorption, diffusion and the time-resolved vibrational response of CO on Ru(0001) and Cu(100) [2], respectively.

A second example illustrates how vibrational (IR and Sum Frequency Generation (SFG)) spectra of water-covered aluminum oxide surfaces can be determined with the help of auto- and cross-correlation functions computed from DFT-based AIMD [3].

Third, the step towards explicitly non-adiabatic surface dynamics is taken in the form of semiclassical, AM1/CI-based “surface hopping”. Specifically, we consider cis-trans isomerizations in densely packed, ordered azobenzene layers, and how they are influenced by excitonic and steric effects [4].

- [1] G. Füchsel et al., PCCP **13**, 8659 (2011); J.I. Juaristi et al., Phys. Rev. B **95**, 125439 (2017).
- [2] R. Scholz et al., Phys. Rev. B **94**, 165447 (2016); R. Scholz et al., to be published.
- [3] G. Melani et al., J. Chem. Phys. **149**, 014707 (2018).
- [4] E. Titov et al., J. Phys. Chem. Lett. **7**, 3591 (2016).

Quantum mechanics for intramolecular reactions and conformational space exploration of organic molecules on metallic surfaces

Mariana Rossi

*Fritz Haber Institute of the Max Planck Society, Berlin, Germany
(corresponding author: M. Rossi, e-mail: rossi@fhi-berlin.mpg.de)*

In this talk, I will address the challenges of sampling the potential energy surface and addressing nuclear dynamics of flexible molecules containing hundreds of degrees of freedom adsorbed on metallic surfaces.

I will give examples of theory challenges faced when sampling the conformational space of rather rigid molecules as well as very flexible ones, like the Arginine amino-acid. In particular, with density-functional-theory based structure searches, we can show how alterations in conformational space appear due to changes in the environment (surface, charge, etc.) and can stabilize different orientations of chiral center with respect to the surface.

Regarding nuclear dynamics, intramolecular hydrogen transfer (IHT) represents a paradigmatic process where nuclear quantum effects and anharmonicity can result in unconventional hydrogen dynamics.

I will show a study of the IHT of porphycene adsorbed on Cu and Ag surfaces at different temperatures, where nuclear quantum effects of zero-point-energy and tunneling are fully included in the dynamics through path-integral based methods.

We predict rates in excellent agreement with experiments and show the importance of heavy-atom tunneling in the reaction. We address the thus-far unexplained temperature dependence of the IHT and reveal that the observed activation energy is related to the energy difference between reactant and product, rather than reactant and transition state.

Simultaneous Detection of Polycyclic Aromatic Hydrocarbons and Inorganic Ions in On-Line Single Aerosol Particle Laser Mass Spectrometry using Molecular as well as Atomic Resonances

R. Zimmermann^{1,2*}, J. Passig^{1,2}, J. Schade¹, R. Irsig^{2,3}, S. Ehlert³, M. Sklorz³, T. Adam^{2,4},
C. Li⁵, Y. Rudich¹

¹ Joint Mass Spectrometry Centre, University of Rostock, Germany

² Joint Mass Spectrometry Centre, Helmholtz Centre Munich, Germany

³ Photonion GmbH, Schwerin, Germany

⁴ Bundeswehr University Munich, Neubiberg, Germany

⁵ Department of Earth and Planetary Sciences, Weizmann Institute of Science, Rehovot, Israel

(* corresponding/presenting author: R. Zimmermann, e-mail:
ralf.zimmermann@helmholtz-muenchen.de)

Polycyclic aromatic hydrocarbons (PAHs) are toxic trace components in atmospheric aerosols. They are bound to airborne particles and transported over long distances. Inhalation of Polycyclic Aromatic Hydrocarbons (PAHs) is a well-known cause of morbidity and mortality, while data on the PAH distribution in aerosols is limited¹. Estimates of PAH transport and degradation pathways would benefit from on-line detection of PAHs along with analysis of the chemical fingerprint of carrying particles to identify the particle emission source (e.g. wood combustion, traffic, coal-fired power plant). In particular, details about the PAHs mixing state are crucial to assess potential health effects. PAHs may either be equally distributed over a large number of particles (internally mixed) or could be highly increased within a specific sub-population (external mixture), inducing strong local effects upon particle-in-lung deposition. Beside this, PAHs are considered for taking a key role in secondary aerosol formation². Consequently, novel on-line characterization techniques that address PAH on a single-particle scale while providing information on their potential source are highly desired.

We report a new and field-deployable technique that yields the single-particle PAH composition by resonance-enhanced multiphoton ionisation (REMPI) along with both positive and negative inorganic ions via LDI (metals, anions, cluster-ions). In particular, heavy metals (e.g. Pb) or redox active transition metals (e.g. Fe, Ni or Zn) contribute to the health impact of inhaled aerosols. Our approach for on-line single particle profiling is based on Single Particle Mass Spectrometry (SPMS)³, where particles are introduced through an aerodynamic lens and detected via laser velocimetry using a pair of cw-lasers. In our technique, the particles are then

firstly heated by an IR-laser pulse ($10.6\ \mu\text{m}$, CO_2 -laser). A few microseconds later the combined ionization step of Resonance-Enhanced Multi-Photon Ionization (REMPI) and Laser Desorption/Ionization (LDI) takes place, using an UV excimer laser light pulse (Fig. 1). With this approach, we present a novel route to obtain the full LDI-information of both positive and negative inorganic ions (metals, anions, cluster-ions; needed for particle source apportionment) in combination with health-relevant PAH by REMPI⁴. In contrast to previous methods, we are now able to address ions from LDI and REMPI in one combined ionization step, acquiring particle source- and aging information. The method has been applied for several combustion aerosols and allows a deepened insight into the mixing state of PAHs. On-line experiments on combustion aerosols demonstrate the methods capabilities to unravel the distribution of health-critical PAHs in the particle phase in real time. We also obtained field study results, where PAHs from ships and biomass combustion in marine and terrestrial aerosols were determined on a single-particle level for the first time.

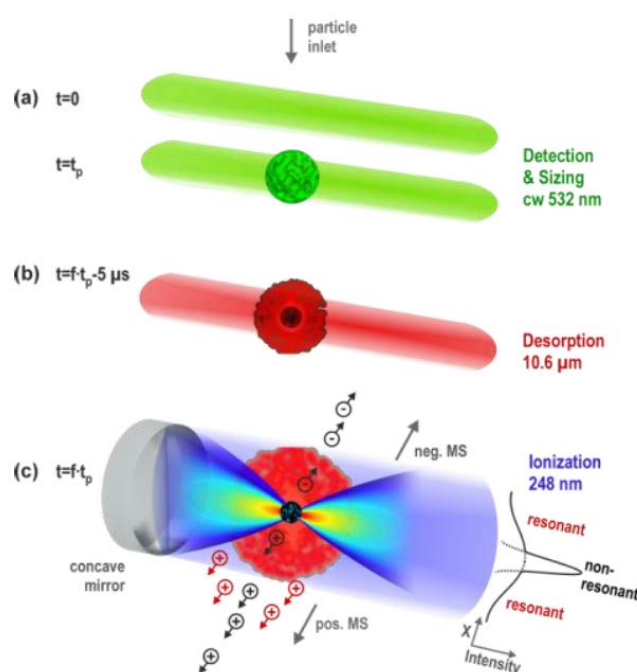


Figure 1. Schematic drawing of the novel ionization procedure⁴: After the sizing by laser velocimetry (a) a IR laser pulse hits the particle for desorption of PAH (b). Then (c) a unfocused laser pulse of $248\ \text{nm}$ wavelength is performing the resonance ionisation of PAH (REMPI, $P \sim 10^7\ \text{W cm}^{-2}$) and the back reflected, tightly focused laser beam hits the particle core for element detection (LDI, $P \sim 10^{11}\ \text{W cm}^{-2}$).

An interesting aspect is the resonance effect in the laser desorption/ionisation process: Experiments with tuneable lasers and different fixed-frequency lasers point out, that resonance enhanced LDI (or RELDI) of elements can be achieved if the ionisation laser wavelengths is in resonance with an atomic line of a relevant element. In fact, iron, which is of particular importance for oxidative stress related health impacts as well as for environmental aspects (e.g.

as micronutrient for plankton growth in remote ocean areas), can be detected by RELDI with greatly enhanced sensitivity using the 248,3 main atomic transition ($\text{Fe}: 3d^6 4s^2 \rightarrow 3d^6 4s 4p$). Energy transfer processes from the ubiquitous iron also support detection of other relevant transition metals. This enable a “double resonance” enhancement (RELDI and REMPI) of two very health relevant species using spatially shaped 248 nm KrF laser pulses (The KrF excimer, which is often is used for the REMPI detection of PAH, by coincidence RELDI excites the 248.3 nm electronic transition of Fe in LDI. Thus the combined LDI and LD-REMPI process detects the most health-relevant PM constituents with increased sensitivity. utilizing molecular (REMPI) as well as atomic (RELDI) resonance. The new method has been applied for several combustion emission-experiments as well as ambient monitoring and allows a deepened insight into the mixing state of PAHs and metals as well as other compounds (e.g. nitrate, sulphate, organic and elemental carbon etc.) and a single particle resolved detection of relevant air toxicants. In Figure 2 the application of the new method is depicted. The single particle laser ionisation mass spectra of two particles from different combustion sources are presented.

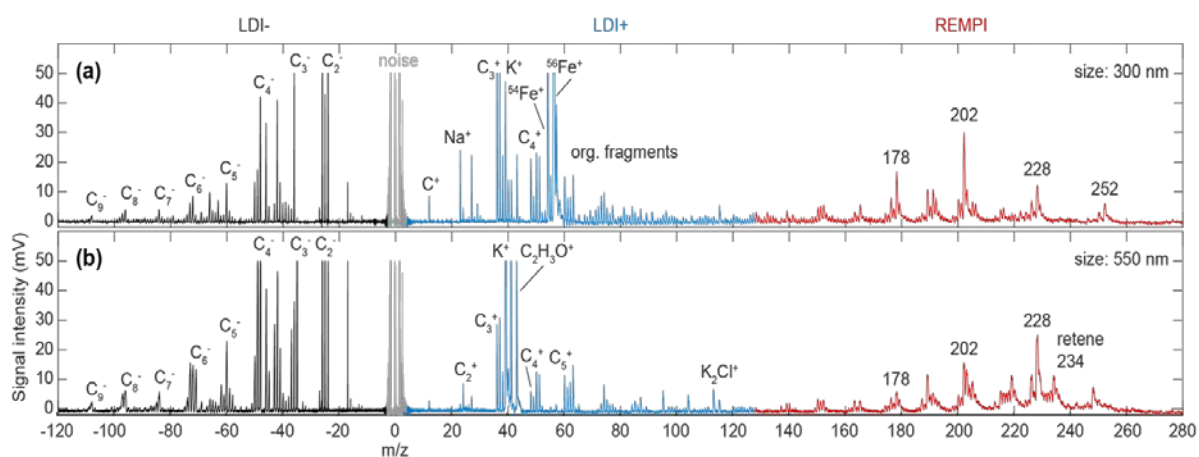


Figure 2. Single particle mass spectra from airborne diesel soot (a) and wood combustion soot (b) particle of 300 and 550 nm diameter, respectively. The red signals are originating from the LD-REMPI process and represent the PAH, the black and blue parts of the mass spectra are due to negative and positive ions for the LDI process.

Furthermore, other transition metals, such as V or Ni are also enhanced (to lower extend) by energy transfer processes from the excitation of the ubiquitous Fe. The latter information is crucial to determine the source- and aging-state of the particles. The system using the REMPI/RELDI approach currently is being commercialized by Photonion.

This work was supported by the German Research Foundation under grant ZI 764/6-1, by the German Federal Ministry for Economic Affairs and Energy (ZF4402101 ZG7), by the Helmholtz International Lab AeroHealth and by Photonion GmbH,

References

- ¹Ravindra K., Sokhi R.S., Van Grieken R., 2008. Atmospheric polycyclic aromatic hydrocarbons: Source attribution, emission factors and regulation. *Atmos. Environ.* 42, 2895-2921.
- ²Shrivastava M., Lou S., Zelenyuk A., Easter R.C., Corley R.A., Thrall B.D., Rasch P.J., Fast J.D., Massey Simonich S.L., Shen H., Tao S., 2017 Global long-range transport and lung cancer risk from polycyclic aromatic hydrocarbons shielded by coatings of organic aerosol. *PNAS* 114(6), 1246-1251.
- ³Murphy, D. M., 2007. The design of single particle laser mass spectrometers. *Mass Spectrom. Rev.* 26, 150–165.
- ⁴Schade J., Passig J., Irsig R., Ehlert S., Sklorz M., Adam T., Li C., Rudich Y., Zimmermann R., 2019 Spatially Shaped Laser Pulses for the Simultaneous Detection of Polycyclic Aromatic Hydrocarbons as well as Positive and Negative Inorganic Ions in Single Particle Mass Spectrometry. *Anal. Chem.* 91, 15.

Precision tests of nuclear spin symmetry and parity conservation in polyatomic molecules

Eduard Miloglyadov, Martin Quack, Georg Seyfang, Gunther Wichmann

Physical Chemistry, ETH Zürich,

CH-8093 Zürich, Switzerland

(corresponding author: M. Quack, e-mail: martin@quack.ch)

Parity and nuclear spin symmetry are approximate constants of the motion, which can be characterized by quantum numbers that are conserved in many fundamental primary processes in molecular physics, such as radiative transitions, inelastic collisions, and even reactions [1]. However, the underlying symmetries are not exact and known to be broken under certain circumstances [2]. In our research we have pursued the study of the corresponding symmetry violations for some time, where in particular our attempts to measure the parity violating energy difference $\Delta_{\text{pv}}E$ between the ground states of the enantiomers of chiral molecules can be considered a major challenge, with no successful experiments worldwide, so far (see the reviews in [2-7] for the recent status). While early theories for $\Delta_{\text{pv}}E$ were clearly incorrect, providing values of parity violating potentials too low by one to even two orders of magnitude for typical benchmark molecules such as H_2O_2 and further ones including simple amino acids (see reviews [2,3,8]), the new orders of magnitude from our theoretical developments in the 1990ies [9-12] have been confirmed in numerous later theoretical publications also by other groups since then (see reviews in [2,7,13] for example). For chiral molecules consisting only of atoms of the lighter elements, which are of particular interest for fundamental studies [2], theory predicts values of $\Delta_{\text{pv}}E$ typically in the range from 0.01 to 1 feV (= femto electron volt 10^{-15} eV) depending on the molecule considered. The current experimental setup has been demonstrated with the test molecule NH_3 to provide a capability of measuring values as low as 0.1 feV [6], presumably extendable to even lower values with some improvements but without requiring major changes. The basic principle for such experiments was proposed in [14,15] and is outlined in Fig 1. One first prepares a molecular quantum state of well defined parity for a (chiral) molecule. In Fig 1. this is a two step process with highly monochromatic laser radiation from optical parameter oscillators, OPO, for example, “selection 1” and “preparation 2”, which prepares a state of positive parity in the example of Fig 1. Because of parity violation this state is time dependent changing its parity according to Eq. (1) for the populations $p^+(t)$ of the state of positive parity and $p^-(t)$ for the complementary state of negative parity

$$p^-(t) = 1 - p^+(t) = \sin^2(\pi \Delta_{\text{pv}}Et/h) \quad (1)$$

In practice the experiment is carried out in a molecular beam expansion, where the time for the evolution of the parity is defined by the time resulting from the flight path for a certain length. In this way evolution times on the order of milliseconds are easily obtainable. By measuring the spectral change when the parity changes from positive to negative as indicated by the schematic spectrum in Fig 1, one can follow the populations $p^+(t)$ and $p^-(t)$. The precision which can be reached is in essence defined by the sensitivity, with which a spectral change can be detected. Thus if a small change in the spectrum following the time evolution in Eq. (1) can be detected with $\Delta_{\text{pv}}E=1\text{feV}$ this would correspond to a spectroscopic frequency difference of about 0.24 Hz. However, the spectroscopic resolution to separate the lines in Fig 1 needs only to distinguish between individual eigenstates (rovibrational levels, perhaps with hyperfine structure [6]), typically something on the order of 1 MHz, depending on the molecule.

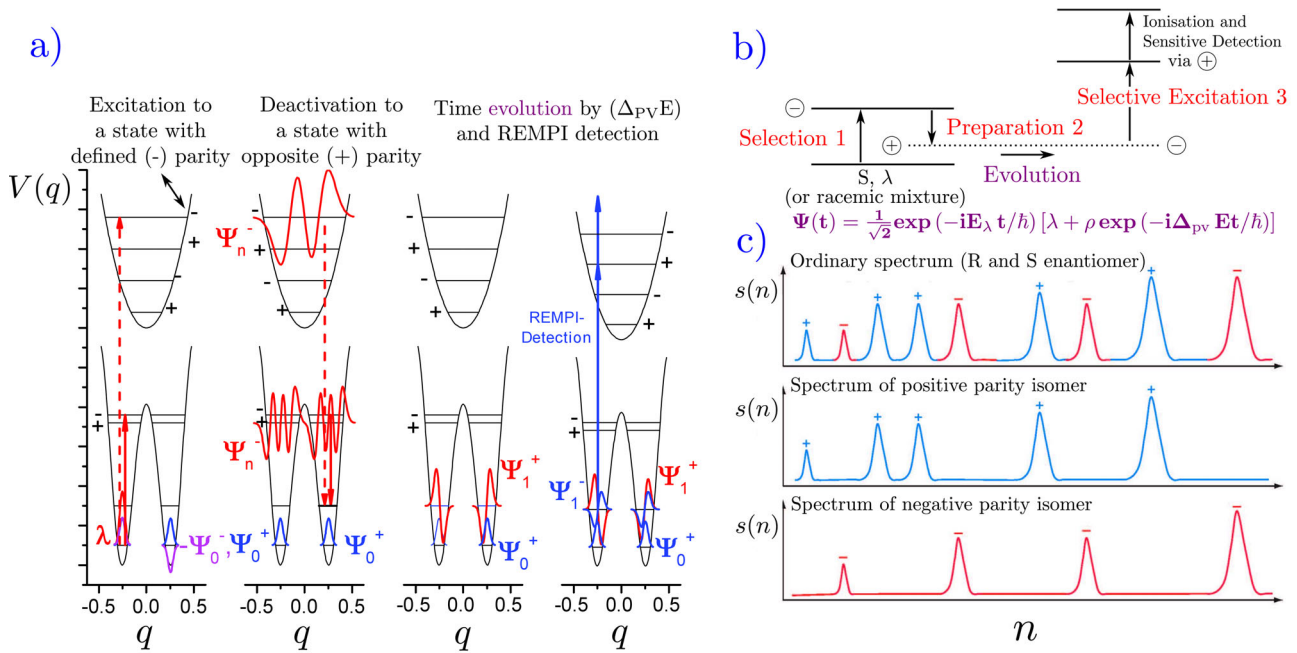


Figure 1: Scheme of the preparation and detection steps for the time resolved experiment to measure $\Delta_{pv}E$. **a)** The transitions to the intermediate states are indicated together with the corresponding wave functions for an excited state with well defined parity close to the barrier of a double minimum potential (full line) or an achiral electronically excited state (dashed line) as an intermediate. The right hand part shows the sensitive detection step with REMPI. **b)** Summary scheme for the three steps. **c)** The spectra of the normal enantiomers (**a)**) and of the selected positive (blue) and negative (red) “parity isomers” (modified after [3,6,14]). n is a reduced frequency difference $(v-v_0)/v_0$, where the frequency spacings between lines are of the order of MHz in order to separate lines connecting states of different parity (+ or -) in the rovibronic, resolved spectrum. The high resolution (Hz to subHz) needed for $\Delta_{pv}E$ is obtained from measuring the time evolution of the spectrum in the middle towards the spectrum at the bottom at very high sensitivity on the ms time scale.

		$\Delta_{pv}E$ / (h Hz)	$\Delta_{pv}E$ /(feV)	
Trisulfane	HSSH:	0.05	0.207	[17,18]
1,2-Dithiine	C ₄ H ₄ S ₂ :	0.34	1.406	[19, 20]
1,3 Difluoroallene	C ₃ H ₂ F ₂ :	0.003	0.012	[21, 22]
Chlorine Peroxide	Cl ₂ O ₂ :	0.017	0.070	[13, 16]

Table 1: Overview of promising axially chiral candidates for the detection scheme depicted in Fig 1.

Thus the effective gain in energy resolution is about 10^6 , which makes this experiment feasible with current high resolution laser systems. Table 1 shows a summary of molecular systems which are available and for which initial spectroscopic studies exist in our work. Very similar considerations apply in the easier studies of nuclear spin symmetry conservation. While one could proceed in exactly the same fashion with a laser selection step as shown in Fig 1, many current studies use as “preparation step” a mixture of nuclear spin symmetry isomers at equilibrium at room temperature, which is rapidly cooled to very low temperature (typically below 10 K) where the equilibrium composition would be very different [23]. By studying whether there is a change in the composition or not, one can test for nuclear spin symmetry conservation. If a change towards the new equilibrium at low temperature is observed one can estimate the rate of nuclear spin symmetry change. Commonly on the short time scale of the molecular beam expansion, nuclear spin symmetry conservation is found, for example for methane CH₄ [23] recently extended to ¹³CH₄ [24] and CD₃H and CH₃X molecules [25] and water H₂O [26, 27]. In our current work we have studied

again the prototypical molecule ammonia [28], for which there has been some debate in the past. We have found nuclear spin symmetry conservation under our experimental conditions. We have for this purpose developed a new molecular beam high resolution OPO-laser-setup for cavity ring-down spectroscopy, which should also be helpful in advancing the spectroscopic studies on the prototypical chiral molecules mentioned in Tab 1, on which further work is in progress. We shall also discuss the relation to fundamental studies of tunneling dynamics in ammonia isotopomers including chiral NHDT [29] and the fundamental aspects of bistructural systems by superposition of isomers leading to a molecular quantum switch [30], the bistructural superposition of left and right enantiomers [31], and somewhat hypothetically left and right skis [32].

Acknowledgement: Help and support from as well as discussions with Andres Laso, Karen Keppler, Roberto Marquardt, Frédéric Merkt, Jürgen Stohner and Daniel Zindel are gratefully acknowledged. We enjoyed financial support from a generous ETH grant and an ERC advanced grant.

- [1] M. Quack, Detailed symmetry selection rules for reactive collisions, *Mol. Phys.*, **34**, 477-504 (1977).
- [2] M. Quack, Fundamental Symmetries and Symmetry Violations from High Resolution Spectroscopy, in "Handbook of High-Resolution Spectroscopy", Vol. 1, chapter 18, pages 659–722, M. Quack, and F. Merkt, Eds. Wiley Chichester, (2011), ISBN-13: 978-0-470-06653-9.
- [3] M. Quack, On Biomolecular Homochirality as a Quasi-Fossil of the Evolution of Life, *Adv. Chem. Phys.*, **157**, 249 – 290 (2015).
- [4] M. Quack, Die Spiegelsymmetrie des Raumes und die Chiralität in Chemie, Physik und in der biologischen Evolution, *Nova Acta Leopoldina NF Band127*, Nr. 412, 119 – 166, (2016).
- [5] E. Miloglyadov, M. Quack, G. Seyfang, G. Wichmann, Precision experiments for parity violation in chiral molecules: the role of STIRAP, *J. Phys. B: At. Mol. Opt. Phys.*, **52**, 11-13, (2019), in K. Bergmann et al, Roadmap on STIRAP applications, *J. Phys. B: At. Mol. Opt. Phys.*, **52**, 1-55, (2019).
- [6] P. Dietiker, E. Miloglyadov, M. Quack, A. Schneider, G. Seyfang, Infrared laser induced population transfer and parity selection in $^{14}\text{NH}_3$: A proof of principle experiment towards detecting parity violation in chiral molecules, *J. Chem. Phys.*, **143**, 244305-1 – 244305-23 (2015).
- [7] M. Quack, J. Stohner, M. Willeke, High-Resolution Spectroscopic Studies and Theory of Parity Violation in Chiral Molecules, *Annu. Rev. Phys. Chem.* **59**, 741 – 769 (2008).
- [8] M. Quack, *Frontiers in Spectroscopy*, *Faraday Disc.* **150**, 533–565 (2011).
- [9] A. Bakasov, T.K. Ha and M. Quack, Ab initio calculation of molecular energies including parity violating interactions, in *Proc. of the 4th Trieste Conference (1995)*, Chemical Evolution: Physics of the Origin and Evolution of Life, 287-296, J. Chela-Flores and F. Rolin eds, Kluwer Academic Publ. Dordrecht, (1996), ISBN 0-7923-4111-2.
- [10] A. Bakasov, T.K. Ha and M. Quack, Ab initio calculation of molecular energies including parity violating interactions, *J. Chem. Phys.* **109**, 7263-7285 (1998).
- [11] R. Berger and M. Quack, Multi-configuration linear response approach to the calculation of parity violating potentials in polyatomic molecule, *J. Chem. Phys.* **112**, 3148-3158 (2000).
- [12] M. Quack and J. Stohner, Influence of parity violating weak nuclear potentials on vibrational and rotational frequencies in chiral molecules, *Phys. Rev. Lett.* **84**, 3807-3810 (2000).
- [13] L. Horný, M. Quack, Computation of Molecular Parity Violation Using the Coupled Cluster Linear Response Approach, *Mol. Phys.*, **113**, 1768-1779 (2015).
- [14] M. Quack, On the measurement of the parity violating energy difference between enantiomers, *Chem. Phys. Lett.* **132**, 147-153 (1986).
- [15] M. Quack, Structure and dynamics of chiral molecules, *Angewandte Chemie* **101**, 588-604 (1989). *Angewandte Chemie (Intl.Ed.)* **28**, 571-586 (1989).

- [16] R. Prentner, M. Quack, J. Stohner, M. Willeke, Wavepacket Dynamics of the Axially Chiral Molecule Cl-O-O-Cl under Coherent Radiative Excitation and Including Electroweak Parity Violation, *J. Phys. Chem. A*, **119**, 12805–12822 (2015).
- [17] C. Fábri, L. Horný, M. Quack, Tunneling and Parity Violation in Trisulfane (HSSSH): An Almost Ideal Molecule for Detecting Parity Violation in Chiral Molecules, *ChemPhysChem* **16**, 3584–3589 (2015).
- [18] S. Albert, I. Bolotova, Z. Chen, C. Fábri, M. Quack, G. Seyfang and D. Zindel, High-resolution FTIR spectroscopy of trisulfane HSSSH: A candidate for detecting parity violation in chiral molecules, *Phys. Chem. Chem. Phys. (PCCP)* **19**, 11738 – 11743 (2017).
- [19] S. Albert, I. Bolotova, Z. Chen, C. Fábri, L. Horný, M. Quack, G. Seyfang and D. Zindel, High resolution GHz and THz (FTIR) spectroscopy and theory of parity violation and tunneling for 1,2-dithiine ($C_4H_4S_2$) as a candidate for measuring the parity violating energy differences between enantiomers of chiral molecules, *Phys. Chem. Chem. Phys. (PCCP)*, **18**, 21976 – 21993 (2016).
- [20] S. Albert, F. Arn, I. Bolotova, Z. Chen, C. Fábri, G. Grassi, P. Lerch, M. Quack, G. Seyfang, A. Wokaun, D. Zindel, Synchrotron-Based Highest Resolution Terahertz Spectroscopy of the ν_{24} Band System of 1,2-Dithiine ($C_4H_4S_2$): A Candidate for Measuring the Parity Violating Energy Difference between Enantiomers of Chiral Molecules, *J. Phys. Chem. Lett.* **7**, 3847–3853 (2016).
- [21] M. Gottselig, M. Quack, Steps Towards Molecular Parity Violation in Axially Chiral Molecules: (I) Theory for Allene and 1,3-Difluoroallene, *J. Chem. Phys.* **123**, 84305-1 – 84305-11 (2005).
- [22] E. Miloglyadov, S. Albert, M. Gottselig, K. Keppler, G. Seyfang, J. Stohner, G. Wichmann, M. Quack, High resolution Fourier transform infrared spectroscopy of 1,3-Difluoroallene, (2019 in preparation).
- [23] A. Amrein, M. Quack, and U. Schmitt, High resolution interferometric Fourier transform infrared absorption spectroscopy in supersonic free jet expansions: carbon monoxide, nitric oxide, methane, ethyne, propyne, and trifluoromethane, *J. Phys. Chem.* **92**, 5455–5466 (1988).
- [24] Z. Bjelobrk, C. Manca Tanner, M. Quack, Investigation of the $\nu_2+\nu_3$ subband in the overtone icosad of $^{13}CH_4$ by pulsed supersonic jet and diode laser cavity ring-down spectroscopy: partial rovibrational analysis and nuclear spin symmetry conservation, *Z. Phys. Chem.*, **229**, 1575–1607 (2015).
- [25] V. Horká-Zelenková, G. Seyfang, P. Dietiker, and M. Quack, Nuclear Spin Symmetry Conservation Studied for Symmetric Top Molecules (CH_3D , CHD_3 , CH_3F , and CH_3Cl) in Supersonic Jet Expansions, *J. Phys. Chem. A* **123**, 6160–6174 (2019).
- [26] C. Manca Tanner, M. Quack, D. Schmidiger, Nuclear spin symmetry conservation and relaxation in water ($^1H_2^{16}O$) studied by Cavity Ring-Down (CRD) spectroscopy of supersonic jets, *J. Phys. Chem. A*, **117**, 10105–10118, (2013).
- [27] C. Manca Tanner, M. Quack, D. Schmidiger, Nuclear spin symmetry conservation and relaxation of water (H_2O) seeded in supersonic jets of argon and oxygen: measurements by cavity ring-down laser spectroscopy, *Mol. Phys.*, **116**, 3718 – 3730 (2018).
- [28] G. Wichmann, E. Miloglyadov, G. Seyfang, M. Quack, Nuclear Spin Symmetry Conservation studied by Cavity Ring-Down Spectroscopy of NH_3 in a seeded supersonic jet from a pulsed slit nozzle, (2019 in preparation).
- [29] C. Fábri, R. Marquardt, A. Császár, and M. Quack, Controlling tunneling in ammonia isotopomers, *J. Chem. Phys.* **150**, 014102 (2019).
- [30] C. Fábri, S. Albert, Z. Chen, R. Prentner, M. Quack, A Molecular Quantum Switch Based on Tunneling in Meta-D-phenol C_6H_4DOH , *Phys. Chem. Chem. Phys.* **20**, 7387–7394 (2018).
- [31] M. Quack, The Concept of Law and Models in Chemistry, *European Review*, **22** (Supplement S1), 50–86, (2014).
- [32] A. M. Q. Zack, Recent Advances in the Physics of Skiing on Surfaces (SOS): Yoctosecond Spectroscopy of Skiing on the Real and Imaginary Time Axes and in the Complex Plane, in *Proceedings of the 10th International Symposium on Atomic, Molecular, Cluster, Ion, and Surface Physics*, Engelberg, Switzerland 21 to 26 January (1996), 305–309 (Eds.: J. P. Maier, M. Quack), VdF Hochschulverlag, Zürich, ISBN 3 7281 2329 3.

Electron-induced processes in novel dielectric gases

Juraj Fedor

J. Heyrovský Institute of Physical Chemistry, Czech Academy of Sciences, Dolejškova 3, 18223

Prague, Czech Republic

(corresponding author: J. Fedor e-mail: juraj.fedor@jh-inst.cas.cz)

Sulfur hexafluoride, SF₆, is widely used in gas-insulated high-voltage equipment due to its excellent dielectric properties and stability under discharge conditions. However, it has an extremely high global warming potential. There is thus an intensive search for a suitable replacement, which has to be a strongly electron-attaching gas and, additionally, it has to fulfill a several other criteria. A number of alternative gases has been suggested as suitable insulators and their properties are being currently intensively probed.

In high-voltage electrical circuits, the electron collisions are the elementary mechanism driving the physics and chemistry of the discharges inception and extinction. We experimentally probe the electron collision processes with candidate insulating gases under single collision conditions. We focus on three elementary channels: (i) electron attachment, (ii) electron impact ionization and (iii) elastic and inelastic electron scattering. All channels are characterized quantitatively, that is, the absolute cross sections are measured using three different electron-molecule collision setups. Apart from providing the cross sections, we focus on the dynamics of atomic nuclei during the scattering, especially in the bond-breaking channels (dissociative ionization [1], dissociative electron attachment and dissociation into neutral fragments).

Support by the company Eaton and by the Technological Agency of the Czech Republic is gratefully acknowledged.

[1] M. Ranković et al., *Phys. Chem. Chem. Phys.* **21**, 16451 (2019).

Unravelling Isomers of Reactive Ionic Intermediates

Sandra Brünken

*FELIX Laboratory, Institute for Molecules and Materials, Radboud University, Toernooiveld 7c, 6525
ED Nijmegen, The Netherlands
(e-mail: sandra.brunden@ru.nl)*

Hydrocarbon and nitrile ions play an important role in the chemistry of planetary atmospheres and the interstellar medium. Laboratory spectroscopic studies of these essential reaction intermediates give valuable insights on their geometrical and electronic structure, and provide accurate transition frequencies needed for their identification in space. Conventional absorption spectroscopy has in the past been successfully applied for spectroscopic studies of molecular ions, but is often hampered by low number densities and spectral congestion due to the multitude of species produced at high excitation energies during their formation process. These limitations can be overcome by performing experiments on mass-selected ions in cryogenic ion trap instruments.

Here I will present laboratory studies of the gas phase spectra of several hydrocarbon and nitrile cations ranging in size from comparatively small systems (e.g., C_3H_2^+ , CH_2CN^+) to polycyclic aromatic hydrocarbon (PAH) cations, made possible by recent developments of sensitive methods for action spectroscopy of cold, trapped ions. A focus will be on infrared experiments and methods to disentangle the isomeric composition of ionic samples, using the unique combination of a cryogenic ion trap instrument interfaced to the infrared free electron lasers at the FELIX Laboratory [1-4]. I will outline how these studies pave the way to investigate isomer-selective reaction kinetics of neutral-ion reactions at astronomically relevant temperatures. Progress towards rotational spectroscopic studies on some of these systems using a novel action spectroscopic scheme based on rotational state-dependent attachment of rare gas atoms to the cold molecular ions will be reported [5-6].

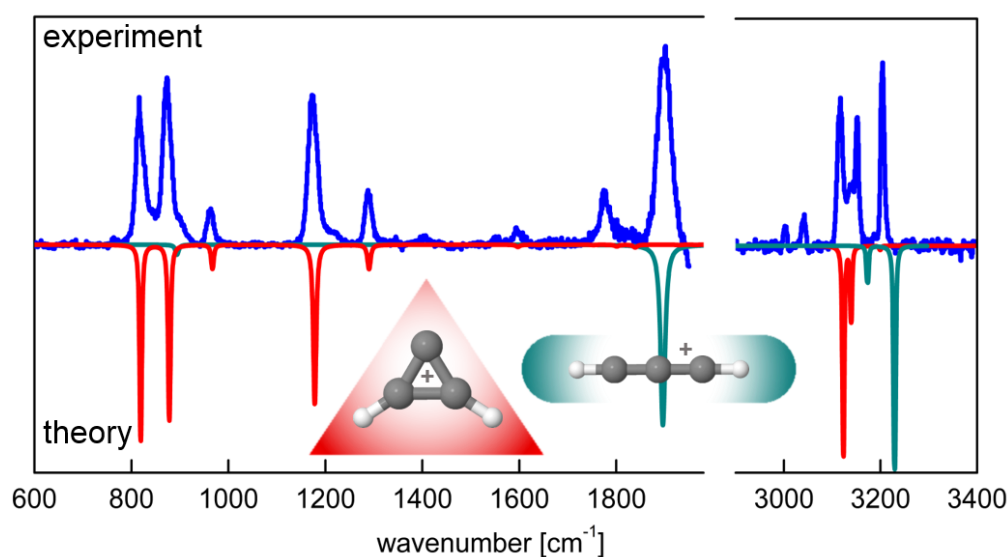


Figure 1: Vibrational spectra of two isomers of C_3H_2^+ recorded using Ne-tagging of cold ions in a cryogenic ion trap in combination with the intense and widely tunable IR-radiation of the FELIX lasers [3].

Support by the Netherlands Organization for Scientific Research (NWO - grant 724.011.002), the German Research Foundation (DFG - grants BR 4287/1-2, SCHL 341/15-1) and the European Research Council (H2020-MSCA-ITN-2016 Program EUROPAH - G.A. 722346) is gratefully acknowledged.

- [1] <https://www.ru.nl/felix/>
- [2] Jusko et al., Faraday Discuss. **217**, 172 (2019)
- [3] Brünken et al., J. Phys Chem. A. **123**, 8053 (2019)
- [4] Jusko et al., ChemPhysChem **19**, 3182 (2018)
- [5] Brünken et al., Astrophys. J. Lett. **783**, L4 (2014)
- [6] Brünken et al., J. Mol. Spectrosc. **332**, 67 (2017)

Combining ultrahigh-resolution ion mobility with cryogenic ion vibrational spectroscopy for the analysis of glycans

Stephan Warnke, Ahmed Ben Faleh, Ali Abi Khodr, Priyanka Bansal, Eduardo Carrascosa, Irina Dyukova, Robert P. Pellegrinelli, Natalia Yalovenko, Vasyi Yatsyna, Lei Yue, and Thomas R. Rizzo

Ecole Polytechnique Fédérale de Lausanne, Laboratoire de chimie physique moléculaire, CH H1 621, Station 6, CH-1015 Lausanne, Switzerland (corresponding author: thomas.rizzo@epfl.ch)

Vibrational spectroscopy of biological molecules is complicated by the coexistence of multiple stable conformers and/or isomers, which causes spectral congestion and hinders analysis. Spectroscopic schemes such as IR-UV double resonance or IR-IR hole burning can help deal with this conformational or isomeric heterogeneity in favorable cases, but neither is universally applicable. New spectral simplification methods are thus needed to push vibrational spectroscopy to increasingly complex biological molecules in a meaningful way. One class of molecules for which this is particularly important is that of glycans, or oligosaccharides.

Despite their biological importance, glycans present a particular problem for analysis arising from the multiple types of isomerism that are simultaneously present. Orthogonal techniques need to be applied simultaneously to have any chance of resolving this isomeric complexity. The most common approach is to combine liquid chromatography (LC) with mass spectrometry (MS), but LCMS cannot distinguish the subtlest isomeric forms. Ion mobility spectrometry (IMS) is being increasingly applied to glycan analysis, but even this powerful technique cannot completely distinguish all glycan isomers. Vibrational spectroscopy, on the other hand, is exquisitely sensitive to the smallest difference between isomeric glycans, particularly when performed at cryogenic temperatures.

We have recently developed a technique that combines ultrahigh-resolution ion mobility spectrometry with cryogenic ion vibrational spectroscopy for the analysis of glycans (1-3). We achieve extremely high resolution ion mobility using structures for lossless ion manipulations (SLIM) (4), which employs traveling-waves generated between a closely spaced pair of printed circuit-board electrodes. Because ions can be made to follow a serpentine path, one can achieve ultra-long path lengths, and hence high resolution, in a compact instrument. This allows us to separate glycan isomers that differ only by the orientation of a single stereogenic center. After mobility separation, we then record a vibrational fingerprint spectrum at cryogenic temperatures, allowing us to compare it with a database constructed from suitable standards.

We will demonstrate here the power of this technique by applying it to a series of glycans of increasing complexity and show our first steps towards making this approach into a useful analytical tool.

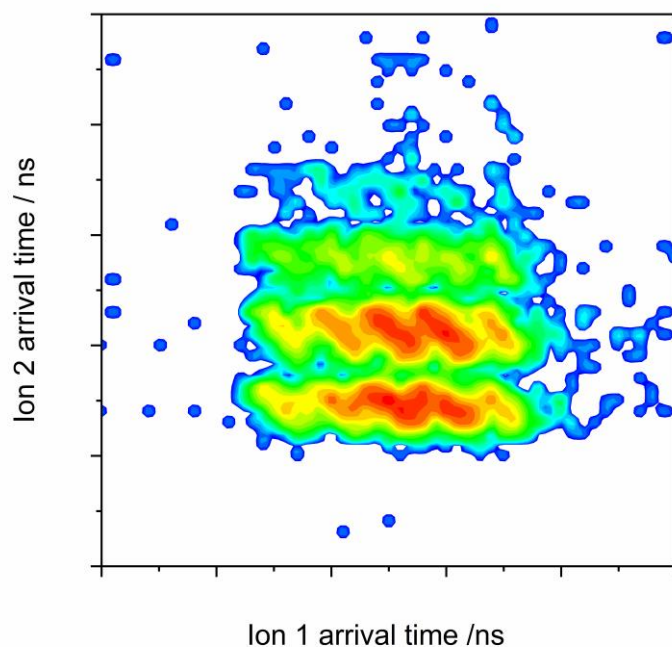
1. S. Warnke, A. Ben Faleh, V. Scutelnic, T. R. Rizzo, Separation and Identification of Glycan Anomers Using Ultrahigh-Resolution Ion-Mobility Spectrometry and Cryogenic Ion Spectroscopy. *J. Am. Soc. Mass Spectrom.* **30**, 2204-2211 (2019).
2. S. Warnke, A. Ben Faleh, R. P. Pellegrinelli, N. Yalovenko, T. R. Rizzo, Combining ultra-high resolution ion mobility spectrometry with cryogenic IR spectroscopy for the study of biomolecular ions. *Faraday Discuss. Chem. Soc.*, (2019).
3. A. Ben Faleh, S. Warnke, T. R. Rizzo, Combining Ultrahigh-Resolution Ion-Mobility Spectrometry with Cryogenic Infrared Spectroscopy for the Analysis of Glycan Mixtures. *Anal. Chem.* **91**, 4876-4882 (2019).
4. A. M. Hamid, S. V. B. Garimella, Y. M. Ibrahim, L. Deng, X. Zheng, I. K. Webb, G. A. Anderson, S. A. Prost, R. V. Norheim, A. V. Tolmachev, E. S. Baker, R. D. Smith, Achieving High Resolution Ion Mobility Separations Using Traveling Waves in Compact Multiturn Structures for Lossless Ion Manipulations. *Anal. Chem.* **88**, 8949-8956 (2016).

Gas-phase Dications: Creation, coincidences, charges and chemistry

Lilian Ellis-Gibblings, Sam Armenta Butt, Eleanor Smith, Will Fortune, Stephen D Price

*Chemistry Department, University College London, 20 Gordon Street, London WC1H 0AJ, UK.
(corresponding author: L. Ellis-Gibblings, e-mail: l.ellis-gibblings@ucl.ac.uk)*

Dications (doubly-charged positive ions) are found in various energetic environments throughout the Universe. Formed *via* photon and electron ionisation, dications have been detected in the atmospheres of Earth, Venus and Io¹. Dications have also been predicted, and their role modelled, in the atmospheres of Titan, Venus and Mars¹. Some molecular dications in the atmosphere contribute to atmospheric depletion² due to the high kinetic energy that is imparted to the charged fragments upon charge-separating dissociation. Dications are also detected in nebulae,³ often via the weak optical recombination lines. Many molecular dications are stable for long periods, and collisional reactions between atomic and molecular dications with surrounding diffuse gases can form new bonds.⁴



Ion pair intensity map of electron ionisation of pyrimidine showing 24:12 m/z to 28:14 m/z pairs detected in coincidence in a mass spectrometer.

At UCL we use several high vacuum experiments to investigate the likelihood of dication formation and the further reactions of these energized species with neutral collision partners. For example, we can measure, using a coincidence mass spectrometer, precursor-specific relative ionisation cross sections (PS-PICS). These PS-PICS show us the relative abundances of the different ionic products (monocations, dications and trications) from single, double and triple ionisation of a given target species. Such investigations often reveal new dications and trications.⁵ When a new long-lived dication is detected we can then investigate the chemistry that

occurs in collisions between this dication and a range of neutral species in a crossed-beam apparatus. Simple mass spectra of the collision products, from the crossed beam apparatus, provide basic information on the bimolecular reactivity⁶ while position-sensitive detection on the product ion pairs can provide the energetics and dynamics of the reactions.⁷

Recent results from the coincidence mass spectrometer include the relative partial ionisation and precursor specific cross sections for electron ionization of PF₃ and NH₃ as well as preliminary work on a more complex cyclic molecule, pyrimidine (see figure). These cross sections can now be normalised to a Binary Encounter Bethe total ionisation cross section calculation,⁸ placing the experimental values on an absolute scale. Recent results revealing the collisional reactivity of the PF₃²⁺ dication, and interactions between Ar²⁺ and O₂ will also be presented. These collisional reactions exhibit a wide range of reactive processes, including single electron transfer, double electron transfer, and bond formation. Chemical bond formation is observed for both PF₃²⁺ + Ar and Ar²⁺ + O₂, with the dynamics and energetics being revealed by position-sensitive coincidence experiments for the latter reaction.

This presentation will detail recent experimental results that are pertinent to understanding the fate of multiply-charged ions in planetary and astrochemical environments. An understanding of dication formation, and the reaction pathways of these species, will aid in interpreting their contribution to the distribution of chemical species in energized environments.

Support by the Leverhulme trust is gratefully acknowledged.

[1] R. Thissen, O. Witasse, O. Dutuit, C.S. Wedlund, G. Gronoff, and J. Liliensten, *Phys. Chem. Chem. Phys.* **13**, 18264 (2011).

[2] S. Falcinelli, F. Pirani, M. Alagia, L. Schio, R. Richter, S. Stranges, N. Balucani, F. Vecchiocattivi, S. Falcinelli, F. Pirani, M. Alagia, L. Schio, R. Richter, S. Stranges, N. Balucani, and F. Vecchiocattivi, *Atmosphere (Basel)*. **7**, 112 (2016).

[3] X.-W. Liu, P.J. Storey, M.J. Barlow, I.J. Danziger, M. Cohen, and M. Bryce, *Mon. Not. R. Astron. Soc.* **312**, 585 (2000).

[4] S.D. Price, J.D. Fletcher, F.E. Gossan, and M.A. Parkes, *Int. Rev. Phys. Chem.* **36**, 145 (2017).

[5] H. Sabzyan, E. Keshavarz, and Z. Noorisafa, *J. Iran. Chem. Soc.* **11**, 871 (2014).

[6] N. Lambert, D. Kearney, N. Kaltsoyannis, and S.D. Price, *J. Am. Chem. Soc.* **126**, 3658 (2004).

[7] W.-P. Hu, S.M. Harper, and S.D. Price, *Meas. Sci. Technol.* **13**, 1512 (2002).

[8] Y.-K. Kim and M.E. Rudd, *Phys. Rev. A* **50**, 3954 (1994).

Recent advancements in surface science instrumentation

Markus Maier, Eleni Anargirou

Scienta Omicron GmbH

65232 Taunusstein, Germany

(Corresponding author: E. Anargirou, e-mail: eleni.anargirou@scientaomicron.com)

We will report on most recent developments at Scienta Omicron regarding Scanning Probe Microscopy at low temperatures and high magnetic fields as well as current state-of-the art of closed-cycle cooling approaches. We will also present the newest developments in the field of photo electron spectroscopy with a focus on XPS.

ZnO: Ultrafast Generation and Decay of a Surface Metal

Lukas Gierster, Sessa Vempati¹, Julia Stähler

*Fritz-Haber-Institut der Max-Planck-Gesellschaft,
14195 Berlin, Germany*

(corresponding author: J. Stähler, e-mail: staehler@fhi-berlin.mpg.de)

¹ *Indian Institute of Technology Bhilai, Raipur-492015, India*

The control of material properties upon laser excitation on ultrafast timescales is a central topic in modern physics. In many strongly correlated materials, light can trigger a photoinduced phase transition (PIPT). In conventional semiconductors, however, the only PIPT is ultrafast melting with intense laser pulses. Here, we show that ZnO undergoes a semiconductor-to-metal transition (SMT) at its surface upon excitation with orders of magnitude lower laser fluence. Generation and decay of the metal phase occur on femto- and picosecond timescales, respectively. The mechanism is based on the strong surface charge induced by photodepletion of deep surface defects, different from intrinsic renormalization effects of the band structure of semiconductors in the high excitation regime. We confirm the PIPT up to near room temperature. As ZnO is transparent and one of the best oxides for nanostructuring purposes, our discovery will likely trigger new device designs based on ultrafast photoswitches. Further, the concept is likely applicable to induce PIPTs in a wide range of semiconductors.

Funded by the Deutsche Forschungsgemeinschaft (DFG, German Research Foundation) – Projektnummer 182087777 - SFB 951.

Nanoscale insights into surface electrochemistry - Au oxidation revisited

Jonas H.K. Pfisterer¹, Masoud Baghernejad¹, Giovanni Giuzio¹, Ulmas Zhumaev¹,
Manuel Breiner¹, Juan M. Feliu², Katrin F. Domke¹

¹ Max Planck Institute for Polymer Research, Ackermannweg 10, 55128 Mainz, Germany
(corresponding author: K.F. Domke, e-mail: domke@mpip-mainz.mpg.de)

² Instituto de Electroquímica, Universidad de Alicante, Apdo. 99, 03080 Alicante, Spain

Gathering molecular-level information about electrochemical interfaces is highly desirable to advance our understanding of – and to ultimately design and control – efficient electrochemical processes that underlie a manifold of ‘green’ energy conversion applications, such as fuel cell or sensitised solar cell operation, electrosynthesis and electrocatalysis or physiological electron transfer. Despite the vast interest in solid/liquid surface chemistry, however, advanced *operando* experimental (and theoretical) tools that provide quasi-atomistic insight into chemical processes at (electrified) solid/liquid interfaces with nanoscale spatial and real-time chemical resolution are still scarce.

In my talk, I will highlight our recent methodological advances with *operando* nearfield Raman spectroscopies that allow us to gain correlated chemical and topographic molecular-level information about, for example, adsorption geometry, chemical interaction and conversion with extreme spatial resolution under reaction conditions. Based on showcase Au oxide formation and reduction during electrochemical water splitting, I will elucidate how our nanoscopic approaches provide valuable new insights into reaction intermediates and site-selective reactivity and thus contribute to an improved mechanistic understanding of potential-controlled metal oxidation. In general, *operando* Raman nanoscopy holds great promise to be employed on a wide range of systems beyond electro-catalytic materials where nano-site activity determines macroscopic device behavior and will aid to push our understanding of the driving forces for chemical and energy conversion to the molecular level.

- [1] Pfisterer et al., Nature Communications (2019). Under review.
- [2] Pfisterer & Domke, Current Opinion in Electrochemistry **8**, 96 (2018).
- [3] Martín Sabanés et al., Angewandte Chemie International Edition **56**, 9796 (2017).

Molecules in interaction with nanoparticles grown on alumina film : the benefits of combined SFG spectroscopy and STM microscopy

Natalia Alyabyeva, A. Ghalgaoui¹, Aimeric Ouvrard, Serge Carrez, Wanquan Zheng, Bernard Bourguignon

*Institut des Sciences Moléculaires d'Orsay (ISMO), CNRS, Université Paris-Saclay,
F-91405 Orsay (France)*

(Corresponding author: Bernard Bourguignon, e-mail: bernard.bourguignon@u-psud.fr)

¹ *Max-Born-Institut für Nichtlineare Optik und Kurzzeitspektroskopie, Max-Born-Strasse 2 a, 12489
Berlin, Germany*

Understanding the interaction of molecules with nanostructures is of increasing importance for applications where the reduction of size and dimensionality of hybrid systems opens the way to control and modify optical and chemical properties: sensors, energy, nanophotonics, plasmonics, molecular electronics, catalysis. Important open questions are the stability of the molecules, the possible enhancement of interaction with light, and the size dependence of electronic, optical and chemical properties, which may all influence the functionality of future devices.

We have studied such issues on an alumina template on Ni₃Al(111) single crystal, which allows to grow high density, ordered clusters. The small size distribution allows to combine spectroscopies and microscopies. STM has allowed to study NP growth and ordering [1], and to observe the formation of an ordered hybrid layer of NPs and organic molecules [2]. Broadband Sum Frequency Generation (SFG) vibrational spectroscopy allows to characterize the adsorption sites as a function of size in a size domain of 4 to 200 atoms, where STM does not provide information on NP size and shape due to tip convolution and proximity of NPs [3]. It also allows to evidence segregation on Pd-Au core-shell clusters. On Pd clusters on MgO clusters, SFG pump-probe experiments have shown that molecules are coupled very differently to hot electrons depending on their location at terraces or edges [4]. Diffusion of CO from terraces to reactive sites at edges was followed in real time [5].

We acknowledge support by the Agence Nationale pour la Recherche (LEMON project ANR-15-CE09-0007).

- [1] N. Alyabyeva, A. Ouvrard, A.-M. Zakaria, F. Charra, B. Bourguignon; App. Surf. Sci. 444, 423 (2018).
- [2] N. Alyabyeva, A. Ouvrard, R. Lazzari, B. Bourguignon; J. Phys. Chem. C 123, 19175 (2019).
- [3] N. Alyabyeva, A. Ouvrard, A.M. Zakaria, B. Bourguignon; J. Phys. Chem. Lett. 10, 624 (2019).
- [4] A. Ghalgaoui, A. Ouvrard, J. Wang, S. Carrez, W. Zheng, B. Bourguignon; J. Phys. Chem. Lett. 8 2666 (2017).
- [5] A. Ghalgaoui, R. Horchani, J. Wang, A. Ouvrard, S. Carrez, B. Bourguignon; J. Phys. Chem. Lett. 9 5202 (2018).

Thiolate-protected metal clusters: Chirality and dynamic nature

Thomas Bürgi

*Department of Physical Chemistry, University of Geneva, 30 Quai Ernest-Ansermet,
1211 Geneva, Switzerland*

(corresponding author: T. Bürgi, e-mail: thomas.buergi@unige.ch)

Chirality at the nanoscale has gained considerable interest in recent years. Chiral nanomaterials have properties that are of interest for applications in chiral technology but also in materials science. In this contribution we will focus on a special class of materials: Thiolate-protected metal clusters. These atomically well-defined objects could be used as building blocks for nanotechnology, as catalysts or as sensors. We will discuss the preparation of chiral gold clusters [1], their chiroptical properties and the transfer of chirality within the ligand shell as well as between cluster and ligand [2].

These clusters, although stable, turn out to be very dynamic. The latter is evidenced by the exchange of metal atoms and ligands between clusters as well as between clusters and surfaces. In addition, chiral clusters can undergo racemization. The latter property is usually unwanted but we will show that the interplay between racemization of a cluster and exchange of a chiral ligand can lead to chiral amplification.

Support by the Swiss National Science Foundation is gratefully acknowledged.

- [1] T. G. Schaaff, G. Knight, M. N. Shafigullin, R. F. Borkman, R. L. Whetten, *J. Phys. Chem. B* **102**, 10643 (2009).
- [2] I. Dolamic, B. Varnholt, T. Bürgi, *Nature Commun.* **6**, 7117 (2015).

Spin excitations and interactions on superconductors – probed and manipulated by scanning tunneling microscopy

Michael Ruby, Benjamin W. Heinrich, Yang Peng, Felix von Oppen, Katharina Franke

*Freie Universität Berlin, Fachbereich Physik, Arnimallee 14, 14195 Berlin, Germany
(corresponding author: K. Franke, e-mail: franke@physik.fu-berlin.de)*

Single-atom spins on superconductors provide a rich variety of interesting phenomena. Here, we explore two regimes of magnetic coupling strength of transition metal atoms on superconductors using scanning tunneling microscopy (STM): At sizeable coupling strength between adsorbate and superconductor, so-called Shiba states arise inside the superconducting energy gap. When the adatoms are brought into sufficiently close proximity, they form extended Shiba bands and may lead to the formation of topological states.

At negligible coupling strength, a very different regime of spin excitations can be explored. The superconductor then acts as a protection for low-energy excited states. This regime can be explored in adsorbed transition-metal porphyrins and allows for tuning their properties with the STM tip.

Carbon Nanoconduits: 2D Materials for Water Purification and Osmosis

Armin Götzhäuser

*Bielefeld University, Physics of Supramolecular Systems and Surfaces,
Universitätsstraße 25, 33615 Bielefeld, Germany
(e-mail: ag@uni-bielefeld.de)*

Clean water is a global challenge, and membrane filtration is a key technology to achieve it. There are growing research efforts to explore the use of ultrathin and two-dimensional materials as nanoconduits for molecular transport and separation [1]. Here, we report on the fabrication, characterization and application of carbon nanomembranes (CNMs) with sub-nanometer channels that prove to be excellent water filters, combining a high selectivity with an exceptionally high water permeance. The CNMs are fabricated via radiation induced cross-linking of molecular monolayers [2]. CNMs fabricated from terphenylthiol (TPT) molecules result in a ~ 1.2 nm thick membrane perforated by channels with diameters smaller ~ 0.5 nm and areal densities of $\sim 10^{18} \text{ m}^{-2}$, *i.e. one sub-nm channel per square nanometer (!)*. When tested as filter membranes, it was found that these CNMs efficiently block the passage of most gases and liquids. However, water passes through the membrane with an exceptionally high permeance of $800 \text{ l m}^{-2} \text{ h}^{-1} \text{ bar}^{-1}$ [3]. This suggests that the water molecules fast, collectively and cooperatively translocate through the channels with a rate of $\sim 60 \text{ molecules s}^{-1} \text{ Pa}^{-1}$.

By conductivity measurements in aqueous salt solutions [4], it has been shown that the sub-nm channels in TPT-CNMs block all ions, including protons, but still allow water to pass through. Comparable to 4 nm thick lipid bilayers of a cell membrane, the CNMs' membrane resistance reaches $\sim 10^4 \Omega \cdot \text{cm}^2$ in 1 M chloride solution. A single CNM channel thus yields a $\sim 10^8$ higher resistance than pores in natural and synthetic channel proteins, as well as in carbon nanotubes. These results motivated the testing of the operation of CNMs as semipermeable membranes. In forward osmosis experiments, the nanomembranes again exhibit an unprecedented high selectivity and water flow rate, two orders of magnitude higher than through commercial membranes. In summary, CNMs are unique systems for studying nanofluidics and they show a great potential for applications in water treatment and osmosis. Their simple and scalable fabrication further enables them to become key materials for a fast and highly selective materials separation.

- [1] H.G. Park, Y. Jung: Carbon nanofluidics of rapid water transport for energy applications, *Chem. Soc. Rev.* **2014**, 43 (2), 565-576.
- [2] A. Turchanin and A. Götzhäuser: Carbon Nanomembranes, *Adv. Mater.* **2016**, 28, 6075.
- [3] Y. Yang, P. Dementyev, N. Biere, D. Emmrich, P. Stohmann, R. Korzetz, X. Zhang, A. Beyer, S. Koch, D. Anselmetti and A. Götzhäuser: Rapid Water Permeation Through Carbon Nanomembranes with Sub-Nanometer Channels, *ACS Nano*, **2018**, 12, 4695.
- [4] Y. Yang, R. Hillmann, Y. Qi, R. Korzetz, N. Biere, D. Emmrich, M. Westphal, A. Beyer, D. Anselmetti and A. Götzhäuser: Ultra-high ionic exclusion through carbon nanomembranes, *submitted*.

Interstellar organic molecules and (anti-)masers

Alexandre Faure¹, François Lique², Antony J. Remijan³, Brett A. McGuire³

¹*Université Grenoble Alpes, CNRS, IPAG, F-38000 Grenoble (France)*

(corresponding author: A. Faure, e-mail: alexandre.faure@univ-grenoble-alpes.fr)

²*Université du Havre, CNRS, LOMC, F-76063 Le Havre (France)*

³*NRAO, 520 Edgemont Rd., Charlottesville, VA 22903 (USA)*

The interstellar medium (ISM) is so diluted (the density is less than 100,000 hydrogen atoms per cm³) that inelastic collisions cannot maintain a local thermodynamic equilibrium (LTE). Atomic and molecular level populations therefore do not follow a simple Boltzmann distribution and non-LTE spectra are the rule rather than the exception. In addition to accurate spectral data, a good knowledge of state-to-state collisional cross sections is thus crucial to properly model the observed spectra and to extract maximum information from the lines (abundance, velocity, density, temperature). While astrophysical models rely almost exclusively on theoretical cross sections, the last decade has seen huge progress in measurements of state-to-state cross sections. Detailed comparisons between quantum calculations and rotationally inelastic scattering experiments have thus allowed to verify theoretical predictions in the cold regime ($T < 50$ K) where quantum effects such as resonances are predominant [1]. Theory has passed all experimental tests so far, demonstrating the reliability of modern collisional data. These tests have been performed on ‘simple’ diatomic and triatomic molecules such as CO [2] and H₂O [3] excited by He or H₂, which are the most abundant colliders in the cold ISM.

Unfortunately, collisional cross sections are also needed for polyatomic molecules with more than 3 atoms, which challenge current computational and experimental capabilities. The main difficulty with large and heavy molecules is their small rotational spacings. From the theoretical point of view, the number of angular couplings between the target and the projectile (He or H₂) increases dramatically with the number of atoms, which makes full quantum calculations very expensive both in terms of time and memory requirements. Still, in recent years, such calculations have been successfully carried out for ‘medium-size’ interstellar species such as H₂CO [4], HC₃N [5], CH₂NH [6], CH₃OH [7] and HCOOCH₃ [8]. An interesting common property of these organic molecules is that they all have rotational transitions presenting (weak) maser emission and/or anti-maser absorption in the ISM. Since the population inversions and anti-inversions are pumped by collisions, any non-LTE model is critically dependent on the precision of collisional cross sections. Inelastic measurements are not available for such large molecules, but related experimental data such as line broadening cross sections can be used to infer accuracy.

We will make a short review of recent comparisons between theoretical and experimental rotationally inelastic cross sections, with emphasis on systems of astrophysical interest. We will show that the theoretical cross sections computed for the above polyatomic organic molecules have allowed to accurately model both maser emission lines and anti-maser absorption lines (see examples in Fig. 1), providing new astrophysical diagnostics for the emitting and absorbing interstellar regions. In addition, we will see that weak (anti-)masers provide unique signals that can help astronomers to robustly identify new and otherwise undetectable molecular species. Finally, we will present the first quantum scattering calculations for the ten-atom propylene oxide ($\text{CH}_3\text{CHCH}_2\text{O}$) molecule, which is the first organic chiral molecule detected in the ISM [9]. This species is larger than any previously treated and, as we will see, was challenging in many aspects [10].

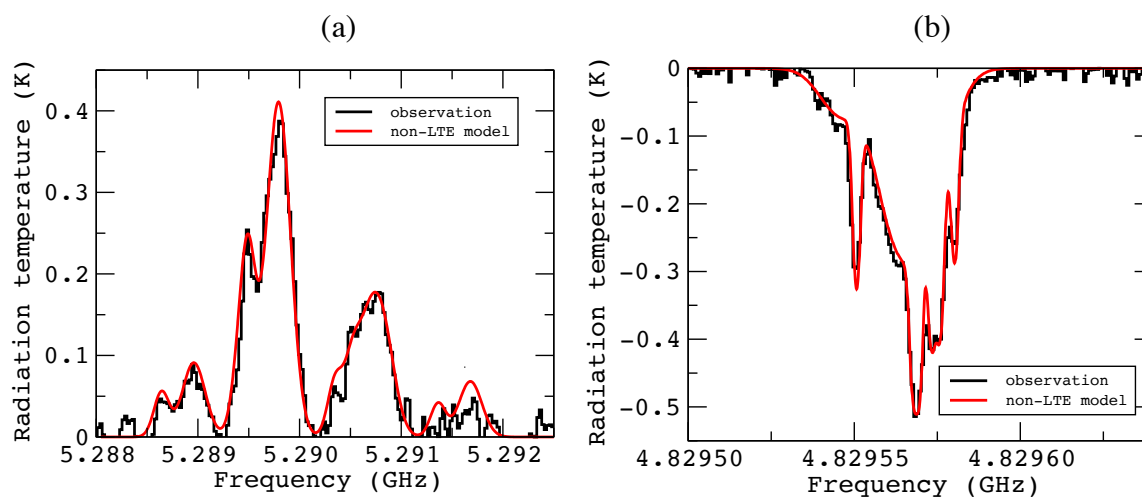


Figure 1: Observational and non-LTE model spectra of (a) methanimine (CH_2NH) $1_{10} \rightarrow 1_{11}$ maser emission transition at 5.29 GHz towards Sgr B2(N) [6] and (b) formaldehyde (H_2CO) $1_{10} \rightarrow 1_{11}$ anti-maser absorption transition at 4.83 GHz towards TMC-1 (work in preparation). Observations were performed with the 100m Robert C. Byrd Green Bank Telescope (GBT).

Support by the French National Program “Physique et Chimie du Milieu Interstellaire” is gratefully acknowledged.

- [1] M. Costes & C. Naulin, *Chem. Sci.* **7**, 2462 (2016).
- [2] S. Chefdeville et al., *ApJ* **799**, L9 (2015).
- [3] A. Bergeat et al., *J. Phys. Chem. A* in press (2019).
- [4] L. Wiesenfeld & A. Faure, *MNRAS* **432**, 2573 (2013).
- [5] A. Faure et al., *MNRAS* **460**, 2103 (2016).
- [6] A. Faure et al., *J. Phys. Chem. Lett.* **9**, 3199 (2018).
- [7] D. Rabli & D. R. Flower, *MNRAS* **411**, 2093 (2011).
- [8] A. Faure et al., *ApJ* **783**, 72 (2014).
- [9] B. McGuire et al., *Science* **352**, 1449 (2016).
- [10] A. Faure et al., *ACS Earth Space Chem.* **3**, 964 (2019).

Electroreduction of water and CO₂: competition or synergism on Mo₂C film electrodes?

Eva-Maria Wernig¹, Daniel Winkler¹, Christoph Griesser¹, Niussha Shakibi Nia¹,
and Julia Kunze-Liebhäuser¹

¹*Institute of Physical Chemistry, University Innsbruck, 6020 Innsbruck, Austria*
(corresponding author: J. Kunze-Liebhäuser, e-mail: Julia.kunze@uibk.ac.at)

The materials class of transition metal carbides (TMCs) has gained importance among electrocatalysts for reduction processes such as the hydrogen evolution reaction (HER) and the CO₂ reduction reaction (CO₂RR). In the CO₂RR, theoretical calculations [1] predict that TMCs are promising alternatives to Cu catalysts due to their preferable ability of breaking the binding energy scaling relations for the corresponding reaction intermediates, which has been experimentally shown to result in less negative onset potentials for hydrocarbon formation on Mo₂C compared to Cu [2]. For a comprehensive understanding of the electrocatalytic properties of Mo₂C towards the CO₂RR and the competing HER in aqueous electrolytes, the present study merges materials science and interface analytics with electrochemistry to unravel the pathways of these complex reactions. We report on the synthesis of Mo₂C films using direct carburization of polycrystalline Mo substrates through carbothermal conversion. Cyclic voltammetry, complemented by rotating ring disc electrode (RRDE) measurements, was used to investigate the electrocatalytic activity of Mo₂C films towards the HER in the absence and presence of CO₂, while changes of the chemical composition at the surface were analyzed with *ex-situ* emission X-ray photoelectron spectroscopy (XPS). Subtractively normalized interfacial Fourier transform infrared spectroscopy (SNIFTIRS) enabled the *in-situ* determination of reaction intermediates at the solid/liquid interface. Gaseous reaction products have been tracked with *online* differential electrochemical mass spectrometry (DEMS) and with gas chromatography.

Support by the Austrian Science Fund (FWF) is gratefully acknowledged.

References:

- [1] Michalsky, R.; Zhang, Y. J.; Medford, A. J.; Peterson, A. A., J. Phys. Chem. C **118**, 13026 (2014).
- [2] Kim, S. K.; Zhang, Y. J.; Bergstrom, H.; Michalsky, R.; Peterson, A., ACS Catal. **6**, 2003 (2016).

Neutralization dynamics of highly charged ions in 2D materials

Friedrich Aumayr

*Institute of Applied Physics, TU Wien, Wiedner Hauptstr. 8-10, A-1040 Wien, Austria
(corresponding author: e-mail: aumayr@iap.tuwien.ac.at)*

For the development of novel devices in the field of optoelectronics and photodetection based on 2D-materials, it is necessary to understand how electrons in low-dimensional materials react to ultrafast external perturbations. As recently shown [1, 2], the electronic reaction of these materials to an extremely strong electric field can be well investigated by the Coulomb field of an approaching slow highly charged ion. In this context, highly charged ions are superior to short pulse lasers since they can probe a very localized area (approx. 1nm^2) around the impact point. Fig. 1 schematically depicts the interaction processes between a freestanding single layer graphene and an approaching highly charged ion, which extracts a lot of charge from a very limited area on a femtosecond time scale. Recharging of the impact area is not instantaneous but retarded due to finite conductivity and allows to probe the local electronic dynamics of the 2D material on this fs-time scale [1]. In addition, a large number of low energy electrons is emitted into vacuum as will be described below.

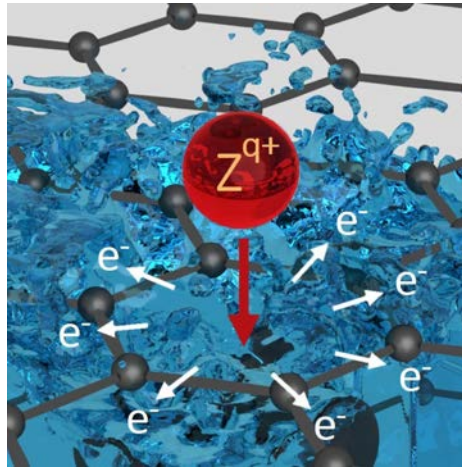


Figure 1: Schematic of the interaction process between a freestanding single layer of graphene and an approaching highly charged ion (HCI), leading to the emission of many low energy electrons [7].

In our experiments we compare the ultrashort time response of different 2D-materials like a single layer of (freestanding) graphene (SLG), MoS_2 and hBN to an incident highly charged ion (typically Xe^{20+} - Xe^{44+}). For this purpose we have constructed and built a multi-

coincidence apparatus [3], which measures the charge state, scattering angle and energy of the ions transmitted through suspended 2D-membranes in coincidence with the number of electrons emitted. From the exit charge state distribution (an example for SLG can be seen in fig. 2) the relevant time scales for the charge transfer along the 2D layer can be derived and the resulting current densities in the material as well as lower limits for the breakdown currents can be estimated [1].

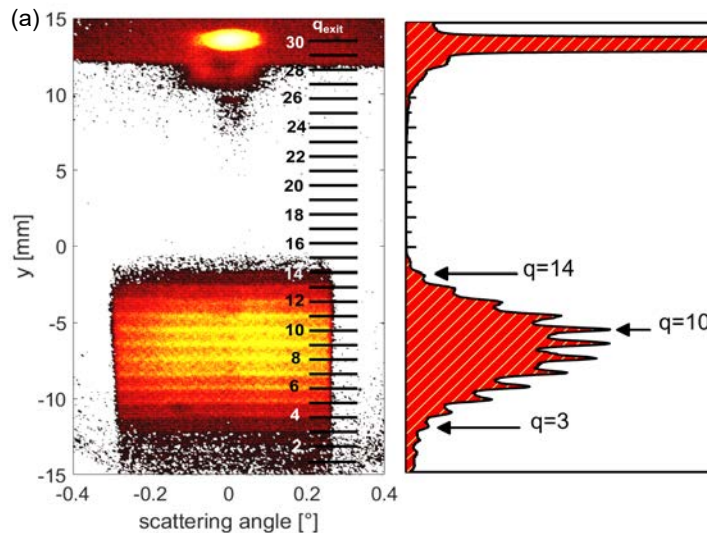


Figure 2: Exit charge state (y -position) vs. projectile scattering angle for 170 keV Xe^{30+} ions transmitted through SLG as recorded on a position sensitive channelplate (left). Counts integrated over scattering angles vs. exit charge state (right) (from [3]).

Depending on the electron mobility, the 2D-materials cannot resupply the lost charges and/or dissipate the deposited energy within a time interval that is small compared to lattice vibrations. Then the resulting Coulomb explosion tears holes in the order of several nanometers into the 2D membrane [4, 5], which are observable in high-resolution (S)TEM investigations. The results of our studies are therefore also of interest for the development of two-dimensional materials with electrons, ions and lasers, with many future applications, such as their use as molecular sieves, for desalination or even for DNA sequencing.

For more than 20 years, there has been a model for the hollow atom (HA) formation and its deexcitation in the vicinity of a solid surface via an auto-ionisation cascade [6]. Our studies of highly charged ion transmission through a freestanding two-dimensional graphene membrane show that ion neutralisation and deexcitation take places within a few fs only and can no longer be explained by the comparatively slow Auger deexcitation cascades [1,2]. In a refined model Interatomic Coulombic Decay (ICD) has now been proposed as the responsible mechanism for the observed fast deexcitation of the initially highly charged ion. Above the

graphene sheet a HA is formed and upon entering the surface, the captured electrons are quenched into inner shells while the de-excitation energy is released by excitation and ionisation of surrounding carbon electrons [2]. The rate of ICD depends on both the interatomic distance, which is small in case of an ion-atom collision, as well as the number of nearest neighbours, i.e. atoms participating in the process. This leads to a significantly higher efficiency of ICD in an embedded environment (solid surface) than in case of isolated gas atoms.

We probe the rapid deexcitation of a HA via ICD by measuring the emitted electrons resulting from one single ion impact on the graphene sheet. We find that the amount of emitted electrons is indeed as predicted by ICD quite high (about 2 times the ion's initial charge state) [7]. Further, we analyse the energy of these electrons (see Fig. 3) and find additional evidence for ICD by measuring that the vast majority of emitted electrons have energies well below 15 eV [7].

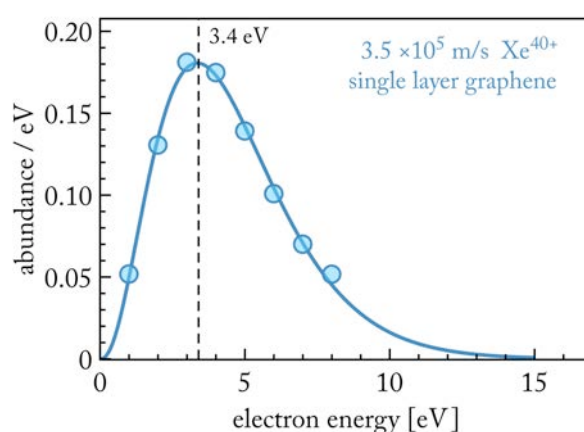


Figure 3: Measured energy distribution of emitted electrons due to 80 keV Xe^{40+} impact on single layer graphene (from [7]).

- [1] E. Gruber, R.A. Wilhelm, R. Pétuya, V. Smejkal, R. Kozubek, A. Hierzenberger, B.C. Bayer, I. Aldazabal, A.K. Kazansky, F. Libisch, A.V. Krashennnikov, M. Schleberger, S. Facsko, A.G. Borissov, A. Arnau, and F. Aumayr, *Nature Comm.* **7** (2016) 13948
- [2] R.A. Wilhelm, E. Gruber, J. Schwestka, R. Kozubek, T.I. Madeira, J.P. Marques, J. Kobus, A.V. Krashennnikov, M. Schleberger, and F. Aumayr, *Phys. Rev. Lett.* **119** (2017) 103401
- [3] J. Schwestka, D. Melinc, R. Heller, A. Niggas, L. Leonhartsberger, H. Winter, S. Facsko, F. Aumayr, and R.A. Wilhelm, *Rev. Sci. Instrum.* **89** (2018) 085101
- [4] R.A. Wilhelm, E. Gruber, R. Ritter, R. Heller, A. Beyer, A. Turchanin, N. Klingner, R. Hübner, M. Stöger-Pollach, H. Vieker, G. Hlawacek, A. Götzhäuser, S. Facsko, and F. Aumayr, *2D Materials* **2** (2015) 035009
- [5] R.A. Wilhelm, E. Gruber, J. Schwestka, R. Heller, S. Facsko, and F. Aumayr, *Appl. Sci.* **8** (2018) 1050.
- [6] A. Arnau et al 1997 *Surf. Sci. Rep.* **27** (1997) 113
- [7] J. Schwestka, A. Niggas, S. Creutzburg, R. Kozubek, R. Heller, M. Schleberger, R.A. Wilhelm, and F. Aumayr, *J. Phys. Chem. Lett.* **10** (2019) 4805.

Small chiral molecules: Progress in synthesis and beyond

Jürgen Stohner

*Zürich University of Applied Science (ZHAW), Institute of Chemistry and Biotechnology (ICBT),
Campus Reidbach RT E309.3, Einsiedlerstrasse 31, CH 8820 Wädenswil, Switzerland,
Email: sthj@zhaw.ch*

Small chiral molecules (C_1 - and C_2 -compounds) are very useful target molecules at the border of chemistry and physics. Major efforts still focus on the attempts to measure parity violating effects in molecular spectroscopy [1-3], the determination of anisotropy in chiral Photon Electron Detachment [4], very precise measurements of the specific rotatory power in gas-phase samples [5], as well as on the determination of the absolute configuration of gas-phase molecules [6,7].

Chiroptical experiments require enantio-pure target molecules. In the past, the resolution of a racemate into its enantiomers was almost exclusively achieved by fractional crystallization [8], a method introduced at the time when “stereochemistry” started with Louis Pasteur separating large crystals of sodium ammonium tartrate with tweezers and a magnifying glass [9].

An alternative separation method is based on gas chromatography. This separation of enantiomers is very difficult when large quantities (order of gram) are involved (“preparative scale”). While a separation on an analytical scale (order of microgram) is possible by using chiral stationary phases, a separation by up-scaling using the same chiral column material and larger preparative columns is largely impossible. The search for column material, which facilitates preparative separation is of utmost importance [10].

We devised a synthetic route to obtain halogenated chiral acetic acids, which serve as precursors to chiral methane and derivatives [11]. Currently, we are working on the synthesis of fluoro oxirane in enantio-pure form by diastereomeric resolution. The racemic target compound has been synthesized already in very good yield and purity. The IR and NMR spectra support this, especially when compared to work reported in the literature [12].

References

- [1] M. Quack, *Angew. Chem. Int. Ed.* **41**, 4618 (2002).
- [2] M. Quack and J. Stohner, *Chimia* **59**, 530 (2005).
- [3] M. Quack, J. Stohner, and M. Willeke, *Annu. Rev. Phys. Chem.* **59**, 741 (2008).
- [4] C. Lux, M. Wollenhaupt, C. Sarpe, T. Baumert, *ChemPhysChem* **16**, 115 (2015).
- [5] P. Lahiri, K.B. Wiberg, P.H. Vaccaro, *J. Phys. Chem. A* **119**, 8311 (2015).
- [6] M. Pitzer, M. Kunitski, A. S. Johnson, T. Jahnke, H. Sann, F. Sturm, L. Ph. H. Schmidt, H. Schmidt-Böcking, R. Dörner, J. Stohner, J. Kiedrowski, M. Reggelin, S. Marquardt, A. Schiesser, R. Berger and M. S. Schöffler, *Science* **341**, 1096 (2013).
- [7] M. Pitzer, G. Kastirke, M. Kunitski, T. Jahnke, T. Bauer, C. Goihl, F. Trinter, C. Schober, K. Henrichs, J. Becht, S. Zeller, H. Gassert, M. Waitz, A. Kuhlins, H. Sann, F. Sturm, F. Wiegandt, R. Wallauer, L. Ph. H. Schmidt, A.S. Johnson, M. Mazenauer, B. Spenger, S. Marquardt, S. Marquardt, H. Schmidt-Böcking, J. Stohner, R. Dörner, M. Schöffler, R. Berger, *ChemPhysChem* **17**, 2465 (2017).
- [8] B. Darquié, C. Stoeffler, A. Shelkovich, C. Daussy, A. Amy-Klein, C. Chardonnet, S. Zrig, L. Guy, J. Crassous, P. Soulard, P. Asselin, T. R. Huet, P. Schwerdtfeger, R. Bast and T. Saue, *Chirality* **22**, 870 (2010).
- [9] L. Pasteur, *C. R. Acad. Sci. Paris* **26**, 535 (1848).
- [10] M. Meister, MSc Thesis, ZHAW Wädenswil (2017); J. Thoma, MSc Thesis, ZHAW Wädenswil (2018).
- [11] M. R. Mazenauer, S. Manov, V. M. Galati, P. Kappeler, J. Stohner, *RSC Advances* **7**, 55434 (2017).
- [12] H. Hollenstein, D. Luckhaus, J. Pochert, M. Quack, G. Seyfang, *Angew. Chem. Intl. Ed.* **36**, 140 (1997).

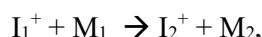
Ion-molecule reactions below 1 K

V. Zhelyazkova, F. B. V. Martins, M. Zesko, K. Höveler, J. Deiglmayr,
and F. Merkt

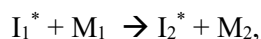
Physical Chemistry Laboratory, ETH Zurich, Switzerland

merkt@phys.chem.ethz.ch

The study of ion-molecule reactions at low collision energies (E_{coll}) or low temperatures below $E_{\text{coll}}/k_{\text{B}} = 10$ K is experimentally challenging because stray electric fields in the reaction volume heat up the ion samples. A potential difference of 1 mV across a reaction region of 1 cm accelerates the ions to 1 meV, which corresponds to heating them up to about 12 K. To overcome this problem and study ion-molecule reactions below 10 K, we have developed a new method, in which the ion molecule reaction takes place within the orbit of a Rydberg electron at high values of the principal quantum number n . In high- n Rydberg states, the Rydberg electron only very weakly interacts with the ion core, so that it does not significantly influence the ion-molecule reaction but shields the ions from heating by stray electric fields. Instead of studying exothermic and barrier-free ion-molecule reactions of the type



we study the reactions



in which I_1^* and I_2^* represent atoms or molecules in high Rydberg states. To reach very low collision energies we use chip-based Rydberg-Stark decelerators and deflectors to merge cold supersonic beams of I_1^* and M_1 and to vary the relative velocity of I_1^* and M_1 [1]. Monitoring the product yield as a function of the relative mean velocity of the two beams, we obtain the relative reaction cross sections as a function of the collision energy [2]. At temperatures below 1 K, we find that the reaction rate coefficients deviate from those estimated with Langevin-type capture models. The deviations become particularly large when M_1 has a permanent dipole or a quadrupole moment.

The talk will present studies of reactions of H_2^+ and He^+ ions (I_1^+) with neutral molecules such as N_2 , H_2 , CH_3F and CH_4 (M_1) at collision energies down to below 1 K and will discuss the observed low-temperature behaviour in terms of the electric dipole and quadrupole moments of M_1 .

[1] Surface-electrode decelerator and deflector for Rydberg atoms and molecules, P. Allmendinger, J. Deiglmayr, J. A. Agner, H. Schmutz, and F. Merkt, *Phys. Rev. A* **90**, 043403 (2014)

[2] New method to study ion-molecule reactions at low temperatures and application to the $\text{H}_2^+ + \text{H}_2 \rightarrow \text{H}_3^+ + \text{H}$ reaction

P. Allmendinger, J. Deiglmayr, O. Schullian, K. Höveler, J. A. Agner, H. Schmutz, and F. Merkt, *ChemPhysChem* **17**, 3596 (2016)

Author Index

Abi Khodr A.	107	Dillinger S.	30
Adam T.	96	Domke K.F.	112
Alducin M.	94	Dowek D.	55
Albertini S.	38	Duensing F.	46
Alyabyeva N.	113	Dulitz K.	75
Amin M.	60	Dyukova I.	107
Anargirou E.	110	Ehlert S.	96
Andreasson J.	73	Eikema K.S.E.	59
Armenta Butt S.	41, 108	Ellis A.M.	38
Armentrout P.B.	30	Ellis-Gibblings L.	108
Arnoldi B.	43	Enache M.	84
Arnolds H.	28	Ernst K.-H.	43, 44, 45, 47, 81, 86
Aumayr F.	120	Espinoza S.	48, 73
Avarvari N.	44, 81	Estillore A.	60
Ayasli A.	92	Faure A.	117
Baghernejad M.	112	Fedor J.	104
Baker B.	84	Feliu J.M.	112
Baljozovic M.	43, 44, 81, 86	Feringa B.L.	26
Ballauf L.	46	Fernandes Cauduro A. L.	43
Bansal P.	107	Field D.	50
Bastian B.	92	Floss G.	94
Bauer K.N.	53	Fortune W.	108
Beck R. D.	31	Franke K.	115
Bedekar A.	45	Fries D.V.	30
Ben Faleh A.	107	Füchsel G.	94
Berger J.	45	Galparsoro O.	58
Berger T.	53	Gallardo A.	86
Bernard L.	44	Gao H.	75, 93
Bernhard C.	53	Garcia G.A.	55
Beyer M.	59	Gatchell M.	38
Beyer M.K.	68	Ghalgaoui A.	113
Bonini Guedes E.	43	Gierster L.	111
Bonn M.	53	Giessibl F.J.	83
Borodin D.	34	Giuzio G.	112
Bourguignon B.	113	Gölzhäuser A.	116
Brablec A.	77	Goian V.	32
Breiner M.	112	Gonella G.	53
Brünken S.	105	Goretzki B.	53
Bucag J.-M.	28	Gottardi S.	84
Bürgi T.	114	Goubert G.	67
Cahlík A.	82, 86	Govers T.R.	55
Carrascosa E.	107	Grenader K.	44
Carrez S.	113	Griesser C.	119
Cassidy A.	50	Grill L.	89
Chen L.	69	Guhl C.	53
Deiglmayr J.	125	Havenith R.W.A.	84
Dill J.H.	43	Hechenberger F.	46

Heinrich B.W.	115	Merkt F.	59, 125
Hellmich U.A.	53	Meyer J.	92
Hertl N.	58	Michaelson T.	92
Hirsch A.K.H.	84	Miloglyadov E.	100
Hoelsch N.	59	Mohrbach J.	30
Höveler K.	125	Monjas L.	84
Horke D.A.	60	Moreno Lopez J.C.	84
Hrodmarsson H.R.	55	Mutombo P.	82
Humpolicek P.	77	Nagata Y.	36, 94
Irsig R.	96	Nahon L.	55
Irziqat B.	43, 45	Neugeboren J.	34
James R.	50	Niedner-Schatteburg G.	30
Jelinek P.	45, 82, 86	Niepel T.S.G.	66, 67
Juaristi J.I.	94	Oncák M.	68
Jungen C.	59	Onvlee J.	61
Jurmanova J.	77	Osterwalder A.	87
Kaiser A.	69	Ouvrard A.	113
Kandratsenka A.	58	Owens A.	61
Kawecki M.	44	Ozaltin K.	77
Kilaj A.	93	Pandey Y.	67
Kitsopoulos T. N.	34	Pantzer J.	32
Klein M.P.	30	Park B.G.	34
Kostov K.L.	32	Pascal S.	82
Kramer Campen R.	36	Pascher T.F.	68
Kranabetter L.	38	Passig R.	96
Krcma F.	62	Pellegrinelli R.P.	107
Krzyzankova A.	62	Peng Y.	115
Küpper J.	27, 60, 61, 75, 93	Pfisterer J.H.K.	112
Kunze-Liebhäuser J.	119	Ploenes L.	75
Laimer F.	38	Price S.D.	41, 108
Larrégaray P.	58	Probst M.	69
Lehocky M.	77	Prokes L.	77
Li C.	96	Quack M.	100
Li J.	84	Quayle J.	28
Li X.	28	Rebarz M.	73
Lindner S.	94	Remijan A.J.	117
Lique F.	117	Rivero U.	93
Loncaric I.	94	Rizzo T.R.	107
Maier M.	110	Roeters S.J.	53
Maier S.	29	Rösch D.	93
Mairena A.	43, 44, 86	Rossi M.	95
Maltseva D.	53	Roth N.	60
Martin K.	44, 81	Ruby M.	115
Martin-Barrios R.	58	Rudich Y.	96
Martins F.B.V.	125	Saalfank P.	36, 94
Mason A.	28	Samanta A.K.	60
Mazankova V.	62, 77	Saribal C.	61
McGuire B.A.	117	Schade J.	96
Meir Z.	90	Scheier P.	38, 46
Melani G.	36, 94	Schlüter A.D.	66
Mendieta J.	45, 82	Schmid A.	43

Schmidt N.	84	Winkler D.	119
Scholz R.	94	Wodtke A.M.	34, 58, 88
Schumann F.O.	32	Worbs L.	60
Schwarzer M.	34	Wurm F.R.	53
Sczzerbinski J.	67	Yachmenev A.	61
Sévery L.	67	Yalovenko N.	107
Seyfang G.	100	Yatsyna V.	107
Shakibi N.	119	Yue L.	107
Shlykov A.	90	Zak E.	61
Sinhal M.	90	Zappa F.	38
Siri O.	82	Zenobi R.	66, 67
Sklorz M.	96	Zesko M.	125
Smith E.	108	Zhelyazkova V.	125
Stadtmüller B.	43	Zheng W.	113
Stähler J.	111	Zhumaev U.	112
Stahel P.	77	Zimmermann R.	96
Steiner A.	30		
Steinrück H.-P.	33		
Stetsovyeh O.	82		
Stienkemeier F.	75		
Stohner J.	123		
Stöhr M.	84		
Stranak P.	75		
Sukuba I.	69		
Sundar S.	45		
Svec M.	82		
Terfort A.	44		
Tiefenthaler L.	38		
Titov E.	94		
Thissen R.	55		
Tilley S.D.	67		
Tomeckova K.	77		
Trunec D.	62, 77		
Ubachs W.	59		
Van der Linde C.	68		
Von Oppen F.	115		
Vempati S.	111		
Viet K.	53		
Vija Meena S.	82		
Voigt J.	43, 81		
Wäckerlin C.	43, 44, 81, 82, 86		
Wang W.	66		
Warnke S.	107		
Weidner T.	53		
Wernig E-M.	119		
Wester R.	92		
Wichmann G.	100		
Widdra W.	32		
Wiehn C.	30		
Wienke M.	44		
Willitsch S.	75, 90, 93		